



## D5.3

---

SECOND REPORT ON NEW TECHNOLOGICAL FEATURES TO BE  
SUPPORTED BY 5G STANDARDIZATION AND THEIR  
IMPLEMENTATION IMPACT

The 5G-SMART project has received funding from the European Union's Horizon 2020 research and innovation programme under grant agreement no 857008.



## Second report on new technological features to be supported by 5G standardization and their implementation impact

Grant agreement number:	857008
Project title:	5G Smart Manufacturing
Project acronym:	5G-SMART
Project website:	<a href="http://www.5gsmart.eu">www.5gsmart.eu</a>
Programme:	H2020-ICT-2018-3
Deliverable type:	Public
Deliverable reference number:	D20
Contributing workpackages:	WP5
Dissemination level:	Public
Due date:	Nov 30, 2021
Actual submission date:	Nov 30, 2021
Responsible organization:	ABB
Editor(s):	Dhruvin Patel, Krister Landernäs
Version number:	1.0
Status:	Final
Short abstract:	This deliverable presents 5G technological features addressing the requirements of the 5G-SMART smart manufacturing use cases. It describes evaluations done relating to three identified technical features, 5G-TSN integration, end-to-end time synchronization, and 5G-supported positioning.
Keywords:	DetNet, 5G-TSN, 5G-based positioning, time synchronization

Contributor(s):	Dhruvin Patel (Ericsson), Krister Landernas (ABB), Daniel Venmani (Orange), Joachim Sachs (Ericsson), Sylvia Lu (UBK), Peter Karlsson (Ublox), Ioannis Sarris (Ublox), John Diachina (Ericsson), Stefano Ruffini (Ericsson), Tore Lindgren (Ericsson), Sara Sandberg (Ericsson), Aleksejs Udalcovs (Ericsson), Marilet De Andrade (Ericsson), David Ginthoer (Bosch), Davit Harutyunyan (Bosch)
-----------------	---



## Disclaimer

This work has been performed in the framework of the H2020 project 5G-SMART co-funded by the EU. This information reflects the consortium's view, but the consortium is not liable for any use that may be made of any of the information contained therein.

This deliverable has been submitted to the EU commission, but it has not been reviewed and it has not been accepted by the EU commission yet.



## Executive summary

5G standardization is progressing with 5G technology by introducing new features to support a wide variety of smart manufacturing use case requirements. This document provides insights to the next steps that are to be taken to further evaluate such features against smart manufacturing use case requirements. All three of the features identified in the first 5G-SMART report on the 5G technological features, i.e., 5G-TSN integration, 5G-based positioning, and time synchronization, are evaluated by selecting appropriate use case scenarios and methodologies. Further, a state-of-art analysis of Deterministic Networking (DetNet) technology is provided and a 5G-DetNet integration architecture is proposed. Based on the current 3<sup>rd</sup> Generation partnership project (3GPP) standards, new scheduling procedures applicable to an end-to-end integrated 5G and TSN (time-sensitive networking) network are proposed. Such scheduling optimization is evaluated against a 5G-SMART trialled use case of the industrial control to control communication. The evaluation shows clear trade-off between complexity and efficiency that can be achieved when using integrated 5G-TSN scheduling optimization. The 5G system (5GS) has various solutions whereby time synchronization can be offered as service to industrial applications. The most demanding time synchronization error budget is defined to be as low as 900ns for industrial applications in an integrated 5G-TSN network (i.e., the time synchronization error introduced when relying on an external Grandmaster clock between ingress and egress points of a 5G system). An in-depth analysis is undertaken which provides details on how a 5GS can support such a time synchronization error budget for a typical smart manufacturing scenario. The results show the need for a Round Trip Time (RTT) based method to determine and compensate for downlink propagation delay between gNB and User Equipment (UE) since this interface is known to be a major source of the time synchronization error introduced by the 5GS. At last, the report provides very detailed evaluations on 5G radio-frequency-based positioning in a realistic industrial environment of a 5G-SMART trial site. The environment is modelled by means of the 3GPP statistical radio propagation channel and with a geometric 3D ray tracing channel. The results show that positioning performance is limited by multipath propagation and the lack of line of sight between the UE to be localized and sufficiently many base stations in certain parts of the factory hall (e.g., in the corners). Further, several recommendations on how to improve positioning performance are provided. The positioning evaluations provide an understanding that performance of positioning does not only depend upon the mechanism used to locate the end device but also on the deployment and radio configuration.



## Contents

Executive summary .....	2
1 Introduction .....	6
1.1 Short summary of 5G-SMART Deliverable D5.1 .....	7
1.2 Objective of the document.....	7
1.3 Relation to other work packages in 5G-SMART .....	8
1.4 Structure of the document .....	8
2 DetNet.....	10
2.1 Standardized DetNet specifications .....	10
2.1.1 DetNet architecture .....	11
2.1.2 Data plane .....	12
2.1.3 Controller plane .....	16
2.1.4 DetNet features for 5G-SMART use cases.....	19
2.2 5G support for DetNet.....	20
2.2.1 Proposed 5G-DetNet architecture .....	21
2.3 Summary.....	23
3 5G-TSN Evaluations.....	23
3.1 Introduction.....	23
3.1.1 C2C use case description.....	23
3.2 TSN scheduling process for 5GS bridges.....	25
3.2.1 Scheduling input parameters .....	27
3.2.2 The schedule computation.....	28
3.2.3 Scheduling output parameters.....	29
3.3 Evaluation of the TSN scheduling process for 5GS bridges .....	29
3.3.1 Impact of wireless channel on 5GS bridge performance .....	30
3.3.2 Wireless channel awareness .....	32
3.3.3 Schedule optimization for 5GS bridge.....	33
3.4 Conclusion .....	37
4 End to End time synchronization Evaluations.....	38
4.1 5G architecture to support time aware network .....	38
4.2 Synchronization network solution over 5GS .....	40
4.2.1 Synchronization of 5GS solution over 5G transport.....	40



4.2.2	Synchronization network solution for 5GS over 5G radio access network.....	42
4.3	Analytical time error analysis .....	42
4.3.1	Time error analysis for transport network, including gNB.....	43
4.3.2	Time error analysis over radio network .....	44
4.4	Link level simulation analysis.....	47
4.4.1	SSB block basic .....	48
4.5	Simulation and result analysis .....	50
4.5.1	Simulation environment.....	50
4.5.2	Simulation goals .....	51
4.5.3	The proposed algorithm to estimate the downlink propagation delay based on process of detection of Primary Synchronization Signal (PSS).....	51
4.5.4	Simulations results .....	52
4.5.5	Inter-correlation technique to detect the peak the UE will detect .....	53
4.5.6	Propagation delay & Time error calculation .....	54
4.6	Study the delay RMS in different SCSs and FFT sizes .....	55
4.6.1	Effect of height on delay RMS.....	56
4.7	Rural Macro (RMa) model in LOS and NLOS.....	58
4.7.1	Discussion of results.....	60
4.8	Conclusions and recommendations .....	61
5	5G positioning evaluations.....	63
5.1	Evaluation methodology.....	63
5.2	Geometric model-based evaluation .....	64
5.2.1	Simulation setup .....	64
5.2.2	LoS probability.....	67
5.2.3	Ranging performance.....	69
5.2.4	Positioning performance.....	76
5.3	Statistical model-based evaluation .....	81
5.3.1	Simulation setup .....	82
5.3.2	Evaluation of LoS probability.....	82
5.3.3	Evaluation of geometric effects on the positioning performance.....	88
5.3.4	Positioning simulation results .....	89
5.4	Comparison between Geometric based model and 3GPP based statistical model .....	93
5.5	Conclusions and recommendations .....	94



6	Summary and Future work .....	97
	References .....	99
	List of abbreviations.....	101



## 1 Introduction

Connectivity plays an important role in digital transformation of smart manufacturing sector supported with seamlessly integrated wired and wireless communication infrastructure. Reliable and secure transport of data in a timely fashion among sensors, actuators and controlling devices is one of the key requirements for a communication infrastructure supporting end-to-end (E2E) connectivity.

In the 5G-SMART project, we focus on key technologies that are fundamental for the transformation of manufacturing. These include 5G-based positioning and E2E time synchronization that are critical for applications such as mobile robotics, automated guided vehicles (AGVs) and augmented reality (AR)-equipped workers. Easy and fast integration of 5G with TSN networks is also key to meet the requirements of flexible production where workflows need to adapt to changing needs. This is empowered by time-bounded communication capabilities and wireless technologies.

An overview of these technology features was provided in a 5G-SMART report released last year [5GS20-D51] (see Section 1.1). In this second report on technology features to be supported by 5G, the focus is on evaluations. Extensive evaluations of identified technical features by choosing relevant methodologies are undertaken and documented in this report. These evaluation results provide answers to how such 5G technical features can fulfil requirements of the advanced smart manufacturing use cases. Additionally, these results provide a general view on how a 5GS should be configured and deployed to meet smart manufacturing use case requirements. Key learnings from these evaluations provide an understanding on how such features can accelerate the adoption of 5G in the smart manufacturing ecosystem.

DetNet, a deterministic transport solution to ensure bounded latency and low data loss over network layer is currently being specified by the Internet Engineering Task Force (IETF). It is seen as a potential technology for future advanced smart manufacturing applications. Within 5G-SMART, an in-depth investigation of the DetNet technology is performed and documented in this report. A brief overview on the standardization aspect of the technology with details on the features and deployment aspects are provided. The report further provides an outlook to upcoming standardization efforts by 3GPP in specifying the interworking of the 5G technology with DetNet. This is realized by proposing an integrated 5G-DetNet architecture foreseen for the smart manufacturing domain.

Internal 5GS time synchronization is an essential functionality in an integrated 5G-TSN based industrial network. The 5GS can offer several internal time synchronization solutions that lead to different amounts of time error when relaying a TSN Grand Master (GM) clock reference value between the 5GS ingress and egress. For the most demanding industrial applications, a time error budget of 900 ns is assigned to the 5GS in an integrated 5G-TSN network. This report provides details on how the 5GS can support such a time error budget.

Reliable positioning with high accuracy is important for navigation and tracking of devices, AGVs and persons in a large set of use cases in smart manufacturing. In this report we evaluate the performance of 5G radio-frequency-based positioning. The industrial 5G deployment used in the 5G-SMART trial site at Fraunhofer IPT institute in Aachen is selected as one realistic environment for evaluations around positioning performance. The environment is modelled both by means of the 3GPP statistical

radio propagation channel and with a geometric 3D ray tracing channel where the specific objects in the trial are included.

### 1.1 Short summary of 5G-SMART Deliverable D5.1

Deliverable D5.1 [5GS20-D51] describes, by considering use cases identified within 5G-SMART project, the required 5G technical features which are not yet standardized or currently being discussed for standardization. Key technical features relating to end-to-end time synchronization, integration of 5G with TSN and 5G-based positioning mechanisms are analysed. A thorough state-of-the-art analysis is performed for each feature. Further, D5.1 develops a system view, lists the potential improvements or gaps observed when comparing the features to use case requirements. The report further provides recommendations towards future standardization and solution development. An overview of the features covered in D5.1 is given in Figure 1.

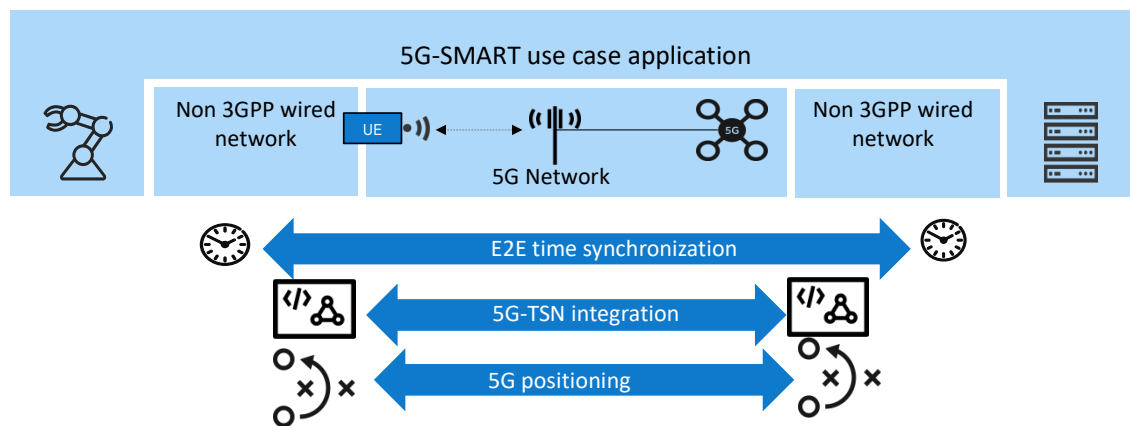


Figure 1: 5G features to support the 5G-SMART use cases

### 1.2 Objective of the document

5G-SMART has identified several advanced technical feature concepts targeting the smart manufacturing domain. A state of the art and gap analysis has been performed and novel 5G features such as time synchronization over 5G, advanced 5G positioning, and solutions on 5G integration with TSN and Industry LAN have been identified as particularly important for manufacturing industries. The analysis has been published in 5G-SMART deliverable D5.1 [5GS20-D51].

In this deliverable, some selected features from D5.1 have been evaluated namely:

- Enhancements of the scheduling procedures in integrated 5G-TSN networks
- Time synchronization of 5G-TSN network, including a time error analysis
- Indoor positioning performance estimated both based on the statistical model used in 3GPP and a geometric model

In addition to the evaluations, an introduction to the advanced technical features of DetNet is also provided.

### 1.3 Relation to other work packages in 5G-SMART

Among the different work packages (WPs) in 5G-SMART, WP5 differs from the 5G-SMART trial work in WPs (WP2-4), which are focused on demonstrating 5G capabilities that are already standardized. WP5 instead investigates new 5G technological features such as 5G-TSN integration, time synchronization and positioning. Figure 2 shows the overall workflow of WP5, it takes input from WP1, specifically use case requirements, and provides output to WP6 with various enhancements of new technological features.

In WP5, new and future-looking 5G technical features are investigated and evaluated against the different use case requirements. The output of the activity is the “development and evaluation of new technical 5G features and concepts beyond trials” as shown in Figure 2. This serves as input to standard development organizations (SDO) and industry fora. Considering different use cases and their requirements, this document provides evaluations on selected 5G technical features, focusing on 5G integration with time-sensitive networking, time synchronization and positioning.

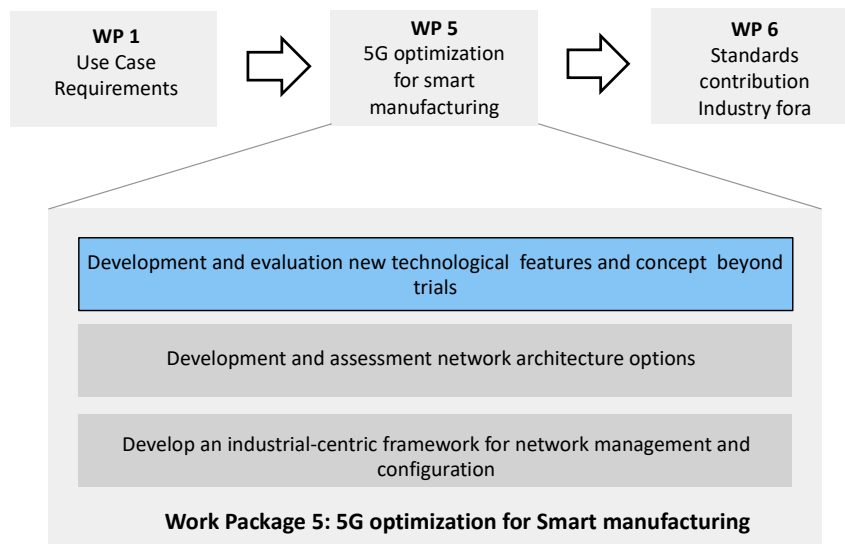


Figure 2 Workflow of WP5

### 1.4 Structure of the document

The 5G technical feature investigation activity within work package 5 (WP5) takes input from 5G-SMART Deliverables D1.1 [5GS20-D11] and D5.1 [5GS20-D51], where 5G-SMART use cases are defined, and technical features are identified and analysed. Figure 3 shows the overall structure of the document.

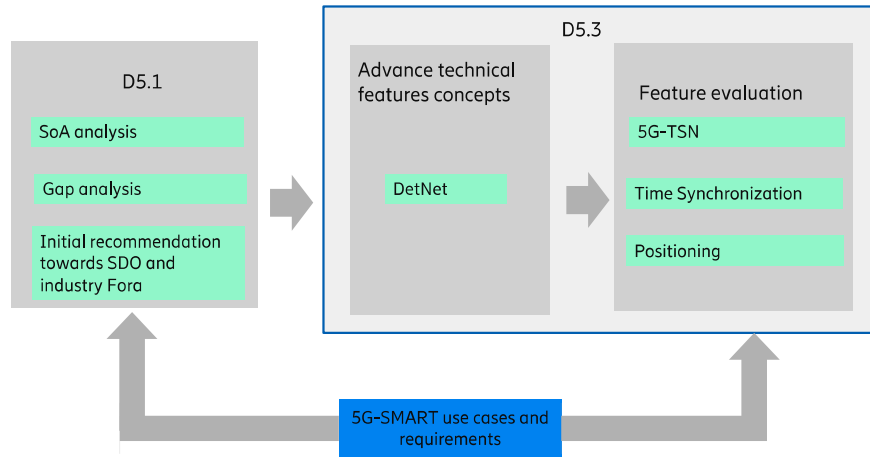


Figure 3: Structure of the document

The deliverable takes a further leap from D5.1 by identifying DetNet as a new set of advanced technical features relevant for smart manufacturing use cases. Section 2 provides details on DetNet and proposed 3GPP 5G-DetNet integrated architecture. Section 3 proposes a new scheduling mechanism for an integrated 5G-TSN network and further describes details on evaluation of the proposed mechanism, by considering industrial control to control communication use case requirements. Section 4 describes the investigation on how 5GS can support time synchronization with a tight time error budget of 900 ns in an integrated 5G-TSN network. Section 5 evaluates the performance of 5G-based positioning in a realistic industrial environment.



## 2 DetNet

As the need for a deterministic transport solution is increasing in a range of application areas including smart manufacturing, the IETF (Internet Engineering Task Force) is specifying deterministic networking (DetNet) standards to ensure the real-time operation with extremely low data loss rates and bounded latency within a network domain. DetNet operates at the Internet Protocol (IP) and Multiprotocol Label Switching (MPLS) layers of networks that are under a single administrative control or within a closed group of administrative control. For its operation (i.e., flow reservation), DetNet requires considerable information about system's resources, node capabilities and their states. Therefore, it is not intended for large groups of domains such as the Internet. There exists a close cooperation between the IETF DetNet Working Group (WG), specifying DetNet standards, and the IEEE (Institute of Electrical and Electronic Engineers) Time-Sensitive Networking (TSN) Task Group (TG) responsible for TSN extensions for the bridged Ethernet. Consequently, there are alignments between these standardization efforts and the incorporated functionality. For instance, the mapping between DetNet flows and TSN Streams, which is required for their interoperation, is specified in dedicated RFC documents. Such interoperation would enable use cases where the deterministic performance at Layer 3 is a pre-requisite to connect multiple TSN sub-networks or to tunnel TSN traffic over larger geographical areas. Furthermore, DetNet as a standard-based solution provides an alternative to proprietary, non-interoperable deterministic Ethernet-based network solutions. Among the magnitude of applications, DetNet can provide end-to-end QoS support for UDP/IP-based transport with OPC Unified Architecture (OPC UA) PubSub. Other applications might be within the industrial machine-to-machine (M2M) communication, discrete and process automation, building automation, and smart grid communication.

### 2.1 Standardized DetNet specifications

The IETF DetNet WG belongs to the Routing Area and focuses its efforts on deterministic data paths operating over Layer 2 (Ethernet) and Layer 3 (IP/MPLS) routed network segments. The determinism of DetNet paths is anchored to the latency, packet loss ratio, jitter, and reliability bounds. At the time of writing, DetNet has reached a technical level of maturity from the data plane standardization perspective, whereas the work on the control and management functionalities is still ongoing. DetNet has defined two data planes: (1) DetNet MPLS from RFC8964<sup>1</sup> and (2) DetNet IP from RFC8939<sup>2</sup>. The main set of standard documents (RFCs) has been endorsed and published, several more are already finalized and just awaiting the publication by the RFC editors, and only few documents are under ongoing development. The list is given below.

Finalised RFCs:

- RFC 8557 "Deterministic Networking Problem Statement", as of May 2019<sup>3</sup>
- RFC 8578 "Deterministic Networking Uses Cases", as of May 2019<sup>4</sup>
- RFC 8655 "Deterministic Networking Architecture", as of October 2019<sup>5</sup>

<sup>1</sup> <https://datatracker.ietf.org/doc/html/rfc8964>

<sup>2</sup> <https://datatracker.ietf.org/doc/html/rfc8939>

<sup>3</sup> <https://datatracker.ietf.org/doc/html/rfc8557>

<sup>4</sup> <https://datatracker.ietf.org/doc/html/rfc8578>

<sup>5</sup> <https://datatracker.ietf.org/doc/html/rfc8655>



- RFC 8938 "Deterministic Networking (DetNet) Data Plane Framework", as of November 2020<sup>6</sup>
- RFC 8939 "Deterministic Networking (DetNet) Data Plane: IP", as of November 2020<sup>7</sup>
- RFC 8964 "Deterministic Networking (DetNet) Data Plane: MPLS", as of January 2021<sup>8</sup>
- RFC 9016 "Flow and Service Information Model for Deterministic Networking (DetNet)", as of March 2021<sup>9</sup>
- RFC 9025 "Deterministic Networking (DetNet) Data Plane: MPLS over UDP/IP", as of April 2021<sup>10</sup>
- RFC 9023: "Deterministic Networking (DetNet) Data Plane: IP over IEEE 802.1 Time Sensitive Networking (TSN)", as of June 2021<sup>11</sup>
- RFC 9056: "Deterministic Networking (DetNet) Data Plane: IP over MPLS", as of October 2020<sup>12</sup>
- RFC 9037 "Deterministic Networking (DetNet) Data Plane: MPLS over IEEE 802.1 Time-Sensitive Networking (TSN) ", as of June 2021<sup>13</sup>
- RFC 9024 "Deterministic Networking (DetNet) Data Plane: IEEE 802.1 Time-Sensitive Networking over MPLS ", as of June 2021<sup>14</sup>
- RFC 9055: "Deterministic Networking (DetNet) Security Considerations", as of June 2021<sup>15</sup>, Currently, the IETF DetNet WG focuses on work items concerning Operations, Administrations and Maintenance (OAM), Controller Plane, and Packet Replication, Elimination, and Ordering Functions (PREOF) for IP data plane. Others are at the final stage. For instance, "DetNet Bounded Latency"<sup>16</sup> is waiting for publication and "Deterministic Networking (DetNet) YANG Model"<sup>17</sup> has passed the Yang validation.

### 2.1.1 DetNet architecture

The DetNet architecture is composed of three planes (Application, Controller, Network). To communicate between them, the southbound and northbound interfaces have been defined (shown in Figure 4).

1) (User) Application Plane, which incorporates a User Agent interacting with an end station and an operator to request DetNet services via an abstract Flow Management Entity (FME),

2) Controller Plane represents a set of entities that perform Control, Measurement, and other Management functionalities. The plane consists of "Controller Plane Function (CPF)" entities, representing a Path Computational Element (PCE), a Network Management Entity (NME), or a

<sup>6</sup> <https://datatracker.ietf.org/doc/html/rfc8938>

<sup>7</sup> <https://datatracker.ietf.org/doc/rfc8939/>

<sup>8</sup> <https://datatracker.ietf.org/doc/html/rfc8964>

<sup>9</sup> <https://datatracker.ietf.org/doc/rfc9016/>

<sup>10</sup> <https://datatracker.ietf.org/doc/html/rfc9025>

<sup>11</sup> <https://datatracker.ietf.org/doc/html/rfc9023>

<sup>12</sup> <https://datatracker.ietf.org/doc/draft-ietf-detnet-ip-over-mpls/>

<sup>13</sup> <https://datatracker.ietf.org/doc/rfc9037/>

<sup>14</sup> <https://datatracker.ietf.org/doc/rfc9024/>

<sup>15</sup> <https://datatracker.ietf.org/doc/rfc9055/>

<sup>16</sup> [draft-ietf-detnet-bounded-latency-07 - DetNet Bounded Latency](#)

<sup>17</sup> <https://datatracker.ietf.org/doc/html/draft-ietf-detnet-yang-11>

distributed control protocol. CPF is a core element of the controller and oversees the computing of deterministic paths. Specifically, one or more CPFs collaborate to implement requests from the FME in a way to respect the pre-flow constraints such as security and latency,

3) Network Plane collectively represents network devices and protocols. It includes the Data Plane and Operation Plane aspects. This plane comprises the Network Interfaces Cards (NICs) in end systems and DetNet nodes.

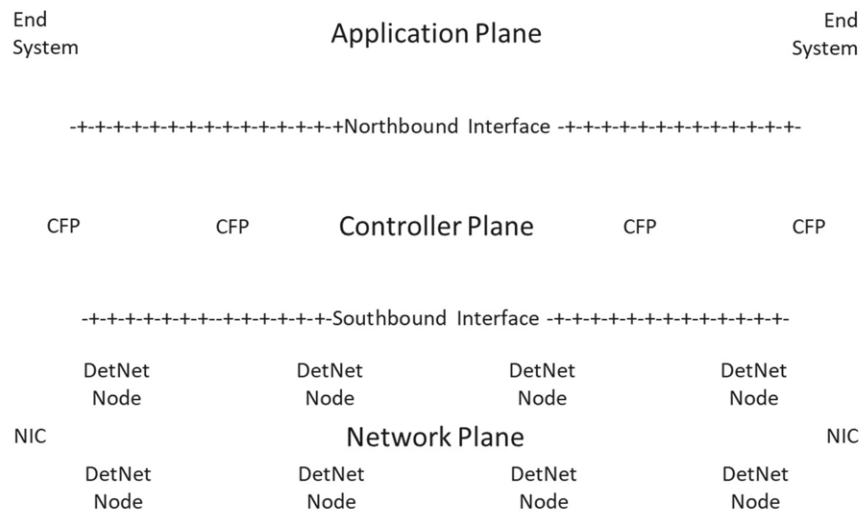


Figure 4 Northbound and Southbound Interfaces in the DetNet Architecture comprises of the Application, Controller and Network Planes [Section 4.4 of RFC 8655<sup>5</sup>]

These planes are separated by Northbound (Service) and Southbound (Network) Interfaces. A Northbound Interface enables the applications in the Application Plane to communicate with the entities in the Controller Plane, whereas a Southbound Interface enables the entities in the Controller Plane to communicate with devices in the Network Plane. For instance, DetNet nodes and NICs use the Southbound Interface to expose their capabilities and physical resources to CPFs and to keep CPFs updated about their dynamic perception of the network topology. In return, CPFs set up the per-flow paths between DetNet nodes after providing the Flow Characterization that is more tightly coupled to the DetNet node operation than a Traffic Specification. A Traffic Specification is a flow abstraction that is used to place a reservation over the Northbound Interface and within the Application Plane.

### 2.1.2 Data plane

The DetNet Architecture decomposes the DetNet related data plane functions into two sub-layers: a service sub-layer and a forwarding sub-layer (see Figure 5). The service sub-layer is used to provide DetNet service protection aiming to mitigate or eliminate packet loss due to equipment failures, including random media and/or memory faults. These types of packet loss can be greatly reduced by ensuring redundancy in the network and spreading the data over multiple disjoint forwarding paths. There are several service protection mechanisms. For instance,



- In-order delivery: a maximum number of packets delivered out-of-order is used as a constraint to limit the impact on the jitter of a flow and the amount of buffering needed at the destination node,
- PREOF includes the Packet Replication Function (PRF), Packet Elimination Function (PEF), and Packet Ordering Function (POF) for use in DetNet edge, relay node, and end-system packet processing. Together these functions ensure DetNet path redundancy, which tackles packet loss caused by device and link failures. The exact mechanisms used for these functions, as well as the order in which a DetNet node applies PEF, POF, and PRF to a DetNet flow, are left open for implementations,
- Packet encoding involves encoding the information in a packet belonging to a DetNet flow into multiple transmission units and combining information from multiple packets into any given transmission unit. It can be used to provide service protection against random media errors,

The forwarding sub-layer supports DetNet services in the underlying network by providing explicit routes and resource allocations to DetNet flows. It uses buffer resources for packet queuing, reservation, and allocation of bandwidth capacity in order to achieve a certain congestion protection (low loss, assured latency, and limited reordering).

- Explicit routes ensure a stable forwarding service and guarantee that DetNet service is not impacted when the network topology changes. A Path Computation Engine (PCE) is able to compute strict and loose paths able to meet the Service Level Agreement (SLA) requirements and assures resources from the network.
- Resource allocation protects DetNet flow from congestion. It is more than simple bandwidth allocation as it includes buffer allocation and queuing disciplines. The resource allocation can be guaranteed by a device configuration. The configuration defines if a particular flow is treated with or without discrimination by using an output port bandwidth reservation as an input to the queue management and the port scheduling algorithm. However, there should be a clear mapping maintained between a DetNet flow and its corresponding resources.

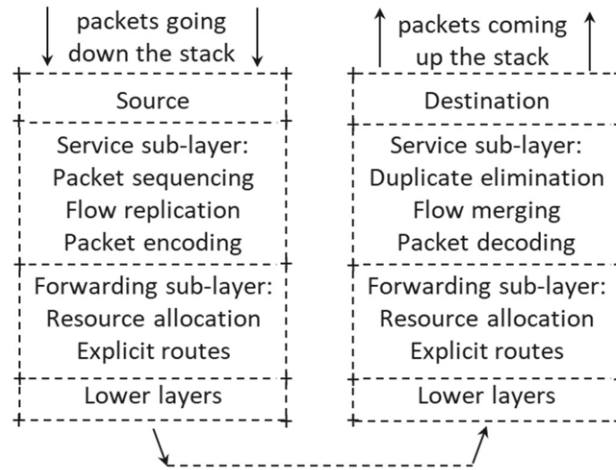


Figure 5 DetNet Data Plane Protocol Stack from RFC<sup>6</sup>

DetNet operates with flows providing them with an extremely low packet loss rates and assured maximum end-to-end delivery latency. There are two different types of flows, and it is important to distinguish between them:

- **App-flow** is a payload (data) carried over a DetNet flow between DetNet-unaware end systems. An App-flow does not contain any DetNet-related attributes and does not imply any specific requirement on DetNet nodes. App-flows can be Ethernet, MPLS, or IP flows. A source and a destination are used as App-flow reference points. One or more App/flows shall be aggregated in the DetNet flow using an N:1 mapping,
- **DetNet flow** includes one or more App-flows aggregated using an N:1 mapping. A flow is identified by the App-flow(s) specific encapsulation using e.g. MPLS labels or IP 6-tuples. DetNet flow starts at the DetNet (DN) Ingress where a networking technology-specific encapsulation may be added to the served App-flow(s) and it ends at the DN Egress where a networking technology-specific encapsulation may be removed here from the served App-flow(s). Consequently, DN Ingress and DN Egress are intermediate reference points for a served App-flow.

RFC 9016<sup>9</sup> uses the concept defined in the IEEE8021Qcc<sup>18</sup> to describe the flow information model. DetNet flows are described using DetNet flow-related parameters:

- *DnFlowID* – a unique management identifier;
- *DnPayloadType* – Ethernet, MPLS, or IP encapsulation;
- *DnFlowFormat* – MPLS or IP, which is set according to the DetNet Packet Switched Networking (PSN) technology;
- *DnFlowSpecification* – SLabel and FLabelStack for MPLS case; SourceIpAddress, DestinationIpAddress, IPv6FlowLabel, DSCP, Protocol, SourcePort, DestinationPort, IPSecSpi;
- *DnTrafficSpecification* – includes metrics such as Interval, MaxPacketsPerInterval, MinPacketsPerInterval, MaxPayloadSize, and MinPayloadSize. Note that these metrics are

<sup>18</sup> <https://1.ieee802.org/tsn/802-1qcc/>

used to allocate resources and adjust queue parameters in network nodes, i.e., specify how the DetNet Ingress transmits packets for the DetNet flow,

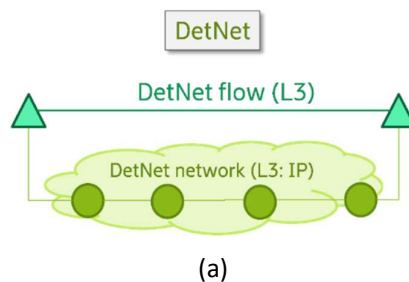
- *DnFlowEndpoints* – point to the ingress interface/node and egress interface(s)/node(s),
- *DnFlowRank* – flow rank 0 to 255 relative to other flows in the DetNet domain where "0" has the highest priority,
- *DnFlowStatus* – the status of the DetNet flow with respect to the establishment of the flow by the DetNet domain, it includes DnIngressStatus, DnEgressStatus, and FailureCode.

Additionally, DetNet flows have the following requirement attributes:

- *MinBandwidth* (in octets per second)
- *MaxLatency* (for a single packet from DN Ingress to DN Egress)
- *MaxLatencyVariation* (in nanoseconds)
- *MaxLoss* (the maximum Packet Loss Rate (PLR))
- *MaxConsecutiveLossTolerance*
- *MaxMisordering* (in some case the out-of-order delivery cannot be tolerated and thus in-order delivery is required, which is indicated by setting its value to 0)
- *DnFlowBiDir* attribute defining that the flow and the corresponding reverse direction flow must share the same path (links and nodes) through the routed or switch network in the DetNet domain.

There are three possible operations for each DetNet flow with respect to its DetNet service at a DN Ingress or a DN Egress: 1) join the flow, 2) leave the flow, and 3) modify the flow. The latter allows initiation of a change of flow specifications (e.g., to change a MaxPayloadSize) while leaving the current flow operating until the change is accepted. It is an advantage in cases when only slight flow changes are required.

DetNet flows offer a DetNet service over a certain network domain. For that, a data-plane solution for DetNet traffic must be created by selecting technology approaches for the DetNet service and forwarding sub-layers separately. There are many possible solutions, yet the fundamental difference is determined by the basic headers used by DetNet nodes. It can be a MPLS label or an IP header. In both cases, IP addresses are used to address DetNet nodes, but the choice impacts the both DetNet data sub-layers. For the service sub-layer, it impacts the basic forwarding logic. For the forwarding sub-layer, the mapping to the subnet technology interconnecting DetNet nodes needs to be performed accordingly. Figure 6 illustrates some of the possible DetNet scenarios.



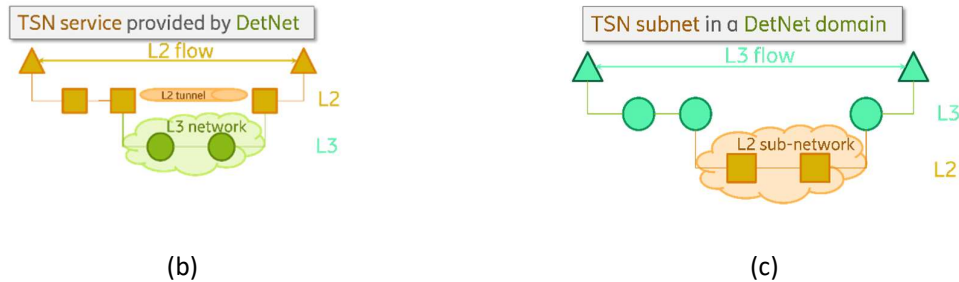


Figure 6 (a) DetNet-enabled IP network, (b) DetNet domain providing a TSN service, and (c) TSN subnet in a DetNet domain

In the first scenario, a DetNet IP network is shown (Figure 6 (a)). DetNet flows are transported over the IP domain using the 6-tuple information carried in IP-layer and higher-layer protocol headers. The 6-tuple is destination address, source address, IP protocol, source port, destination port, and Differentiated Services Code Point (DSCP). No DetNet-specific fields are added to support DetNet IP flows and thereby the end-to-end service protection cannot be provided at the DetNet layer. Instead, it can be provided on a per link and per sub-network basis, at least within the current specifications. However, the Packet Replication, Elimination and Ordering Function (PREOF) for DetNet IP has been recently proposed and described in the draft document<sup>19</sup>. The sub-network can represent a Time-Sensitive Networking (Ethernet, L2), MPLS network, or other network technology that can carry DetNet IP traffic. The first option is in focus for smart manufacturing scenarios.

Some TSN domain(s) may be initially confined to a certain deployment area like a particular machine or production station, e.g., with a focus on maintaining tight latency bounds among a set of local entities. Connecting services over larger distances, like a controller-to-controller use case, may need to extend beyond a confined TSN domain. DetNet enables to provide a service over such TSN domain boundaries, while using TSN transport services within the TSN sub-networks. Specifically, in the second scenario, a TSN Stream is “tunneled over a DetNet segment” and thereby extending the TSN service over a larger reach as illustrated in Figure 6 (b). This allows some devices to remotely become part of a TSN domain at another location. For this, some TSN devices are connected via a L2 VPN type of service provided by a DetNet domain to the remaining nodes of the TSN domain. The third scenario (Figure 6 (c)) leverages TSN as a subnet technology for a DetNet network. This can be relevant in large industrial installations, where e.g. multiple TSN domains are deployed locally and DetNet is used for communication between them. In both cases, the mapping between DetNet flows and TSN streams is required; and the procedure is drafted in RFC 9024 and RFC 9023/RFC 9037.

### 2.1.3 Controller plane

DetNet Controller Plane aggregates aspects traditionally associated with the Control and Management Planes separately. For instance, the Control Plane is responsible for the instantiation and maintenance of flows, allocation and distribution of flow-related information, and active in-band or out-of-band information distribution to support DetNet functions. The Management Plane statically provisions DetNet network nodes using appropriate Yang models and performs Operations, Administration and Maintenance (OAM) tasks, including e.g. active/passive performance monitoring as well as

<sup>19</sup> <https://datatracker.ietf.org/doc/draft-varga-detnet-ip-preof/>



connectivity and fault/defect management, to ensure DetNet performance and detect outages or other issues. Consequently, there are a number of requirements that DetNet Controller Plane must fulfil, especially if the automation of DetNet service provisioning and monitoring is the goal. The full list of requirements is specified in I-D document "Deterministic Networking (DetNet) Controller Plane Framework"<sup>20</sup>. However, here we just mention the most notable, for instance:

- Dynamic creation, modification (including (de-)aggregation), and deletion of DetNet flows. This requirement includes e.g., explicit path determination, link, link bandwidth, node buffer and other resource reservations, and specification of required queueing disciplines.
- Origination of flow instantiation requests from an end application, as a result of static provisioning, or from a centralized SDN controller or distributed signalling protocols.
- Support of queue control techniques, for instance, a credit-based shaper (IEEE 802.1Qav), time-gated queues governed by a rotating time schedule based on synchronized time (IEEE802.1Qbv), synchronized double (or triple) buffers (IEEE802.1Qbu), and Ethernet packet pre-emption (IEEE802.1Qbu and IEEE802.3br).
- Ability to advertise, to adjacent network nodes or network controller, static or dynamic node and link resources.
- Provisioning of flow identification information for each node in the path, since it may differ depending on its location in the network and its DetNet functionality.
- Monitoring of DetNet flow performance, continuity, and connectivity checks, testing and monitoring of PREOF (if applicable) in the DetNet domain.

Furthermore, the Controller Plane must ensure an operation in a converged network domain that contains both DetNet and non-DetNet flows. The presence of DetNet flows reduces the bandwidth available for non-DetNet flows. However, the Controller Plane is responsible for the prevention of so-called starvation of non-DetNet traffic. Finally, the Controller Plane must adopt to DetNet domain topology changes, e.g., link/node failures, additions, and removals.

Further, let us discuss possible DetNet Control Plane architectures. There are three possible classes:

1. Fully centralized SDN-like control plane,
2. Fully distributed control plane utilizing dynamic signalling protocols,
3. Combined (partly centralized and partly distributed) control plane.

In this report, we focus on the first option as we believe that one is more likely to be considered and implemented first. The standardization in IETF is more advanced for the fully centralized SDN-like control plane. Additionally, a fully centralized SDN-like controller model is generally considered more scalable compared to a fully distributed counterpart.

---

<sup>20</sup> <https://datatracker.ietf.org/doc/html/draft-ietf-detnet-controller-plane-framework>

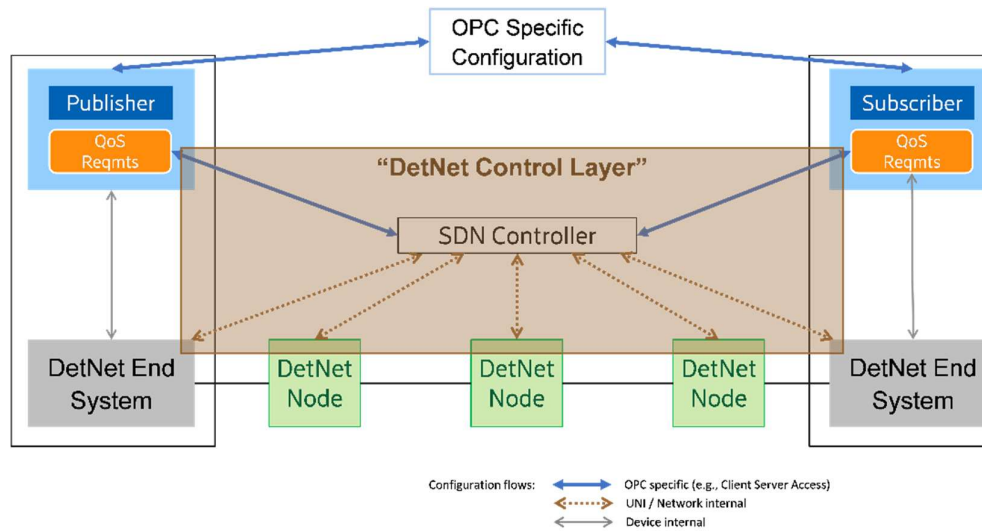


Figure 7 OPC UA and DetNet Configuration

In the case of a fully centralized configuration, flow information is transmitted from a Centralized User Configuration or applications via an Application Programmable Interface (API) or northbound interface to an SDN Controller as shown in Figure 7. The SDN Controller is the sole source of routing and forwarding information for the domain. It performs node configurations for DetNet flows relying on e.g., NETCONF protocol and Yang model. A draft document, containing the specification for the DetNet Yang model for configuration and operational data for DetNet flows, already exists: Deterministic Networking (DetNet) Yang Model<sup>21</sup>. However, extensions of protocols are required to incorporate DetNet-specific features and parameters. Besides, there exist additional issues worth bringing up. For instance:

- Explicit paths are required in DetNet to provide a stable forwarding service and guarantee that DetNet services are not impacted due to changes in the network topology. These paths need to meet strict Service Level Agreement (SLA) requirements and traffic specifications imposed directly and indirectly from the application. Such paths can be computed by a Path Computation Engine (PCE) in the Controller using the network information collected from the DetNet domain. However, loose explicit paths also can be acceptable for DetNet service assuming that the beforehand calculated path is able to meet the SLA requirements,
- Resource reservations is not a straightforward bandwidth allocation since it may also require the allocation of buffer size and required queuing disciplines during the flow forwarding stages. Furthermore, the allocated resources must be sufficient to execute the DetNet service sub-layer functions such as the PREOF,
- To avoid packet loss, DetNet service protection is supported via the PREOF. Consequently, PREOF requires the ability to compute and establish a set of multiple paths between the point(s) of packet replication, packet elimination and ordering. The mapping of DetNet member flows to explicit path segments must be ensured. Yet, these features may require the protocol extensions,

<sup>21</sup> <https://datatracker.ietf.org/doc/html/draft-ietf-detnet-yang-11>



- PREOF provides some challenges for DetNet IP data plane, as RFC 8939 does not provide a solution for mapping of sequence information. Adding sequencing information is under discussion<sup>22</sup>.

Additionally, other issues and gaps might emerge on later stages.

#### 2.1.4 DetNet features for 5G-SMART use cases

This section provides a brief overview of the DetNet inbuilt capabilities that makes it suitable for smart manufacturing use case.

##### *Applicability over existing Ethernet standard*

The standardization is the key enabler for an ecosystem where component/device vendors can create interoperable products promoting the competition among vendors and better cost performance. The standards-based networks provide an alternative to many proprietary, non-interoperable deterministic Ethernet-based network solutions. However, DetNet should not be perceived as a new kind of networks as it is based on extensions to existing Ethernet standards, e.g., IEEE 802.1 TSN, to provide the deterministic performance at Layer 3. That may lead to use cases allowing DetNet to interconnect two or more TSN LAN islands using a standardized router operating with DetNet-specified data flows.

##### *Coexistence of deterministic and best-effort traffic*

DetNet aims at ensuring the fair coexistence of time-sensitive traffic and non-time-sensitive, so-called best-effort, traffic in the same unified network. In addition, DetNet flows can be used to support the hard separation of various users' deterministic performances. For instance, DetNet flows can be strictly isolated and/or provided with the explicit paths offering a particular user with bandwidth, latency and reliability guarantees that cannot be impaired by other users' traffic (placed in other DetNet flows). Furthermore, the bandwidth reserved for a DetNet flow but not used by its owner is made available for best-effort traffic until the owner resumes transmission, i.e., usage of the reserved bandwidth. Note that such temporarily available bandwidth cannot be relocated to other DetNet flows as they must have own reservations.

##### *Scalable size and wide range of timing parameters*

DetNet networks can cover a very small area (e.g., inside a single industrial machine) or span over a large territory involving many hops over radio, microwave or fiber-optic links. In any case, a DetNet network must be centrally administered and therefore DetNet solutions are not intended for unbounded decentralized networks such as the Internet. They are left outside the DetNet scope. In addition to a geographical size, DetNet networks can be small/large in terms of number of flows. Moreover, the number of flows in a given DetNet network can be very different and can grow faster than the number of nodes and hops in the path. So, DetNet shall ensure the scalability of number of flows to satisfy requirements for any given application. Furthermore, each DetNet flow can be configured to assure very different traffic requirements (the worst-case maximum/minimum latency, maximum packet loss, etc.). For instance, "low latency" and "maximum packet loss rate" may imply very different parameter bounds depending on the application. Consequently, the mechanisms for

<sup>22</sup> <https://datatracker.ietf.org/doc/draft-varga-detnet-ip-preof/>



specifying DetNet flow parameters (e.g., MaxLatency, MaxLoss) include wide ranges and, from architecture point of view, there is nothing that could prevent arbitrarily high/low requirements from being implemented in a given network.

*High reliability, availability and quality assurance.*

Mechanisms embedded in DetNet (such as PREOF, explicit paths) are expected to ensure arbitrarily high availability, e.g., 99.9999% (so called, “six nines”) uptime or up to 12 nines<sup>4</sup>. Yet, DetNet itself does not make any assumptions about a level of reliability and availability that may be requested by a service; instead, it defines parameters for communicating the corresponding requirements within the network. Besides, DetNet flows are isolated from each other and from the best-effort traffic, so that even if the network is saturated with traffic, the configured DetNet flows are not adversely affected, and the starvation of the best-effort traffic is avoided. The DetNet controller ensures that, by accepting the flow only if the requested service level can be met (as opposed to accepting the flows but then not delivering the requested service), and by terminating the flow that starts misbehaving. Furthermore, DetNet flows are expected to be protected against devices failure, deliberate attacks, misbehaving devices, etc., which together with the previous properties contribute to high determinism.

## 2.2 5G support for DetNet

5G networks continue to reinforce their positions for critical industrial applications for which low guaranteed latency and extremely low packet loss are of importance. The 3GPP Release 16 has standardized specifications (see Sections 5.27 and 5.28 in TS 23.501 [3GPP20-TS23501]) enabling to integrate the 5G network into a TSN network. For instance, 5GS may act as a logical bridge for TSN. Therefore, Release 16 of the specifications enables only Ethernet (Layer 2) based use cases. In other words, 3GPP Release 16 only supports time-sensitive networking (TSN) operating on Layer 2 (Ethernet), while with Release 17 the 3GPP extends the 5G capabilities by introducing general mechanisms to support time-sensitive communications (TSC) that enable IP and Ethernet which can be non-TSN based use cases. Specifically, it includes the exposure functionality, allowing external applications (i.e., application functions (AFs) from a trusted domain or a 3<sup>rd</sup> party) to request time synchronization services and deterministic QoS from the 5G network. However, many applications may require/prefer IP-based TSC solutions with deterministic QoS as adding the native Ethernet support may be costly and thereby prohibitive for most deployments. Consequently, the 5G support of a TSN-like solution but operating in the IP network domain is required. However, the existing exposure procedure for IP applications in the 3GPP Rel-17 is not aligned with the DetNet framework. Specifically, there is no central controller (such as the TSN AF for the Ethernet) for the IP network domain, and AFs directly communicate their request to the 3GPP network. Such approach excludes the possibility for a central controller to map and manage resources in the network domain, which in general case may also include non-3GPP IP nodes or links. Consequently, the Rel-17 approach has poor scalability and is suitable for small-size deployments where all IP user plane nodes belong to the 3GPP network or when non-3GPP network nodes are limited.



### *3GPP efforts toward DetNet integration*

To enable the 3GPP support for DetNet, a new study item description (SID)<sup>23</sup> has been proposed for Rel-18 focusing on the extension of the TSC framework. Its scope is limited and includes only IP-based DetNet considerations. Other aspects, such as an MPLS-based DetNet solution, handling the multicast DetNet communications, and the support for the edge DetNet node functions, are kept out of scope. Furthermore, a fully centralized DetNet configuration with a Centralized Network Configuration (CNC)-like entity, performing routing and forwarding tasks, is considered. In such the configuration, an entity that performs mapping between the IETF specified DetNet network and the 3GPP specified network is required in order for 5GS to act as a logical DetNet IP router. The same approach as for the IEEE TSN is reused and a DetNet AF is defined to provide mapping between the central DetNet controller entity and the 5GS (see Figure 8). The mapping involves translation of DetNet traffic profile and flow specification to 5GS QoS parameters and TSCAI. DetNet, similarly as TSN, solely operates and is concerned about the worst-case values for the end-to-end latency, packet delay variation, and out-of-order packet delivery. Average, mean, or typical parameter values are not considered to be significant as they do not characterize the ability of a real-time system to perform its tasks. For instance, a priority-based queuing scheme may ensure a better average latency to a data flow than DetNet, yet it may not be a suitable option for services with deterministic QoS requirements due to its worst-case latency.

#### **2.2.1 Proposed 5G-DetNet architecture**

Figure 8 illustrates the proposed 5G-DetNet architecture which is described in the work item description (WID) and submitted to the 3GPP Service and System Aspects (SA) WG2. In the proposed configuration, the DetNet AF interfaces a DetNet controller and represents the 3GPP network part. A fully centralized SDN-type DetNet controller is assumed in this scenario. Thereby, the DetNet controller controls DetNet flows in a certain DetNet domain and interworks with the DetNet AF. Normally, the DetNet AF is considered trusted and thus directly interacts with the PCF. However, it's possible that the DetNet AF is not considered to be trusted, in case it belongs to a 3<sup>rd</sup> party, and thus requires a Network Exposure Function (NEF) for authorization and communication with the PCF (not shown in Figure 8).

---

<sup>23</sup> [https://www.3gpp.org/ftp/tsg\\_sa/WG2\\_Arch/TSGS2\\_146E\\_Electronic\\_2021-08/INBOX/Revisions/S2-2105500r01.zip](https://www.3gpp.org/ftp/tsg_sa/WG2_Arch/TSGS2_146E_Electronic_2021-08/INBOX/Revisions/S2-2105500r01.zip)

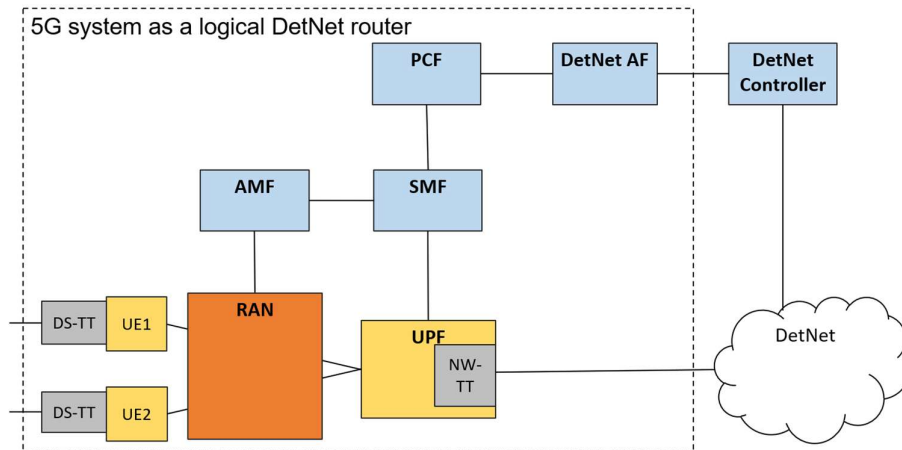


Figure 8 System architecture view with 5GS appearing as a logical DetNet IP router, where DS-TT—device-side TSN translator, UE—user equipment, RAN—Radio Access Network, AMF—Access and Management Function, SMF—Session Management Function, PCF—Policy Control Function

#### Envisioned DetNet AF functionalities:

- Collect the control and management information (including the network topology and routing paths) from the 5GS. The collection procedure may rely on the control signalling using, e.g., the Port Management Information Container (PMIC) and User Plane Node Information Container (UMIC) mechanisms and the containers content. The information may include IP addresses assigned to UEs over the individual PDU sessions and information about neighbours that are reachable over N6 and N19 interfaces. The latter may be obtained using a neighbour discovery protocol, e.g., an interior gateway protocol (IGP) that runs over that interface. The information may be delivered to the DetNet AF from the UPF or UEs side. In the first case, the NW-TT provides the information and the UPF send it via the SMF and PCF to the DetNet AF within the UMIC or PMIC. In the second case, the DS-TT provides the IP addresses and signals them from the UEs side. Alternatively, this information may be pre-configured in the DetNet AF,
- Receive an explicit route request from the DetNet controller, convert the received configuration information to 3GPP domain, and determine whether the explicit route request conflicts with the 3GPP systems topology and routing information,
- Accept/reject the explicit flow routing information depending on its alignment with the current routing in the 5GS or update, when applicable, the routing within the 5GS.
- Respond to the DetNet Controller and provide the necessary information so that it has the complete knowledge of the DetNet network and thereby can set up DetNet flows with the targeted QoS requirements,
- Store the explicit route information provided by the DetNet Controller, including the flow and interface specifications, so that information can be used to determine a PDU session associated with a given flow.



## 2.3 Summary

The IETF is specifying DetNet standards intended to provide a deterministic transport solution over Layer 3 (IP/MPLS) routed networks. DetNet ensures time-sensitive features that guarantee extremely low packet loss rates, bounded latency, and high reliability (including in-order packet delivery). Hence, DetNet has similar features as the IEEE-standardized TSN, which operates at Layer 2 via Ethernet frames and whose integration with 5G is supported starting from 3GPP Release 16 and 17. Meanwhile, DetNet has reached a technical level of maturity from the data plane standardization perspective, however, control and management functionalities are still incomplete; the work is ongoing in the IETF. Nonetheless, there is a study item proposal for 3GPP Release 18 on the extension of the TSC framework to support DetNet. At the time of writing, the study item description (SID) discussion is still ongoing, and decisions about new Release 18 SIDs have not been made. Yet, companies' interest and support for DetNet are undeniable.

## 3 5G-TSN Evaluations

### 3.1 Introduction

The IEEE 802.1 Time-Sensitive Networking (TSN) is foreseen to bring unification and convergence to the industrial Ethernet domain. TSN comprises a set of standards that can enable different mechanisms such as synchronization, redundant transmission, or traffic shaping depending on the application requirements. This high level of configurability provides the potential for TSN to find widespread application in different areas. Especially in the future factory environment, where flexibility and customization play an increasingly important role, TSN is expected to act as the convergence layer between different technologies to enable a holistic communication system. The extension of TSN with wireless capabilities has been an ongoing topic, where 5G is seen as a promising solution to achieve seamless integration and widespread application. The integration of 5G into a TSN network is standardized in the 3GPP starting with Release 16 [3GPP20-TS23501].

The standard describes the integration of 5G as a logical TSN bridge. The seamless interoperation is achieved by introducing user and control plane translator functions to support TSN. The state-of-the-art has been described in a previous 5G-SMART deliverable, D5.1 [5GS20-D51] with focus on QoS mapping between 5G and TSN, including potential 5G reliability enhancements to support the stringent TSN requirements. The gap analysis performed in the work revealed that a closer investigation of end-to-end stream configuration is necessary to make the 5G-TSN integration efficiently applicable.

The aim of the following evaluation is to provide an overview of the scheduling procedures in an end-to-end integrated 5G and TSN network based on the current standard. We then investigate current limitations and indicate potential enhancements to improve the end-to-end schedule generation process. The evaluation of the presented end-to-end scheduling mechanism has been performed on a 5G-SMART use case involving control-to-control (C2C) communication with its stringent requirements [5GS20-D11].

#### 3.1.1 C2C use case description

In manufacturing plants, processes and tasks are usually planned in advance by supervisory instances such as the Manufacturing Execution System (MES). Typically, pre-planning is also used for the



communication networks, where an end-to-end configuration and scheduling takes place before production is executed. One example of such an industrial use case, namely, TSN/Industrial LAN over 5G, targeting control-to-control applications is considered in the Reutlingen factory trial of the 5G-SMART project. A detailed description of that use case can be found in 5G-SMART Deliverable D1.1 [5GS20-D11].

Table 1: C2C use case from D1.1 [5GS20-D11]

Communication	Periodicity	Determinism	Symmetry	Transfer interval [ms]	Data length [Byte]
C2C traffic	Periodic	Deterministic	Symmetrical	[4-10]	In the order of 500

Performance requirement metric	Value
Data rate [Mbit/s]	$r_{DL} : [0.4 - 1] \quad r_{UL} : < [0.4 - 1]$
Latency [ms]	$< \text{transfer\_interval}$
Jitter [ms]	$< 0.5 \times \text{transfer\_interval}$
Communication area [m $\times$ m]	a typical factory area (100 $\times$ 100)
Communication density [device/m <sup>2</sup> ]	$< 10$
Transmission reliability [%]	$\geq 99.999$
Velocity [m/s]	Not relevant

This kind of control-to-control applications usually comprise some sort of control task, e.g. motion control commands with safety critical properties, for which the timely exchange of control information between different controllers is of paramount importance in order to achieve high performance guarantees. The main KPIs for this application type are summarized in Table 1.

From the requirements it becomes apparent that careful resource planning and network configuration is mandatory to meet all KPIs. C2C traffic requires low jitter, bounded latency, and high reliability to consistently maintain the communication cycles with transfer intervals in the lower millisecond region. The fact that mobility is not considered, and traffic characteristic are deterministic, meaning the timing of transmissions and packet sizes are known in advance, makes this use case suitable for the integrated 5G and TSN network. TSN supports the usage of ‘scheduled traffic’, where resources are configured in advance via egress port shaping rules, as detailed in the following.

### 3.2 TSN scheduling process for 5GS bridges

To support scheduled traffic over a network including 5GS bridges, the centralized configuration model must be used as shown in Figure 9. The centralized user and network configuration instances

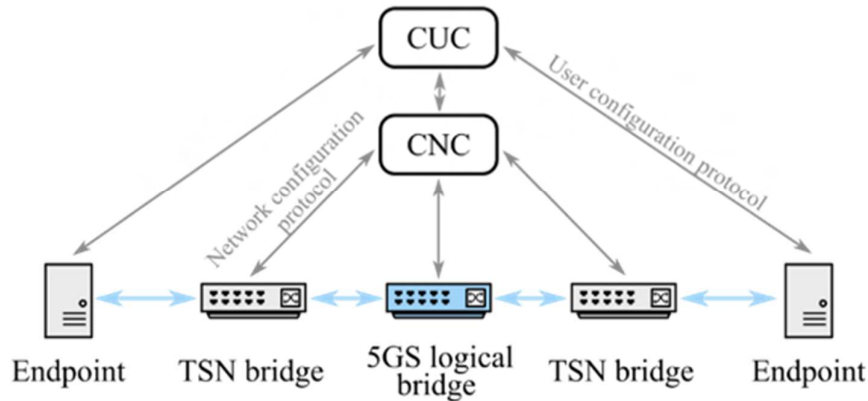


Figure 9: Centralized Configuration Model for TSN

(CUC and CNC, respectively) collect information about the network and streams, and remotely configure each bridge and endpoint.

The 3GPP standard [3GPP20-TS23501] describes the necessary measures to let the 5G network participate in the TSN network as a logical bridge. The 5GS supports TSN translator functions on the user plane and a TSN application function (TSN AF) on the control plane to provide the necessary interfaces towards the external network. Furthermore, the standard describes several internal procedures and enhancements to support time-sensitive communication. This includes, for example, the time-sensitive communication assistance information (TSCAI) and 5G QoS Identifier (5QI), which provide relevant information about the streams to support e.g., the 5G RAN. It can then allocate a Data Radio Bearer (DRB) with periodicity, packet delay budget (PDB), packet error rate (PER) and maximum data burst volume (MDBV) attributes suitable for a specific data stream relayed through a 5GS. A detailed overview of the integration model is given in [5GS20-D51], while the bridge configuration process is described in [5GS20-D52].

In this report, the focus is on the initial schedule calculation process, which takes place in the CNC. Another relevant aspect of the CNC is the admission of new TSN streams and subsequent re-calculation of the schedule. To speed up this process, heuristics can often be used to adjust the initial schedule, which is however not in the scope of this work. While the scheduling itself is not standardized and is up to the implementation, the input and output parameters of the scheduling process are defined in the standard. Hence the possibilities to optimize the end-to-end schedule is limited by the available parameter exposed by the network to the CNC. Simplified, the scheduling process consists of three basic steps. Initially, endpoints and bridges provide input parameters. TSN endpoints provide their capabilities to the CUC, while the Talkers additionally provide the stream/application requirements to the CUC. The CUC communicates with the CNC to provide user requirements on a per Stream ID basis. TSN bridges forward their capabilities to the CNC directly.

1. Based on the input parameters, the CNC determines a suitable schedule that maintains all requirements of all concurrent streams,
2. The schedule is then translated to a TSN configuration which includes scheduling and policing information e.g., the Gate Control Lists (GCL) and Per-Stream Filtering and Policing (PSFP). The configuration is then forwarded and applied to all endpoints and bridges.

The information exchange of this process is depicted in Figure 10. Since the integration of 5G is described as a black-box model, the CNC has no knowledge about the existence of a wireless network. The 3GPP specification TS 23.501 [3GPP20-TS23501] only describes functionalities to let the 5G system behave like a TSN bridge by providing the bridge capability exposure to the CNC, as also shown in Figure 10. The scheduling itself is hence limited by the parameters supported in the current IEEE 802.1Q standard [IEEE18-8021Q]. The TSN AF is responsible to determine and expose this input to the CNC.

Using the capabilities of all bridges in the network and application requirements as input, the CNC determines a suitable schedule. The CNC issues the TSN bridge configurations, which is then interpreted in the 5G system. This includes a mapping of the TSN traffic class to a suitable internal 5QI, and the provisioning of the TSCAI and 5QI to the gNB for allocation of DRB resources suitable for the radio interface portion of a QoS flow supported between the ingress and egress points of the 5GS bridge.

The available input and output parameters in the scheduling process are described in the following section. Note that only selected parameters relevant for the scheduling process itself are listed. An exhaustive parameter list of the managed bridge objects is provided in the IEEE 802.1Q standard [IEEE18-8021Q] and its amendments, most importantly in P802.1Qcc [IEEE18-8021QCC].

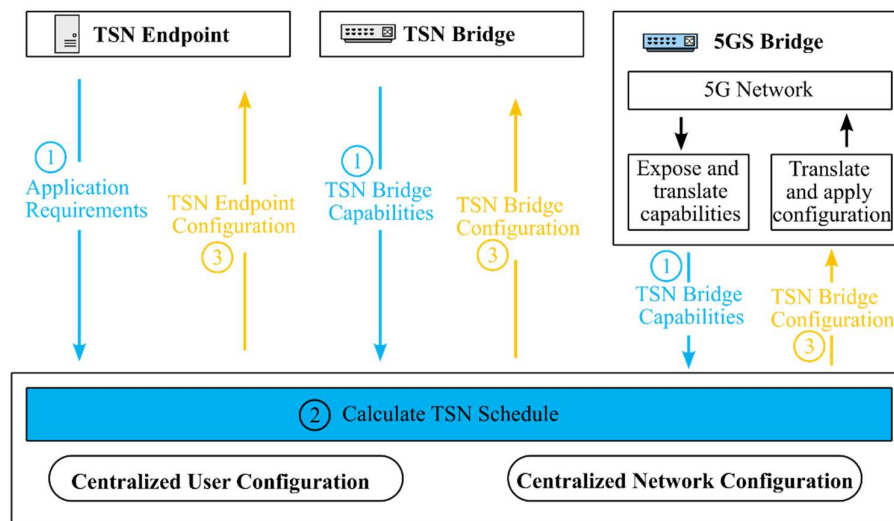


Figure 10: TSN Schedule determination process

### 3.2.1 Scheduling input parameters

Each bridge in the network exposes characteristics/capabilities to the CNC, such that the CNC can determine a feasible scheduling configuration based on the application requirements.

Table 2 TSN bridge parameters exposed to CNC



 <b>TSN Bridge</b> parameters exposed to CNC relevant for scheduling as defined in IEEE 802.1Qcc		
Propagation Delay	Bridge Delay	Stream Parameter Table
txPropagationDelay	IndependentDelayMin	MaxStreamFilterInstances
	IndependentDelayMax	MaxStreamGateInstances
	DependentDelayMin	MaxFlowMeterInstances
	DependentDelayMax	SupportedListMax

Table 2 shows the parameters that being exposed by TSN bridge towards CNC. The bridge delay is defined as the delay of a frame as it is relayed through the bridge (i.e., from bridge ingress to egress). The delay consists of a value that is independent and a value that is dependent on the frame length. The delay is given as the best and worst-case per design without any scheduling or queuing delay. It is the task of the CNC scheduler to determine the impact of transmission selection. The propagation delay is defined as the time a frame travels after exiting an egress port of one station and entering the ingress port of a neighbouring station.

The stream-specific parameters represent the PSFP capabilities of the bridge, i.e. how many different streams a bridge can distinguish, if PSFP is supported. This represents an important information to the schedule computation software to determine the supported streams and control list capacity prior to computation.

Additionally, to the bridge capabilities, stream requirements are provided by the TSN Talker endpoint to the scheduler over the CUC (shown in Table 3).

Table 3: Stream Requirements by a TSN Talker

 <b>TSN Talker</b> parameters exposed to CUC relevant for scheduling as defined in IEEE 802.1Qcc	
Traffic Specification	User to Network Requirements
Interval	NumSeamlessTrees
MaxFramesPerInterval	MaxLatency
MaxFrameSize	
TransmissionSelection	
EarliestTransmitOffset	
LatestTransmitOffset	
Jitter	

Again, the list is limited to the relevant parameters for the schedule computation process. Note that this list of traffic parameters is not compulsory by the standard for the centralized configuration

model. When using a CUC, the operation and exchange protocols are up to implementation. Nonetheless, the values fully specify the scheduled traffic properties and can hence be used for the centralized model, as also mentioned in IEEE 802.1Q Annex U [IEEE18-8021Q].

The C2C use case introduced initially can be directly translated into such a TSN Talker object. It specifies the requirements regarding transfer interval, latency, and jitter and packet size. The transmission offset parameters define the time frame within which the application can send out its frame respective to its interval cycle. After the schedule has been determined, the CUC will then feedback the exact time point within the tolerable offset range at which the application should sent out its frame. The parameter *NumSeamlessTrees* defines the number of independent transmission paths required by the application if multiple transmission paths as defined in IEEE 802.1CB are to be applied.

### 3.2.2 The schedule computation

Based on the input parameters described in the previous section, the CNC determines the TSN schedule. The common approach to formulate and solve such a scheduling task is depicted in Figure 11. In the first step, the system model based on the network topology and properties provided as input to the scheduler is established. Based on this model and the stream requirements, a scheduling problem can be formulated which usually consists of decision variables and several constraints. The decision variables describe the scheduling choices, i.e. the assignment of frames to transmission resources. The constraints limit the scheduling choices to the bridge capabilities and stream requirements, hence defining a feasible solution space (if one exists). The task of the solver is to find a set of decision variables such that all constraints are satisfied. Such a schedule is said to be feasible. To find a good – or even the best possible – solution, the user can define objective functions. These can be single or multi-objective functions that represent usually cost function which the solver aims to minimize, e.g. the latency. Different approaches to formulate and solve such a problem exist, e.g. constraint programming (CP), satisfiability modulo theories (SMT) or (mixed-)integer linear programming ((M)ILP). A common issue with such optimization problems is the scalability. With increasing number of streams and complex network models, the number of decision variables and, hence, the solution space increases rapidly, resulting in very long computation times. Heuristics play an important role to control the complexity and find trade-offs to the optimality of the solution.

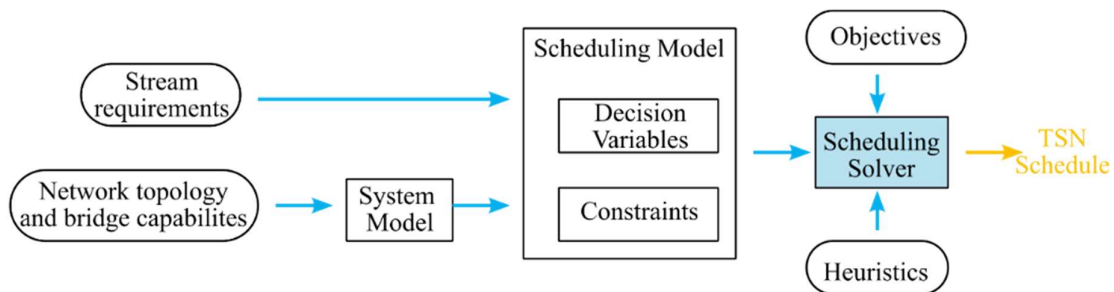



Figure 11: Solving the TSN scheduling problem

### 3.2.3 Scheduling output parameters

After successful determination of a schedule, the CNC provides the bridge configuration to the respective TSN bridges. The relevant configuration parameters derived directly from the schedule are shown exemplary in Table 4: TSN Bridge Configuration example

Table 4: TSN Bridge Configuration example

 <b>TSN Bridge</b> configuration parameters determined by scheduling as defined in IEEE 802.1Q standard		
Traffic Class Table	Gate Parameter Table	Stream Gate Instance Table
	GateEnabled	PSFPGateEnabled
	AdminBaseTime	PSFPAdminBaseTime
	AdminControlList	PSFPAdminControlList
	AdminControlListLength	PSFPAdminControlListLength
	AdminCycleTime	PSFPAdminCycleTime

The schedule output determines the priority of each traffic class via the Traffic Class Table object. The scheduled bridge operation as described in IEEE802.1Q is defined on a traffic class granularity. The Gate Parameter Table fully determines the egress shaping at each port of the bridge. The *AdminControlList* specifies the opening and closing times of gates for traffic classes relative to a known time scale, which is repeated after *AdminCycleTime*. In addition to traffic scheduling at the egress port, per-stream filtering can be performed at the ingress of the bridge to better control multiple streams belonging to the same traffic class and hence same priority. This per-stream operation can be optionally provided with the Stream Gate Instance Table.

In the 5GS bridge, the scheduling output is again translated and applied internally in the 5G system (c.f. Figure 10). The Gate Parameter Table is applied to the egress ports of the logical bridge. 5G supports a hold and forward buffer to achieve deterministic behaviour and maintain the predefined schedule in the presence of jitter introduced e.g. by the 5G system. The stream-based information from the Stream Gate Instance Table can be leveraged in the 5G system to provide QoS information on a stream basis. This allows e.g. to distinguish different TSN streams of the same traffic class that are multiplexed to the same QoS flow and hence potentially enable more efficient radio scheduling. Based on bridge configuration provided by the CNC, the TSN AF initiates a mapping of the TSN traffic class to a suitable internal 5QI and provides the TSCAI and 5QI to the gNB for allocation of a suitable DRB resource. TSCAI includes the flow direction, periodicity, burst arrival time, and survival time of the stream whereas 5QI identifies critical flow attributes such as PDB, PER and MDBV. The periodicity can be directly determined from the *PSFPAdminCycleTime* and the burst arrival time from the *PSFPControlList*. It is then up to the 5GS bridge internal processing to reserve necessary DRB resources for this stream, e.g. via persistent scheduling methods.

### 3.3 Evaluation of the TSN scheduling process for 5GS bridges

The integration of 5G into TSN as a black box has many advantages, most importantly the simple integration for the end-user and hence a potentially high level of acceptance. TSN acts as a convergence layer that hides the complex procedures in a 5G network. The scheduler has no



possibilities to distinguish the 5GS bridge from a regular TSN bridge. However, the wireless 5GS bridge behaves quite different compared to a standard wired TSN bridge. Such a simplification could potentially result in inefficient resource usage.

In this section, we evaluate possible effects of introducing additional input parameters to the 5GS bridge and additional exposures from the 5GS bridge to improve the end-to-end configuration of the network. One possibility to assist the 5GS internal stream handling to better match the requirements of the TSN streams is to bring application requirements closer to the network to maintain their QoS. An approach in this direction has been already made with the introduction of the survival time into the TSCAI [3GPP20-TS23501]. The survival time can be optionally used to inform the 5G RAN about a stream's tolerances to consecutive packet losses such that it can adjust its internal prioritization to avoid an application failure due to excessive packet drops. Even within a fixed TSN schedule, the underlying 5G system can adapt e.g. redundancy or robustness of the applied coding scheme if the risk of exceeding the survival time reaches a certain threshold. However, it is not clear how this value can be provided to the 5GS bridge. It cannot be task of the CNC as it only forwards bridge configuration that reflects the application requirements of the stream and is not foreseen to directly transport stream requirements to the bridges. This type of parameter must hence be provided by the application layer, e.g. by some engineering tool of the application.

Another possibility to achieve a better integration is to extend wireless exposures over the TSN domain, as shown in the following sections.

### 3.3.1 Impact of wireless channel on 5GS bridge performance

Wireless and wired systems are inherently different on the physical layer, which is observable from the different performance each system can deliver. While wired systems are very reliable and consistent in terms of packet errors and achievable data rate, this is not the case for wireless systems. Channel variation caused by fading and shadowing due to dynamic environments, mobility and multipath propagation result in a comparably higher packet error rate and varying throughput.

Assigning a periodic schedule, as required by C2C applications, to a wired bridged network is straight forward. A bridge usually operates at a constant data rate, allowing to compute schedules in advance (if overall traffic demand is known a-priori) and achieve deterministic behaviour during operation. A TSN schedule will remain feasible as long as the applications behaves as intended. In a 5GS bridge, however, the achievable rate for a given amount of transmission resources depends on the current channel condition. There is hence a risk that a schedule could become infeasible if the 5GS cannot provide enough resources in a timely manner to all services (e.g., due to inherent differences between the time base used by applications relative to the time base used for scheduling 5GS radio resources).

There are two options to tackle this problem. First, for each port pair and each stream in a 5GS bridge, the assigned time slots and resources must be overprovisioned to account for the worst-case channel conditions, such that there are always sufficient reserved resources to deliver the QoS guarantees. Second, the CNC must perform a re-scheduling to maintain a feasible bridge configuration. Re-scheduling of radio resources can be done in real-time but such an event must be recognized early enough, thereby representing an increased complexity in resource management and a likely reduction in radio resource utilization efficiency.

Furthermore, the spatial dimension of the bridges has to be taken into consideration when comparing TSN and the 5GS bridges. While the TSN bridge performs switching within a few centimetres of the physical device, the logical 5GS bridge can switch ports that are around 100 meters apart. In an industrial setup, where e.g. a centralized virtual controller on an edge server and the corresponding field device can be very far apart, the endpoints could still connect over a single 5GS bridge. In a wired TSN scenario, on the other hand, multiple bridges and hops are likely required to cover greater distances, which in turn increases the solution space of the scheduling problem and hence its complexity.

The difference in switching performance and resulting effect on the scheduling for a wired TSN bridge compared to a 5GS bridge are indicated in Figure 12 and Figure 13, respectively. In a TSN bridge, independent paths  $p_1$  and  $p_2$  between different port pairs can achieve independently their maximum achievable rate  $r_{\max}$  through the switching fabric. The achievable rate per path is constant and can be scheduled independently by the CNC. (Note: switching fabric of wired bridges is usually ideal (non-blocking).)

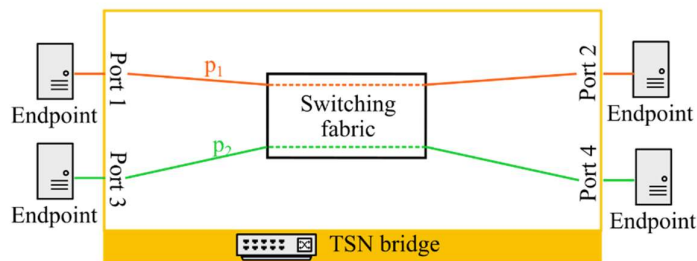


Figure 12: Independent transmission paths in a TSN bridge

The 5GS logical bridge however is exposed to physical effects such as fading, shadowing and multipath propagation. Although the considered use case considers no mobility (c.f.), a high variability is nonetheless possible. Operation in factory environments is known to be harsh due to high degree of mobility in the environment itself, and densely deployed machines and production goods with reflective surfaces. Without mitigation efforts, these effects can be noticeable on the higher layers in form of performance degradation and overall, a lower reliability. The 5GS applies adaptive modulation and coding (AMC) by choosing a suitable modulation and coding scheme (MCS) to maintain a trade-off between reliability and throughput according to a predefined target error rate. In order to provide a constant target throughput level for the TSN streams, the 5GS can adjust the resources provided to a guaranteed service. In Figure 12 the data radio bearer (DRB) assignment over time is schematically shown for two transmission paths  $p_1$  and  $p_2$  over independent port pairs. Unlike in the TSN bridge, the port pairs cannot be seen as independent anymore, as multiple UEs are usually sharing the wireless resources in the same cell. There is a maximum number of DRBs available per time slot, which must be assigned to at least all paths with guaranteed services in the network. Following the logical bridge model, the internal resource assignment is hidden from the TSN system, and it is therefore the task of the 5G system to schedule the streams internally such that a configured minimum throughput level at a configured maximum error rate can be ensured for each path. To guarantee sufficient resources for all TSN-streams even under worst-case conditions, admission control limits the number of guaranteed services to provide sufficient resource reserves in case needed. How much of the

available bandwidth of a transmission path can be provided by the 5GS logical bridge for TSN streams is an important information to calculate the TSN schedule. This number depends on different factors, such as the QoS requirements of the stream or the maximum resource demand the 5GS must provide in the worst-case. The potential for fluctuation of transmission resources allocated to different paths is usually not completely random but shows a correlation between neighbouring endpoints. Some channel effects such as shadow fading can be caused by dynamic environmental changes such as moving machines in a factory environment. The resulting temporal obstruction of line-of-sight communication in dense networks usually affects multiple neighbouring UEs. Knowledge of these channel-related characteristics could potentially be used in the TSN schedule calculation process to assign resources more efficiently. (Note: 5GS as a virtual TSN bridge is like a bridge with a non-ideal switching fabric.)

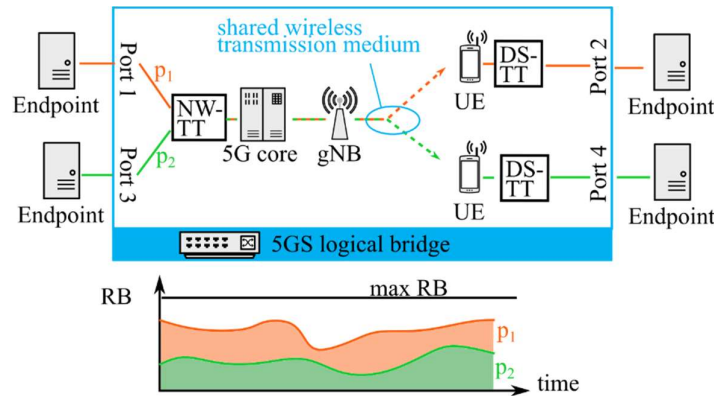


Figure 13: Dynamic allocation of DRBs to transmission paths with guaranteed services in a 5GS bridge

### 3.3.2 Wireless channel awareness

Based on the logical integration model, only the standardized exposures and parameters originating from the wired domain are available for the schedule computation. The task of the TSN AF is to translate the 5GS bridge internal characteristics according to the available parameters shown in Table 2. The variations of the wireless transmission medium and the corresponding radio resource management need to be translated into the dependent and independent delay parameters based on a worst- and best-case estimation.

A more resource effective approach would be to characterize the dynamics of the channel and forward that information to the CNC for further processing in the scheduling process. Establishing this form of wireless awareness would allow the 5GS to indicate different characteristics, such as the level of variation in the channel (e.g. if a UE is mobile or stationary), the probability that the data rate falls below a certain threshold, or the correlation of channel dynamics between different UEs.

However, such changes have a strong impact on the overall architecture from a standardization perspective. In the TSN domain, the 5GS bridge would not be completely hidden anymore. Instead, TSN must establish wireless awareness, which would not only require the 3GPP to define the respective exposures from the 5G system, but also introduce new parameters in the IEEE TSN

standard, such that the exposures can be leveraged in the CNC for schedule computation. In the context of IEEE P802.1dj<sup>24</sup>, where configuration enhancements for TSN as amendment to the standard are formulated, such a proposal has already been made. The authors in [MS+21] propose to introduce a LinkDelayVariability parameter which describes a delay CDF instead of the current minimum and maximum delay value as described in Table 2.

### 3.3.3 Schedule optimization for 5GS bridge

In classical TSN systems based on Ethernet with no link variability, the schedule computation process is a standard constraint problem. The scheduling model consists of constraints, if a candidate solution meets all constraints, a schedule is said to be feasible. Using a well-defined objective function, a proper schedule is determined, and the bridges are configured accordingly.

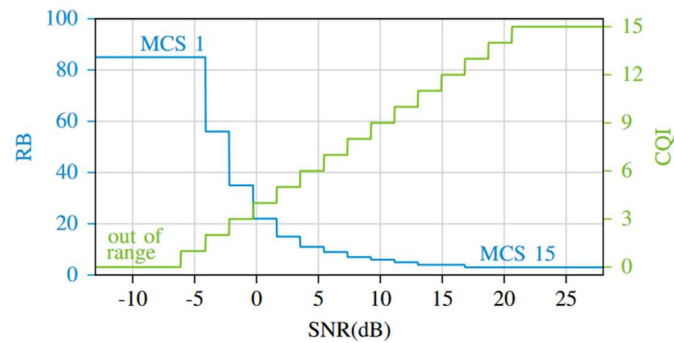


Figure 15: Mapping of SNR to CQI and MCS with the required DRBs for a 125-byte packet

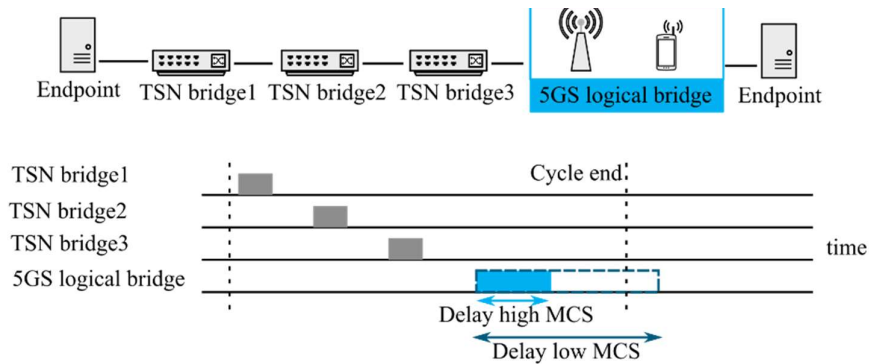


Figure 14: Schedule for 5GS Bridge with variable delay

In wireless systems with variable delay, a schedule could be feasible only with a certain probability. The task of a scheduler is hence to find a schedule that meets the application tolerance requirements. The effect of the channel state, represented as the signal-to-noise ratio (SNR), on the instantaneous scheduling decision inside the 5GS is shown in Figure 14. Under a lower SNR, and hence lower channel

<sup>24</sup> "P802.1Qdj – Configuration Enhancements for Time-Sensitive Networking," [Online]. Available: <https://1.ieee802.org/tsn/802-1qdi/>.

quality indicator (CQI), the 5GS bridge must select a lower MCS to maintain a low error rate and requires a higher number of DRBs to transmit, in this example, a 125-byte packet. While in traditional networks packets can be delayed until the channel is in a better state, this is not possible for time-critical applications. The low transfer intervals given for e.g. the C2C use case in Table 1. is in the lower millisecond range and hence requires immediate transmission even under adverse conditions. With different MCS levels, also the delay can vary, depending on the available system bandwidth and packet size. The effect on a fixed TSN schedule under varying delay is shown in Figure 14: Schedule for 5GS Bridge with variable delay. The schedule must be designed such that the system remains feasible with a given tolerance level, allowing all frames to be transmitted in order before the cycle ends.

Another parameter of interest to the scheduling computation process is the correlation between different ports. As shown in Figure 13, even independent port-pairs are bound to the same shared resource and can experience correlated channel variation based on the underlying physical effects of the channel. The correlation can have an impact on the worst-case estimation when performing e.g. stream aggregation.

Figure 15 shows 4 bridges in a line topology with 3 streams between different endpoint pairs. When transmitting with the same cycle time and offset, streams can be aggregated on the TSN bridges into a single gate cycle on the respective egress ports. On the 5GS bridge, the streams split up to independent egress ports and UEs. Nonetheless, the UEs must share the transmission resources internally. We assume that resources can be dynamically shared between the UEs, which makes the total worst-case delay for delivering all frames to all endpoints the crucial parameter that determines the feasibility of the schedule. Here, correlation between the UEs additionally influences the required resource allocation. Under high correlation, there is a non-negligible probability that the worst-case estimation delay per UE (and hence port) can occur simultaneously, leading to an overall higher resource requirement.

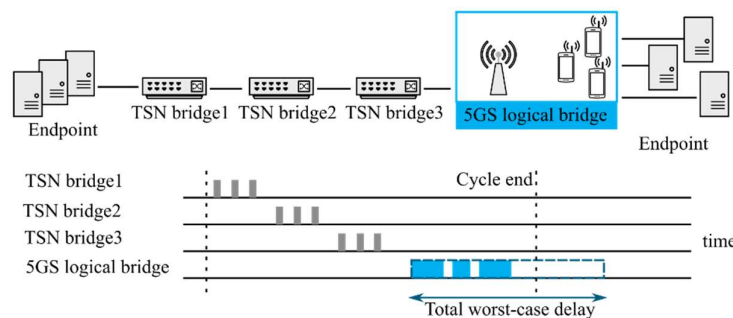


Figure 16: Schedule for 5GS bridge with variable delay and multiple endpoints

The impact of this effect on the schedulability is investigated via system-level simulation in the following. Using a MILP solver to compute schedules and the OMNeT++ framework to simulate the scheduling in the TSN and 5G network, different schedule optimization strategies have been investigated. Since the simulation investigates the resource handling inside a 5GS bridge, we consider a single radio cell in which multiple UEs are served. The network layout is shown in Figure 18.

Multiple clusters  $C_i$  are defined, where several endpoints are in close distance, representing e.g. a larger production machine or different machines performing coordinated tasks. Devices within a cluster are either connected over individual UEs or aggregated over a single UE. The E2E streams defined in this simulation study are aligned with the C2C use case requirements described in Table 1. The values are drawn randomly, for the interval time between 2 ms and 10 ms, and for the packet size between 50 and 250 bytes. The hyper period, i.e., the smallest interval of time after which the periodic patterns of all the tasks are repeated, of the calculated schedule is 10 ms, in which a total of 50 streams are served.

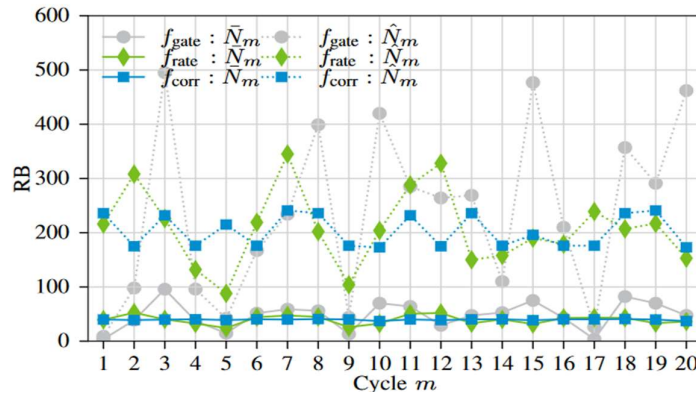


Figure 17: Mean and peak total resource demand in RB per cycle under different schedule optimizations

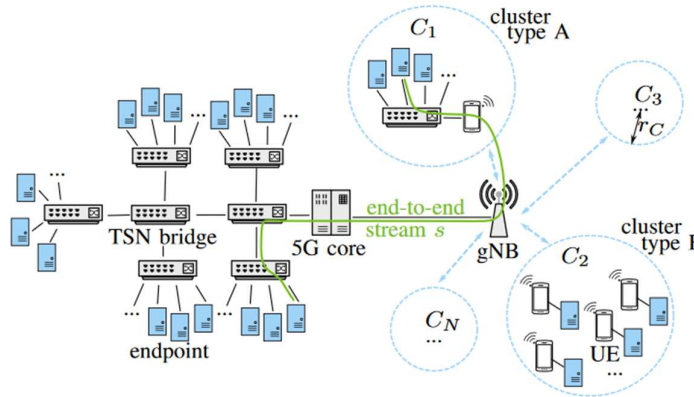


Figure 18: Network layout for simulation analysis

The complexity and degrees of freedom in the schedule computation process grows rapidly with the number of streams, which becomes apparent even for this simple setup. Hence simplifications such as stream aggregation, where multiple streams with the same cycle time are being combined, are crucial to handle the device density. Considering for example only the C2C use case, the number of streams at a device density of  $<10$  per  $m^2$  (c.f. Table 1) can become already quite large in manufacturing deployments. In the following, different optimization strategies to aggregate streams are investigated.

To reduce complexity, the system model considers quantized time windows of 0.5 ms, in which frames from different streams are jointly forwarded towards their respective endpoint. Considering the 10 ms hyper period, the schedule consists hence of 20 of such time windows or cycles. At each time window, multiple frames arrive at the 5GS and must be forwarded by sharing the available DRBs. A more detailed model description to this study is provided in [RG+21].

Figure 17 **Error! Reference source not found.** shows the mean  $\bar{N}_m$  and peak  $\hat{N}_m$  RB demand for each of the cycles under different optimization strategies for stream aggregation:

1.  $f_{\text{gate}}$  minimizes the number of egress gate cycles, hence achieves the best stream aggregation,
2.  $f_{\text{rate}}$  optimizes the data rate distribution over time, leading to similar number of transmitted bytes over each of the 20 cycles,
3.  $f_{\text{cor}}$  aggregates only the streams which have the lowest correlation to each other.

While the first optimization approach is sometimes used in TSN systems to minimize gating events by merging streams with the same cycle time and transmission path, the results show that the performance on the 5GS bridge is not optimal. Especially in cases as shown in cluster  $C_1$  in Figure 18, a strong aggregation over highly correlated paths can lead to long burst durations that become difficult to deliver in time, once the channel condition degrades due to e.g., temporal obstruction of the link. Since the 5GS is expected to provide service guarantees for the TSN streams, it must hence provide the most resources of the three compared optimizations to operate under this TSN schedule. The second optimization reduces the peak data rate per time window but is unaware of the channel condition. Since the actual resource demand depends on the CQI and hence MCS, we observe still an uneven resource demand in different time windows. Knowledge of the channel condition, especially in the static case where not much fluctuation is expected, can be helpful to design better TSN end-to-end schedules with lower peak DRB demands. The third optimization takes channel condition and correlation into account and can maintain a more stable resource utilization throughout the entire schedule. This becomes especially useful when operating under a resource constraint, which is usually the case for wireless systems. If e.g., only a fixed number of DRBs is available to the assigned network slice to operate the time-sensitive C2C applications, it is beneficial to remain below the threshold to achieve the lowest risk of unschedulability. The risk of such an event under different DRB constraints per cycle  $\hat{N}_c$  is shown in Figure 19. The advantage of this optimization is that potentially more streams

with guaranteed service requirements can be supported by the 5GS bridge, as we can make more relaxed assumptions on the worst-case resource requirement of the individual TSN-streams.

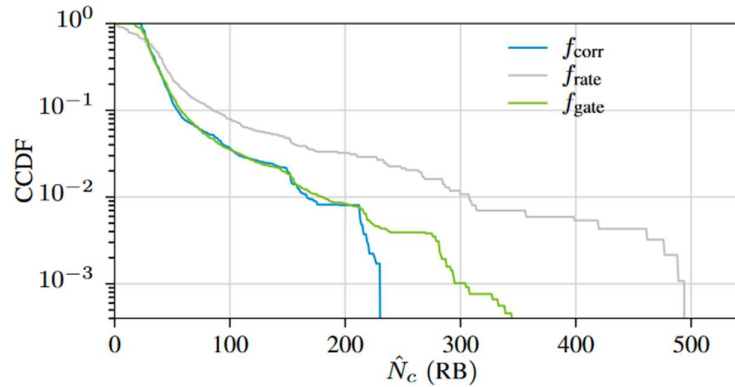


Figure 19: CCDF of schedule infeasibility risk under different schedule optimizations

### 3.4 Conclusion

We have investigated how TSN streams can be scheduled based on standardized bridge capabilities and stream requirements in an integrated TSN and 5G network. The results here have shown that the CNC can design better TSN schedules if more information about the actual bridge capabilities, especially regarding the channel conditions of a logical 5G TSN bridge, are made available. The focus of the conducted simulation study was on quantifying the feasibility of a given TSN schedule in a network where channel variation in the 5G TSN bridge occurs. Additional capabilities considered in the schedule generation process include

- Variability of the link. For example, a mobile UE will have a much larger channel quality variability compared to a static UE.
- Channel quality classification. Such a classification can be used to determine the average resource demand of a UE. For example, a UE in the cell edge requires more resources than in the cell centre.
- Correlation of UEs. A factor that quantifies how strongly different paths within the 5GS bridge experience similar channel effects.

The downside of using these additional values is however the increased complexity, as the simple black-box integration of the logical 5GS bridge does not apply anymore. There is a clear trade-off between complexity and efficiency that can be achieved with the integrated TSN and 5G network concept. From the final result graph, one could already observe that such a precise optimization only brings significant value if the application has very stringent requirements on the latency and reliability. This is especially the case when the utilization of the network is high. The less critical the requirements, and the more resource reserves are available, the less important a precise schedule optimization becomes.



## 4 End to End time synchronization Evaluations

Time synchronization is one of the main building blocks for IEEE 802.1 TSN-based time-aware industrial networks. There are different industrial applications in the factory automation domain, which depend on the clocks to be tightly synchronized, e.g.:

1. High accuracy demand (in the order of microseconds) is put forth by factory deployments of industrial robots, in, e.g., coordinated move of 2 (or more) robot arms.
2. Building on simultaneous communication under few tens of microseconds, a motion control system requests that up to 100 actuators and sensors are guaranteed clock synchronicity in the order of one microsecond, or even below.

The first 5G-SMART Deliverable on the technical features [5GS20-D51] investigates the time synchronization specifications from standard development organization (SDO)s such as ITU, IEEE and 3GPP. Key gaps for realizing E2E time synchronization in integrated 5G-TSN networks were identified therein.

3GPP has proposed new mechanisms in Release 16 in order for the 5GS to interwork with a TSN network. In this context, 3GPP has modelled the 5GS as IEEE 802.1AS time aware system in an integrated 5G-TSN network. The most demanding time synchronization error is defined to be as low as 900 ns for industrial applications in an integrated 5G-TSN network between the ingress and egress points of a 5GS (i.e., the 5G system end-to-end time error budget) [3GPP20-22104]. Within 5G system the radio link between a base station and user equipment (UE) is considered to have a major contribution towards this 5G time error budget. Here, the uncertainty introduced from estimation of the downlink propagation delay, which is used to adjust the 5G reference time made available to a UE, is a major factor.

Taking this as a baseline, this report takes a further leap on evaluating the E2E time error budget for a given 5GS deployment. In this report we investigate how a 5GS should be designed to satisfy the above mentioned 900 ns requirement. An in-depth analytical evaluation of the 5G reference time error introduced based on the two different delay estimation method is performed. In this context, a set of synchronization error components within the E2E path of a 5GS are identified and investigated. It is concluded from the analytical analysis that the Round Trip Time (RTT) based propagation delay compensation method can achieve lower time error compared to Time Advanced (TA) based method.

As an extension to analytical evaluation, the report further provides details on the link-level simulation analysis performed for RTT based propagation estimation method to investigate the suitable radio configuration parameters required to ensure 900 ns time error budget in 5GS. Further based on such evaluation, list of recommendations on 5GS deployment is provided for a given deployment model.

### 4.1 5G architecture to support time aware network

IEEE 802.1AS specifies a mechanism to ensure accurate TSN time reference delivery across the TSN network. A time synchronization model is specified wherein connected time aware systems support the generalized Precision Time Protocol (gPTP). gPTP is used for relaying master clock information from a source node serving as gPTP master clock to multiple end stations. A time aware system in the context of the TSN network can either be an TSN end-station or a TSN bridge. It can include support for more than one gPTP instance. Residence time of each gPTP relay node and propagation delay

between two gPTP relay nodes are the two main parameters that should be precisely calculated to ensure precise master clock time synchronization over the end-to-end path (i.e., between the gPTP master clock and a TSN end-station). The uncertainty introduced when determining the value of the residence time of each gPTP relay node between the gPTP master clock and the end stations must be known. Also, to meet the master clock synchronization requirement, the propagation delay between each pair of gPTP relay nodes in the E2E path must be determined with an acceptable level of uncertainty. In an integrated 5G-TSN network, the ingress to egress (I2E) of the 5GS is only part of the overall E2E path and is considered as a time aware system using Ethernet-based connectivity. Note that the 5GS is modeled as a TSN bridge where corresponding ports are at the TSN Translators (TT) which are located at the edge of the 5GS. Both Device-Side TT (DS-TT) on User Equipment (UE) side and a single Network-Side TT (NW-TT) on User Plane Function (UPF) side support IEEE 802.1AS functions such as gPTP packet handling and timestamping.

When considering a gPTP relay node, the precise calculation of the residence time for gPTP packets should be calculated between their ingress and egress points (e.g., a DS-TT and NW-TT when a 5GS serves as the relay node). To enable this, 3GPP has specified a mechanism to timestamp all incoming gPTP packets from DS-TT or NW-TT with an internal 5G reference time. This internal 5G reference time is provided by the 5G internal clock to all the user plane nodes (UE, gNB and UPF). Paper [IG+20] provides further details on 5G-TSN integration as specified by 3GPP in Release 16 specification. Four possible time synchronization scenarios relevant for industrial networks are supported by the 5GS as shown in Figure 20. From Release 17, the Best Master Clock Algorithm (BMCA) functionality is supported at the NW-TT to satisfy the requirement of running BMCA in a centralized location. Additionally, 3GPP Release 17 has specified the capability of the TSN Application Function (AF) to: (i) activate/deactivate the time synchronization service, (ii) determine the functionalities to be supported by the 5GS (such as whether 5GS can act as grandmaster), and (iii) configure the gPTP instances. Release 17 also specifies support for PTP instances (according to IEEE 1588-2019 and provisioned by a given PTP profile), including the possibility to configure the 5GS to operate as a Boundary Clock, Transparent Clock, or Time Aware System, and the use of IP-based connectivity for time synchronization.

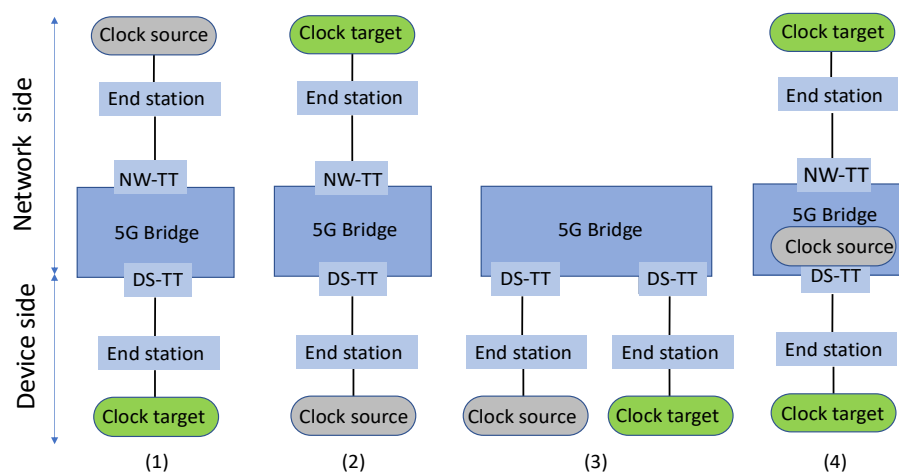


Figure 20 5G time sync solutions



For alternatives 1, 2 and 3 in Figure 20, the first process is time synchronization of 5G user plane nodes, that in addition to supporting the operation of the 5G system, also ensures precise calculation of the 5GS residence time experienced when relaying the TSN GM clock between the 5GS ingress and egress nodes (e.g., between DS-TT and NW-TT per option 2 of Figure 20). The second process is TSN time synchronization realized by relaying the master clock from the source node (TSN-GM) to the target nodes (TSN end-stations) realized using the IEEE 802.1AS mechanism. The time error introduced between these two nodes should be below 900 ns. A special case is where 5GS acts as master clock source for the connected TSN networks (alternative 4 in Figure 20). In this case the timing source for these two processes is the same and is provided by the 5GS internal clock master.

In this report we refer to the 5GS clock master as “5G GM” (“5G Grandmaster”) which serves as the source clock for the internal 5G reference time. This can be considered as a PTP grandmaster (i.e., as per IEEE1588, the PTP synchronization master) and serves as the Primary Reference Time Clock (PRTC) as defined by ITU-T. The PRTC is a device that is typically implemented with an integrated Global Navigation Synchronization System (GNSS) receiver (e.g., Global Position system (GPS)) and that is the actual source of time synchronization for the network.

The independence of the two synchronization processes brings flexibility in time synchronization deployment, e.g., when upgrading an existing deployment. For example, if a mobile operator has already deployed a 5GS in one area, to further support the use of gPTP for factories in 5G coverage, only the UPF, gNB and UE need additional enhancement to support the use of internal 5G time synchronization. Also, if 5G is added to a fixed TSN network with time synchronization, the TSN time synchronization is not modified due to the introduction of 5G. The rest of report focuses only on the internal 5G time synchronization process between a DS-TT and NW-TT.

## 4.2 Synchronization network solution over 5GS

5G internal time synchronization is an integral and essential part for the operation of the 5GS. Radio network components (base stations) in 5GS already support a form of time synchronization necessary to support advanced radio transmission, such as Time Division Duplexing (TDD) operation, CoMP (Coordinated Multipoint Transmission) and carrier aggregation. Paper [IG+20] provides more details on the time synchronization solution and requirements. The fundamentals of the internal 5G time synchronization process lies in the internal distribution of the 5GS master clock provided by GNSS as explained in [IG+20]. There can be multiple options regarding where the 5G GM clock can reside, based on how the transport and radio networks are deployed. The internal 5G time synchronization process includes the transmission of 5G reference time information across the fixed transport network and the radio network portions of the 5GS.

### 4.2.1 Synchronization of 5GS solution over 5G transport

The synchronization of 5GS relies on accurate distribution of 5G reference time information from a synchronization master time source towards the end-clients (i.e., the gNBs) and, in order to support 5G time synchronization solutions for time aware industrial networks, towards UPF/NW-TT. One first approach is to deploy GNSS receivers at every base station. A stable GNSS receiver is capable of providing accuracy of about  $\pm 100$  ns, a value that is suitable for existing and emerging technology demands.



Even though this is considered as the simplest of all the solutions, it has its own set of drawbacks. Some of them include the management and cost of deploying GPS receiver antennas across every base station, installation issues (sky visibility, indoor deployment), risk of jamming (intentional or accidental). In any case, backup references would be required to keep time/phase synchronization requirements in case of GNSS failures. This resulted in development of complementing solutions that could be combined with the use of GNSS receivers and involving the use of time protocol-based technologies capable of supplying the level of accuracy required over packet switched networks.

#### *PTP telecom profile*

The Precision Time Protocol (PTP) specified by IEEE 1588 (latest version is in IEEE1588-2019) was the protocol selected by the industry for precise distribution of timing information from the master node providing the 5G GM clock to the nodes requiring the synchronization information (e.g., the clock in the gNB) [SR+21].

The IEEE 1588 standard specifies a protocol to synchronize clocks running on individual nodes of a distributed system. The initial objective of this protocol was to deliver time/phase synchronization with high accuracy (sub-microsecond) in Local Area Network (LAN) environment. It was then updated and complemented by profiles for use in specific industries. In case of Telecom applications, the related profiles have been developed by ITU-T with a target to distribute phase/time with  $\pm 1.5 \mu\text{s}$  timing accuracy. It has to be noted that the concept of time synchronization is very close to the notion of phase synchronization; the difference lies in associating labels (timestamps) to the significant phase instants; they can be interchangeably used here. In its basic form, PTP protocol behaviour can be characterized as a typical Master-and-Slave type signalling exchange. While the slave clock is always embedded in the gNBs (and UPF/NW-TT), the master clock could be placed anywhere in the network (pre-aggregation, aggregation, core) based on operators needs and strategies.

Several standards and recommendations have emerged out over a very short time span that resulted in this protocol finding its way within the operator networks. Several mobile operators worldwide are deploying PTP to transfer time/phase across their network. For the application in Telecom environments ITU-T has specified 2 profiles for the distribution of time synchronization: G.8275.1 and G.8275.2 [ITU20-G82751] [ITU20-G82752].

G.8275.1: The first one, called PTP profile with full timing support from the network, is based on a "hop-by-hop" architecture; it implies that the network nodes between the PTP master and the PTP end clocks are "PTP-aware" (they process the PTP messages with implemented hardware functions to improve the performance of PTP). This approach allows for better control on the end-to-end performance.

G.8275.2: The second one, referred to as PTP profile with partial timing support from the network, requires only some of the intermediate network elements to support PTP functions. The complexity here lies in the fact that, when every network element does not support the PTP function, from an operational point of view, it becomes extremely tedious to set-up the flow of the PTP messages across the network elements (e.g., set up of the IP unicast path, that is not required for the multicast transmission in G.8275.1). One major problem with this approach is that the performance can be significantly impacted by traffic load and the achievable performance may change over time (e.g., due to changes in the network).



#### 4.2.2 Synchronization network solution for 5GS over 5G radio access network

Delivery of internal 5G reference time over the radio network is an essential component in supporting an internal 5G end-to-end time synchronization solution and is in the focus of the remaining discussion below. One mechanism specified by 3GPP is based on the existing synchronized operation inherent to the 5G radio access network, where UE and base station maintain the synchronization for NR frame transmission. These frames are identified by system frame number (SFN). The base station (gNB) acquires the internal 5G reference time value from the 5G GM and maintains this acquired 5G reference time on an ongoing basis as well as periodically projecting the value it will have when a specific reference point in the system frame structure occurs at the BS antenna reference point (ARP). A System Information Block (SIB)/Radio Resource Control (RRC) unicast message embeds this information consisting of the internal 5G reference time value and the corresponding reference point (reference SFN) is then transmitted to a UE. The frequency of this message is up to implementation. Depending on the cell size, it may be necessary to adjust the 5G reference time to reflect the downlink propagation delay experienced by a UE at the point in time to which the 5G reference time applies. Hence, compensation for propagation delays is an important function and depends upon on the cell size and target end-to-end synchronization requirement.

#### 4.3 Analytical time error analysis

This section provides an analysis of the details of the time uncertainty experienced in the E2E chain of 5GS. This also includes the error components observed in each individual link in the E2E chain. Time error is the difference in value between the clock time maintained by a clock target (e.g. a UE) and clock source (e.g. a gNB) at any given time instant. This error is always relative between these two clocks and can change over time. For the time error analysis, a typical manufacturing scenario of integrated 5G-TSN network is considered as shown in Figure 21. The scenario relates to alternative 1 from Figure 20 showing the possible 5GS time synchronization solutions. For a given scenario (shown in Figure 20) the steps below are to be followed for time synchronization between the TSN-GM and a TSN end station. These steps require that a 5G reference time is first distributed to the NW-TT and DS-TTs within the 5GS.

1. A downlink Ethernet frame carrying a gPTP event message is received at the NW-TT ingress port. Based on the 5G GM reference time, the  $T_{si}$  timestamp is generated and embedded in the gPTP message (as a suffix field).
2. The NW-TT forwards the gPTP message towards the DS-TT via UPF. The UPF determines the destination (set of 5G Quality of Service (QoS) flows over which PTP message are forwarded) depending on the state of the PTP ports.
3. On receiving the gPTP message at DS-TT, a  $T_{se}$  timestamp is generated. The timestamping is done based on the 5G GM reference time at DS-TT.
4. The DS-TT retrieves the  $T_{si}$  from the suffix field of the gPTP message and calculates the residence time of the message within the 5G system ( $T_{si} - T_{se}$ ). This residence time is then embedded in the gPTP message while forwarding it to the TSN end station. Further, the TSN end station utilizes the embedded residence time to recover the TSN GM reference time.

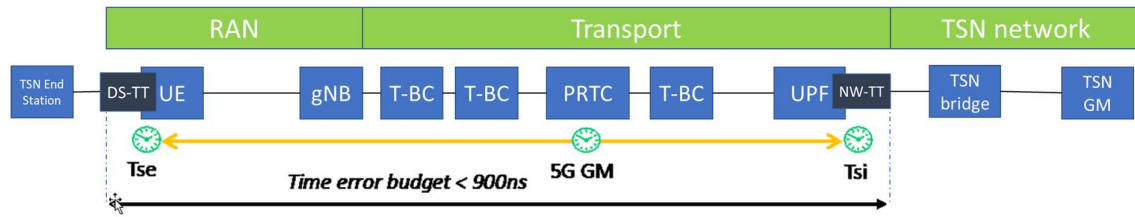


Figure 21 Time error analysis

As mentioned in section 4.1, a precise calculation of the residence time experienced when transporting a TSN-GM related signalling through a time aware system is important to achieve an accurate time synchronization to the TSN end-stations. This means that the time error introduced by the 5GS time reference to generate  $T_{si}$  and  $T_{se}$  timestamps (where the difference between  $T_{si}$  and  $T_{se}$  timestamps determine the 5GS residence time) should be below 900 ns. The error introduced when determining the 5GS residence time consists of the total time error accumulated when distributing 5G reference time over two paths:

1. Time error accumulated during delivery of 5G reference time from PRTC to DS-TT. This path needs to ensure acceptable time synchronization error is introduced over transport network (PRTC to gNB) and radio network (gNB to UE).
2. Time error introduced over path from PRTC to NW-TT. This path needs to ensure acceptable time synchronization error is introduced over transport network.

Concerning the radio network, 3GPP working group RAN1 has agreed on allowing a worst-case per radio link interface time error budget of 275 ns for the use case where two radio links are involved in the 5GS ingress to egress path, including errors due to misalignment of gNB downlink transmissions [3GPP21-2010837]. For simplicity, the contribution of the radio link interface time error budget due to misalignment of gNB downlink transmissions (~65 ns) can instead be allocated as part of the transport network timing error. Due to that, as an initial reference, we can assume that the time error budget over a single radio link is around 200 ns. Thus, for the scenario shown in Figure 20, a 700ns time error can be assigned to all remaining sources of time error introduced when transporting a TSN-GM clock time between the 5GS ingress and egress points. The figures for the error between the DS-TT and UE can be assumed to be different for different implementations, e.g. it can be in the range of 50 ns. This leaves a 650 ns error budget for the transport network timing error i.e, the total error between the gNB Tx antenna and NW-TT shown in Figure 21. This allows for some degree of flexibility regarding the number of hops on the transport network that can be supported behind the radio access network. The remaining section provides time error analysis of the 5G transport and radio network.

#### 4.3.1 Time error analysis for transport network, including gNB

ITU-T recommendations, in particular G.8271.1 specify engineering rules/guidelines to achieve the desired time synchronization performance between a PRTC and a gNB, when clocks compliant with ITU-T recommendations G.8272, G.8273.2 and 8273.3 are used. With reference to the example shown in Figure 21 it is possible to estimate the maximum absolute time error introduced between the DS-TT and NW-TT interfaces when measuring the 5G residence time of a TSN GM clock using ingress and egress timestamping. In this section we focus on the time error between output of the gNB towards

the radio interface and the NW-TT interface towards the TSN network. A PTP-aware transport network implementing the G.8275.1 [ITU20-G82752] time profile can be utilized for the internal 5G network time synchronization solution. Mapping this model on the above selected scenario (Figure 21), we have a packet network consisting of a chain of Telecom Boundary clocks (T-BC) (or Telecom Transparent Clocks, T-TC) between the 5G GM (combined PRTC/T-GM according to ITU-T terminology) and the end application time clock. The end application time clock is the clock maintained by the UPF/NW-TT at one end and gNB at the other end. The gNB terminates the PTP timing flow and uses it to generate the 5G reference time which it distributes to UEs over the radio interface. Depending upon the deployment and number of the T-BCs between these end points, the end application time clock could be adjusted to reduce the time error. The above mentioned ITU-T recommendations specify the minimum equipment tolerance to phase and time error that shall be provided at the boundary of packet networks at phase and time synchronization interfaces. This allows for determining the various time error budgets to be assigned to each individual link comprising the transport network.

In the example shown in Figure 21 we assume that the error introduced by the PRTC/T-GM to be approximately the same when sending the PTP timing signals towards the gNB and towards the UPF/NW-TT. Therefore, its contribution to the relative time error between the DS-TT and NW-TT can be assumed negligible. A total of 4 T-BCs of G.8273.2 class C are assumed in the synchronization chain. The (low frequency) time error they introduce (as a combination of constant and dynamic time error which are 10 ns and 10/2 ns respectively) is  $Err_{T-BC}$ , which is in the order of 50 ns (following the methodology described in G.8271.1 where constant time error is accumulated linearly and dynamic time error is accumulated as noise power). Additionally, the time error  $Err_{Fiber}$  from the fiber connectivity between all network equipment should be considered (this is due to asymmetries generated for instance in 2-fiber transmission systems). Hence, the maximum time error for the above two paths (PRTC to NW-TT and PRTC to gNB) is given by below equation, where  $Err_{gNB}$  is the error introduced by the gNB towards the radio interface:

$$Tmax\ time\ error - transport = Err_{T-BC} + Err_{Fiber} + Err_{gNB}$$

Based on the above equation and as per the guidelines from G. 8271.1, the maximum network limits of phase and time error of 650 ns for the transport network (including the gNB) can be fulfilled. In fact, with 50 ns generated by the T-BCs, and 400 ns allocated to the gNB including some margin for failure conditions (see G.8271.1), 200 ns would still be available for time errors due to fibre asymmetries or other transport related asymmetries (e.g., that could be introduced by the OTN layer). Note that 400 ns for the gNB is a combination of a budget allocated to failure conditions and errors introduced during normal conditions by the gNB (this includes the  $Err_{BS,DL,Tx}$  component defined in section B). If more T-BCs are considered in case of a necessity for a longer chain, then one needs to implement a better compensation of fibre asymmetries and/or less budget for gNB failure conditions.

#### 4.3.2 Time error analysis over radio network

In a radio network the time error is introduced by two main sources between the gNB antenna and UE antenna:

1. Error source 1: The time error observed during transmission of the 5G reference time from the base station and its reception at the UE ( $Err_{BS,DL,Tx} + Err_{UE,DL,Rx}$ ).  $Err_{BS,DL,Tx}$  is not considered in this analysis as this is part of the gNB  $Err_{gNB}$  budget.

2. Error source 2: Error introduced in the estimation of the propagation delay ( $PD_{error}$ ) for downlink (gNB to UE) which is used to compensate for the downlink propagation delay.

$$T_{max \text{ time error} - radio} = Err_{UE,DL,Rx} + PD_{error}$$

This above equation shows the total time error introduced over the radio link between gNB and UE. "Error source 1" includes the uncertainty due to UE downlink frame timing detection. Considering the Synchronization Signal Block (SSB) as the downlink signal for timing estimation, the minimum timing error ( $Err_{UE,DL,Rx}$ ) of  $\pm 139$  ns can be assumed for 15 kHz downlink subcarrier spacing (SCS). In this report, two propagation delay estimation methods are analysed.

Following this, in section 4.4 total time error over radio network between gNB antenna and UE antenna has been evaluated based on the link level simulation. Rest of the below section provides details on the analytical analysis of the time error budget.

#### Timing advance based propagation delay estimation

Timing Advance (TA) [3GPP21-38213] was originally used for uplink timing control for NR transmissions with the purpose of aligning multiple uplink transmissions from different UEs in time when received at the base station. Timing advance for each UE is calculated well in advance by the base station. The TA value is basically a negative offset between a start of a downlink slot and the start of that same slot in uplink. This calculation is based on an estimate of the propagation delay. Considering a TA based method for propagation delay compensation estimation, the equation below shows the different factors contributing to the propagation delay estimation error.

$$PD_{error} = \frac{Err_{UE,DL,Rx} + Err_{UE,UL,Tx} + Err_{BS,UL,Rx} + Err_{TAG}}{2}$$

The sum of  $Err_{UE,DL,Rx}$  and  $Err_{UE,UL,Tx}$  refers to the time error introduced by the UE continuously attempting to align its uplink transmissions with respect to its downlink receptions, which is basically the UE transmit error (denoted as  $T_e$  in [3GPP21-38133]). Here, the UE performs transmissions of uplink frames after detecting the downlink frame and adding the timing advance (TA). According to the specification [3GPP21-38211], considering 15 kHz SCS for the uplink signal, the error value can be calculated as below.  $T_c$  is the basic timing unit  $T_c = 1/(480 \cdot 10^3 \cdot 4096)$  sec.

$$T_e = \pm 12 \cdot 64 \cdot T_c = \pm 391 \text{ ns}$$

$T_c$  details can be found in the report [3GPP21-38211]. The error  $Err_{BS,UL,Rx}$  is the uncertainty with which the gNB acquires uplink frame timing. The error value can be affected by how accurately it determines the difference between when an uplink slot has been received and when the slot should have been received if the UE was perfectly aligned.  $Err_{BS,UL,Rx} = \pm 100$  ns has been proposed as a realistic value in 3GPP [3GPP21-2010837].  $Err_{TAG}$  indicates the uncertainty due to TA command granularity. The maximum value of this error is half of the TA granularity in the existing NR specification, which can be calculated as below. Here  $\mu = 0$  for 15 kHz SCS.

$$Err_{TAG} = \pm 8 \cdot 64 \cdot T_c / 2^\mu = 512 \cdot T_c = \pm 260 \text{ ns}$$

Based on the above values, 375.5 ns of  $PD_{error}$  is observed. This shows that the TA based method for propagation delay estimation is not suitable for time synchronization solution when 200 ns value of time error budget is considered.

#### Round trip time (RTT) based propagation delay estimation

The RTT method is based on the 3GPP defined physical layer measurement capabilities between UE and gNB [3GPP21-2010837]. This measurement mechanism at the UE and the gNB is controlled by higher layers (e.g., medium access control layer) and can be utilized to estimate accurately the propagation delay. In particular,  $UE_{Rx} - Tx$  and  $gNB_{Rx} - Tx$  time differences are defined (see Figure 23) which can be used to accurately estimate the propagation delay.  $UE_{Rx} - Tx$  is the time difference between UE reception of a downlink subframe containing a positioning reference signal (PRS) and UE transmission of the uplink subframe containing a sounding reference signal (SRS). Here, the SRS transmission in the uplink is in the subframe closest in time domain to the received downlink subframe containing the PRS.  $gNB_{Rx} - Tx$  is the time difference between gNB reception of an uplink subframe containing an SRS and a gNB transmission of a downlink subframe containing the PRS that is closest in time to the subframe containing the SRS received from the UE. Practically, a UE can calculate the measurement  $UE_{Rx} - Tx$  and transmit the value to the gNB which can be further used to estimate the propagation delay based on the equation shown below,

$$Delay = \frac{(UE_{Rx} - Tx) + (gNB_{Rx} - Tx)}{2}$$

The time uncertainty associated with the estimation of time difference between reception and transmission of reference signals at both UE and gNB are  $Err_{gNB,RxTxDiff}$ ,  $Err_{UE,RxTxDiff}$  as shown in Figure 22. Also, the time error  $Err_{RxTxDiff,report}$  reflects the time error due to the granularity of the reporting of the  $UE_{Rx} - UETx$  time difference to gNB. Hence,  $PDerror$  can be estimated as below.

$$PDerror = (Err_{gNB,RxTxDiff} + Err_{UE,RxTxDiff} + Err_{RxTxDiff,report})$$

$$Err_{gNB,RxTxDiff}, Err_{UE,RxTxDiff} = \pm 90 * Tc = \pm 45.8 \text{ ns}$$

So far, 3GPP working group RAN4 has not defined an accuracy requirement on the  $UE_{Rx} - Tx$  and  $gNB_{Rx} - Tx$  calculation. For the estimation, maximum values as proposed in [3GPP20-38901] are assumed. In the 3GPP [3GPP21-38133] mapping tables are provided for the  $gNB_{Rx} - Tx$  time difference where the granularity ranges from  $1 * Tc$  to  $32 * Tc$ .

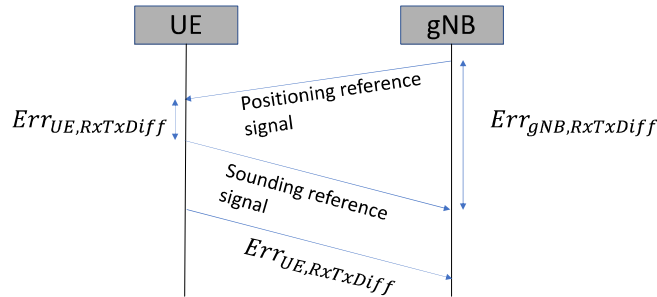


Figure 22 Error component of RTT based propagation delay estimation



Assuming the largest granularity of  $32 * T_c$ , the uncertainty due to the granularity of reporting the  $Rx - Tx$  time difference  $Err_{RxTxDiff,report} = (32 * T_c) / 2 = 8$  ns. Based on the equation above,  $(45.8 + 45.8 + 8) / 2 = 49.8$  ns is the total estimated  $PD_{error}$ .

Table 5: Total time error for considered scenario

Radio		UE	Transport	Total Error	Expected synchronization accuracy
Method	Total error				
TA based	514 ns	50 ns	650 ns	1214.5 ns	> 900 ns
RTT based	188.8 ns	50 ns	650 ns	888.8 ns	< 900 ns

Table 5, shows the total time errors from two propagation delay estimation methods. From the above analysis it can be observed that the RTT based method will incur significantly less time error compared to the legacy-based TA method when determining a value for propagation delay compensation. Additionally, it can be noted that for the RTT based method uplink and downlink reference signals are used to calculate propagation delays, while the TA based method is based on the legacy SFN synchronization between UE and gNB. In particular, for the TA based method, the time error (sum of  $Err_{UE,DL,rx}$  and  $Err_{UE,UL,tx}$ ) observed during UE's continuous operation of aligning itself with base station has a major contribution towards the overall time error budget. This makes the TA method less promising compared to the RTT method considering that ongoing pressure to reduce these timing errors even further may materialize. Moving forward, only the RTT based method is able to satisfy the 900 ns time error requirement. In addition, for the TA based method a significant optimization would be required on the transport side (275 ns) and that would imply the introduction of strong constraints in terms of number of clocks that can be supported as well as on the resiliency design (lower budget for holdover) and / or control of fiber asymmetries. In turn this means increased costs and challenges for the network operators. Furthermore, 3GPP Release 18 is working on a solution where the timing of the 5G system itself may be used by the connected devices (e.g., smart grid, financial sector) to increase their resiliency to failures experienced by external TSN GM clocks (see [3GPP20-22104]). This implies in some cases, very tight E2E (5GS ingress to egress) synchronization requirements for the TSN GM clock timing delivered between the ingress and egress of the 5GS will be observed. For these cases an advanced solution for controlling the radio propagation delay error such as that offered by an RTT based method will be crucial.

Taking RTT method as baseline, next section performs the time error analysis utilizing link level simulation.

#### 4.4 Link level simulation analysis

Taking RTT method as a baseline, this section provides details on the link level simulation analysis performed to investigate suitable radio configuration parameters (e.g., subcarrier spacing, UE antenna height, etc.) that can achieve the time error budget assigned for the radio network part of 5GS. Before going into details on time error analysis, the section below provides basic understanding on the 5G synchronization process.



#### 4.4.1 SSB block basic

In the 5G New Radio (NR) radio interface, synchronization signal block (SSB) is specified as a signal block that is required for initial access of a user equipment (UE) to the radio access networks [3GPP21-38331].

Before getting into details of SSB, we shall look into initial 5G synchronization process over the radio access network (initial access processes). Synchronization is a process in which a mobile terminal (UE) obtains the time and frequency of the wireless network and is also a pre-requisite for the terminal to access the network. The UE needs to know on which frequency and at what time the network sends it messages. The synchronization process is therefore a series of operations performed by the terminal to determine the frequency and time information. The transmission direction from gNB to UE is known as the downlink and the reception direction from UE to gNB is called the uplink. Thus, there are two types of synchronization, one is uplink synchronization and the other is known as downlink synchronization.

Downlink synchronization is the mechanism where the UE detects the frame boundary and symbol boundary. This detection process is implemented by a UE processing SSBs. Uplink synchronization is a process where the UE determines which frequency resources and time periods to use for transmitting data.

Generally, the gNodeB needs to process multiple UEs, thus the network side must ensure that each UE uplink transmissions arrive at the network without interference from other UEs (i.e., the network has to ensure that the uplink signals from every UE should be time aligned according to their distance from the antenna of their common serving cell). The mechanism by which this is ensured is called the Random-Access Channel (RACH) procedure.

The SSB comprises a primary synchronization signal (PSS), secondary synchronization signal (SSS), and physical broadcast channel (PBCH) [3GPP21-38211] as presented below in Figure 23 and Figure 24. An SSB block is 4 Orthogonal Frequency Division Multiplexing (OFDM) symbols long (1-symbol PSS, 1-symbol SSS, 2-symbol PBCH) and 200 subcarriers wide. OFDM is utilised in 5G New Radio access technology. OFDM is form of multi-carrier modulation scheme that transmit data over number of orthogonal sub-carriers.

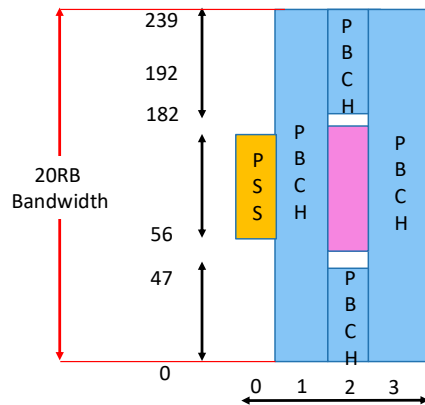


Figure 23 Format of SSB Block

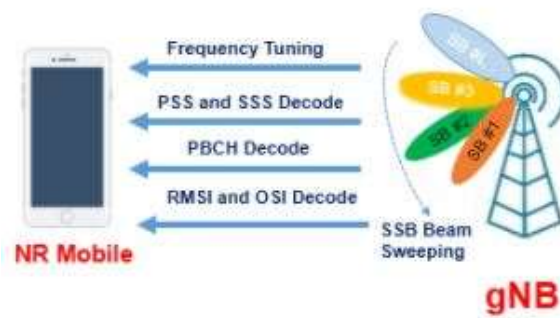


Figure 24 5G-NR cell access

**Primary Synchronization Signal (PSS):** The PSS is the first signal transmitted by gNB, and it occupies the center 127 resource elements of the 240 block.

**Secondary Synchronization Signal (SSS):** one of 336 possible sequences of the SSS comes to OFDM symbols later and also occupies the centre 127 resource elements.

**Broadcast Channel or PBCH:** which carries the master information block with the essential set of information to get started completes the SSB.

The main uses for the SSB are initial synchronization and cell search as well as cell search of neighbour cells when they are in range. It also provides a first piece of information about suitable beamforming or in other words the relative position of the base station.

Cell search is the procedure by which a UE acquires time and frequency synchronization with a cell and then decodes the Cell ID of that cell. A UE can access a 5G NR cell in Standalone mode following steps presented below.

#### *SSB transmission*

SSBs are transmitted in a batch by forming an SS Burst (one SSB per beam) that is used during beam sweeping by changing the beam direction for each SSB transmission. The SSB can be transmitted with



different subcarrier spacings that can range from 15 kHz to 240 kHz. A collection of SS Bursts is referred to as an SS Burst Set. The maximum number of SSBs in an SS Burst is frequency-dependent and it can be 4 (below 3 GHz), 8 (3 to 6 GHz), or 64 (6 to 52.6 GHz). Currently used frequency 3.5 GHz in France 5G networks is in the range of mid-band frequencies (3 to 6 GHz).

#### *Difference between LTE sync signal and 5G sync signal*

The synchronization signal generation method is different based on the technology. The PSS in LTE is a Zadoff-Chu sequence of length 62; and the PSS in NR is an m sequence of length 127. The SSS in LTE is an m sequence of length 62, while the SSS in NR is a gold sequence of length 127. The number of PCI is different. 504 PCI is defined in LTE, which is divided into 168 groups, corresponding to 168 SSSs; each group contains 3 cells, corresponding to 3 PSSs. NR defines 1008 PCIs, which are divided into 336 groups, corresponding to 336 SSSs; each group contains 3 cells, corresponding to 3 PSSs. The Synchronization signal time domain and frequency domain position are different in both. The frequency domain and time domain positions of LTE PSS, SSS and PBCH are fixed in the system and always occupy the central frequency part of the system bandwidth. PSS and SSS and PBCH do not have a strict binding relationship. However, in 5G, PSS, SSS and PBCH are bound together, known as SSB. The subcarrier spacing of different LTE subcarrier spacing is fixed to 15 kHz, whereas the PBCH subcarrier spacing in NR varies according to the frequency band.

#### *5G synchronization process*

It is precisely due to the difference in synchronization signals between NR and LTE that the 5G synchronization process is different from LTE. Beamforming is commonly used in NR, and the synchronization signal SSB is transmitted on different beams. Therefore, one goal of the Synchronization process is for a UE to find the optimal beam. This process is done by determining the SSB's index. In the 5 ms period, the index of the SSB and the beam are in a one-to-one correspondence. By determining the index of the optimal SSB, the optimal beam direction can be found. By determining the frequency domain position of the SSB, it can be based on other parameters ( $k_{ssb}$ ,  $NCRB^{SSB}$  etc).

## 4.5 Simulation and result analysis

### 4.5.1 Simulation environment

For simulations we are using MATLAB, which is a multi-paradigm programming language developed by MathWorks. MATLAB allows implementation of algorithms, plotting of functions and data, and the major advantage is interfacing with programs written in other languages.

MathWorks provide many tools like 5G Toolbox<sup>25</sup>. It provides standard-compliant functions and reference examples for the modelling, simulation, and verification of 5G New Radio (NR) communications systems.

The toolbox supports link-level simulation and test waveform generation and other ready functions that can be used for link level synchronization study. The "5G Toolbox" is utilized for the presented time synchronization investigation.

---

<sup>25</sup> <https://de.mathworks.com/products/5g.html>

#### 4.5.2 Simulation goals

The synchronization budget (propagation delay + delay error) can be evaluated by detecting a PSS signal and by using 5G NR parameters. We evaluate the total budget of (propagation delay + error) for different (SCS 15 kHz to 240 kHz), for 3.5 GHz only 15 and 30 kHz. We investigate the impact of the frequency of timing messages from the gNB on synchronization performance.

#### 4.5.3 The proposed algorithm to estimate the downlink propagation delay based on process of detection of Primary Synchronization Signal (PSS)

The following steps (see Figure 25) are involved in the process of detection, estimation, and correction when a PSS is transmitted from the BS to the UE, and are needed in order to calculate the propagation delay value:

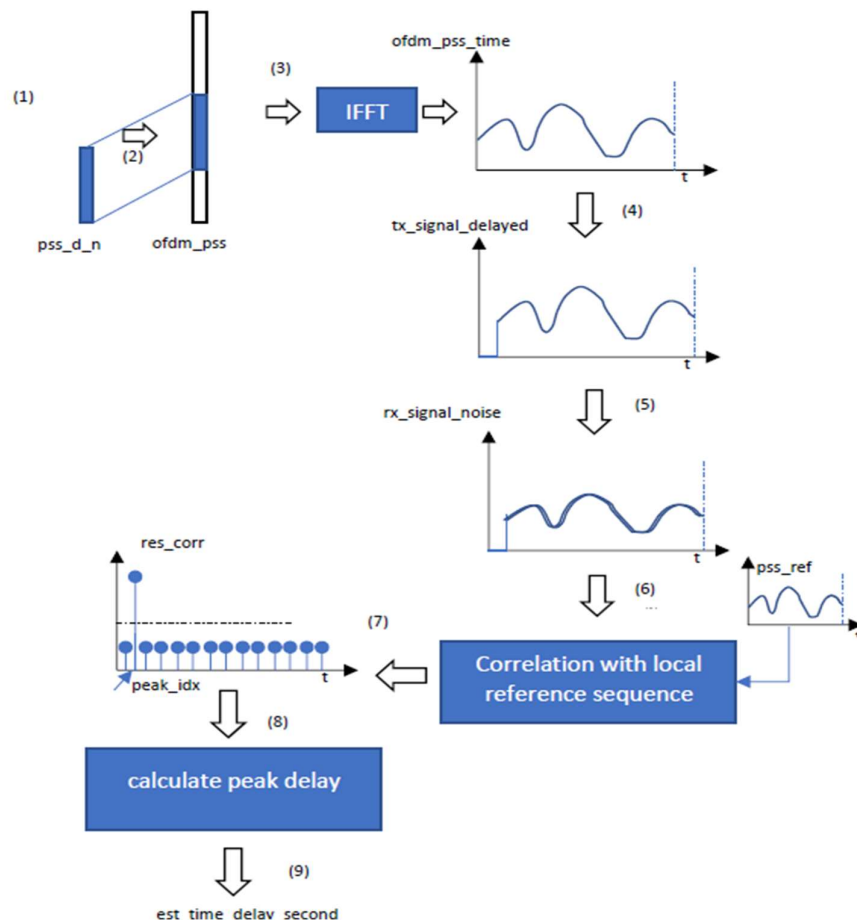


Figure 25: Description of the process of detection of time delay

Steps:

- 1) Generation of the PSS sequence (with a length of 127) according to 3GPP 38.211 [3GPP21-38211] section 7,
- 2) Mapping PSS sequence to subcarriers inside the cell bandwidth,

- 3) Apply IFFT to transform PSS sequence into signal to be transmitted,
- 4) Add delay to transmitted signal,
- 5) Add channel gain and noise to signal,
- 6) Receive the signal,
- 7) Perform correlation with the local reference PSS sequence,
- 8) Correction peak detection,
- 9) Calculate peak delay.

#### *Detection of the delay error*

To detect the value of the error we use the RMS delay spread formula which is the difference between the ideal value of delay (which depends on the distance between the BS and the UE and the value of speed of light C) and the estimated value of delay (which is detected using the peak of the transmitted downlink signal at the UE side), the accuracy of which depends also on distance from the BS.

Value of downlink UE reception error:

$$\text{Err}_{\text{UE,DL,rx}} = \frac{1}{N} \sum_{i=1}^N |\text{Delay, est, } i - \text{Delay, ideal}|$$

RMS (Root Mean Square) of downlink UE reception error value:

$$\llbracket \text{RMS} (\text{Err}) \rrbracket_{\text{UE,DL,rx}} = \sqrt{\left( \frac{1}{N} \sum_{i=1}^N |\text{Delay, est, } i - \text{Delay, ideal}|^2 \right)}$$

Table 6 Parameters of simulations

Parameter	Value
Center frequency	3.5 GHz
Bandwidth	20 \ 40 MHz
ADC TX converter gain	90 dB
ADC RX converter gain	90 dB
Tx power at antenna output	20\30\50 MHz
nFFT size	2048\4096
SCS	15\30 kHz
Distance Between BS and UE	Min 50 m – Max 200 m
<u>Parameters for Rural Macro (RMa):</u>	
height of the base station	35 m
height of UE	1.5\3\6 m
avg. street width	20 m
avg. building height	5 m
channel	AWGN

#### 4.5.4 Simulations results

##### *The transmitted signal from base station*

We generate a PSS sequence according to 3GPP 38.211 and transform it to Tx signal (Figure 26) that would be sent by base station at 30 dBm sending power toward a receiver, this signal received at the UE in (Figure 27) is a delayed signal.

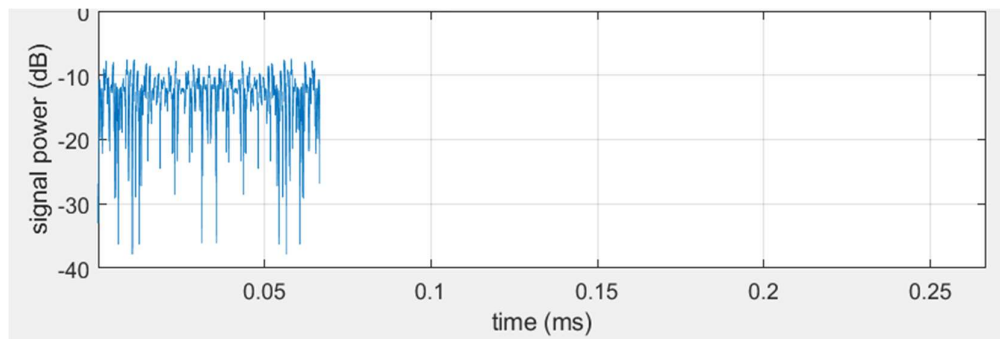


Figure 26: Tx signal from Base Station

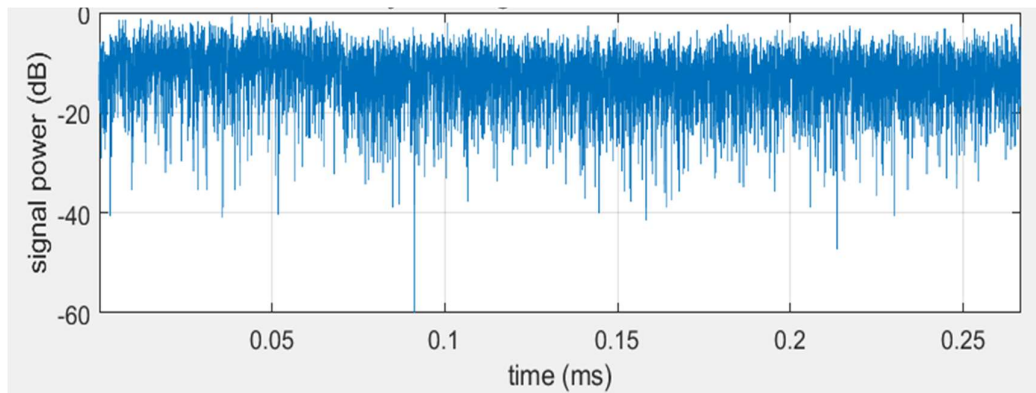


Figure 27 Delayed Tx signal that UE will receive

#### 4.5.5 Inter-correlation technique to detect the peak the UE will detect

The received signal at the UE then will be correlated with local reference PSS sequence, we obtain a peak of signal that corresponds to our received signal at the UE (shown in Figure 28). The desired propagation time that we need to know from signal detection correspond to the time of the peak. Then we can use the RMS error formula to calculate the value of RMS for each detected value of time delay.

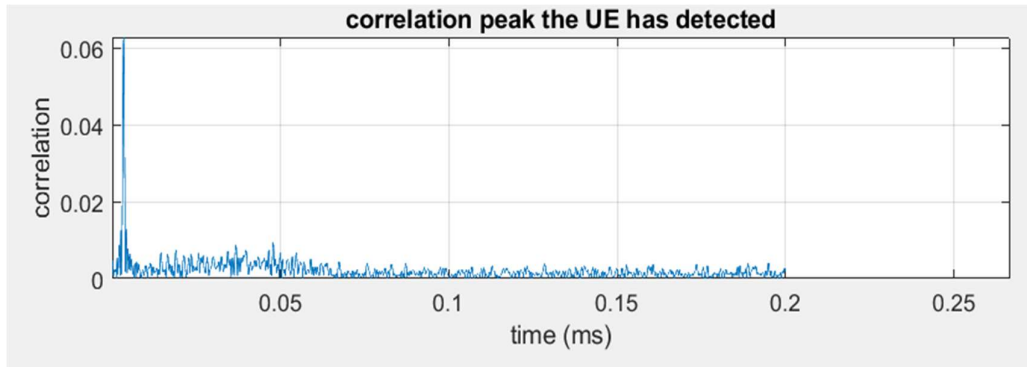


Figure 28 Correlation peak which the UE detected

#### 4.5.6 Propagation delay & Time error calculation

*Study the distance between UE and gNB in terms of synchronization budget:*

To get accurate values of propagation delay and the delay error we simulated the scenario with varying parameters including Tx power, subcarrier spacing and FFT size. Below are the results.

**Tx power = 30 dBm, SCS= 15 kHz, FFT= 2048**

- For a requirement of **400 ns** between the BS and the UE the correspondent values are:  
**d=100 meter:**

*Ideal delay = 0.333333(us), Estimated delay = 0.358073(us), error = 0.024740(us)*

*RMS (delay error) (us) = 0.010263*

*Estimated delay + RMS = 0,368336 (us)*

- For a requirement of **300 ns** between the BS and the UE the correspondent values are:  
**d=80 meter:**

*Ideal delay = 0.266667(us), Estimated delay = 0.292969(us), error = 0.026302(us)*

*RMS (delay error) (us) = close to zero (due to high SNR)*

The values of detected propagation delay and errors are dependents to the value of Tx\_power, when the SNR is too high the detection of the error becomes difficult.

**Tx power = 20 dBm, SCS = 15 kHz, FFT= 2048**

- For a requirement of **400 ns** between the BS and the UE the correspondent values are:  
**d=90 meter:**

*Ideal delay = 0.300000(us), Estimated delay = 0.325521(us), error = 0.025521(us)*

*RMS (delay error) (us) = 0.065183*

*Estimated delay + RMS = 0,390704 (us)*

- For a requirement of **300 ns** between the BS and the UE the correspondent values are:



**d=70 meter:**

$Ideal\ delay = 0.233333(us), Estimated\ delay = 0.227865(us), error = -0.005469(us)$

$RMS\ (delay\ error)\ (us) = 0.039482$

$Estimated\ delay + RMS\ (delay\ error) = 0.267347(us)$

Table 7 below summarizes the above results:

Table 7 Summary of simulation results for distance between gNB and UE.

Tx Power (dBm)	SCS kHz	Maximum allowed time error (ns) between gNB and UE via OTA technique (defined in 3GPP TS 22.104)	Distance (m) required between gNB and UE
30	15	400	100
30	30	300	80
20	15	400	90
20	30	300	70

From the above results we notice that the value of propagation delay depends on distance, where we have estimated the corresponding distance for each value of propagation delay and RMS error.

The RMS error can be lower at higher values of Tx transmission power due to high SNR, same thing can be observed for propagation delay. For same time error allowed and same SCS (SCS = 30 kHz) we gain 10 meters more for (30 dBm) than (20 dBm) of Tx power.

#### *Comparison of the results with LTE synchronization requirements*

To validate the above proposed method for the propagation delay estimation, a cross verification is performed by estimation of the delay with LTE radio information. Ideally, it is known that for 1 km usually the accuracy synchronization requirement in LTE is around 3  $\mu$ s.

**Hence for the  $d = 1000$  meter:**

$Ideal\ delay = 3.333333(\mu s), Estimated\ delay = 3.352865(\mu s), error = 0.019531(\mu s)$

The requirement of 3 (us) is respected for a distance of 1 km which correspond to LTE coverage BS radius. The value of Estimated delay= 3.352865 us can be improved by rising the  $Tx\_power$  and by applying less noise.

Or in other words, in order to cross-verify the above table estimated values of distance between the gNB and the UE in the context of 5G, we tried to determine the maximum distance between the eNB and UE in the context of 4G, where +/- 1.5  $\mu$ s between eNBs is defined. In this case, the distance obtained in 1 km, i.e. 1000 m, which respects the maximum coverage range in the case for 4G.

#### **4.6 Study the delay RMS in different SCSs and FFT sizes**

In the below simulations, we estimate the mean time error vs. distance between the gNB and the UE for different FFT sizes (2048 and 4096) and different SCSs (15 kHz and 30 kHz).

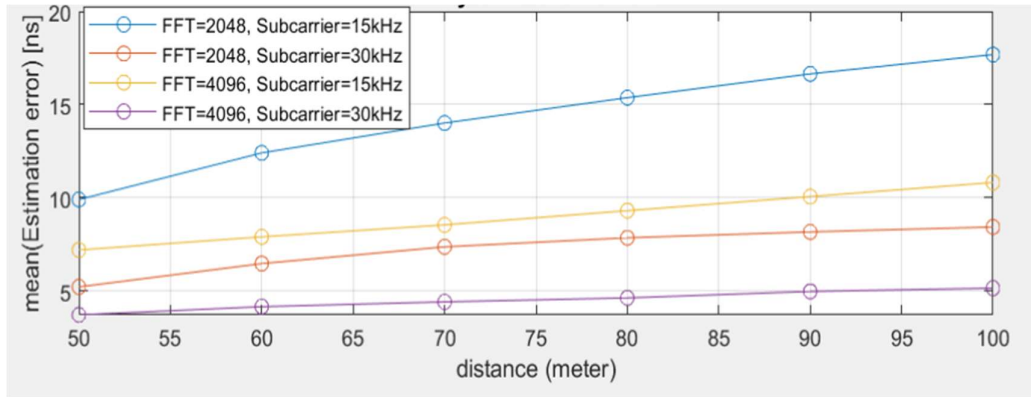


Figure 29 Value of RMS delay vs gNB-UE distance

At 50 meters: the value of RMS delay is different for each SCS and FFT value, as the distance increase the RMS delay increases in parallel but in different speeds. The RMS value of mean time error delay is much higher for (SCS=15 kHz, FFT=2048) than (SCS=30 kHz, FFT=4096). IN 5G-NR, frame structures of different numerologies are made to be adaptive, i.e., the length of (shortened) transmission time intervals (TTIs) and subcarrier spacing should be designed according to the richness of the channel. In the time domain, the subframe length of NR is 1 ms, which is composed of 14 OFDM symbols using 15 kHz subcarrier spacing and normal CP. This is doubled, i.e. 28 OFDM symbols for 30 kHz. And therefore, in 5G NR numerology with a higher SCS value, i.e. 30 kHz compared to 15 kHz, higher the throughput because of the number of radio frames per time slot being doubled. And similarly, higher the SCS, the lesser is the TTI due to the reduced length of the sub-frames. And therefore, the time error which is encountered is reduced.

#### 4.6.1 Effect of height on delay RMS

Moving forward, we shall consider the heights of the BS and the UE in our simulations by using the reflection channel mode which is depicted in report<sup>26</sup>.

In this reflection channel model, the effective channel gain will be much smaller than Line of sight (LOS) channel because of the cancellation effect when combining the signal from the direct path and the reflected path. So, to guarantee the same downlink (DL) delay estimation performance, the transmission power from the base station need to increase. Here in the simulation, it is increased from 20 dBm to 50 dBm (100 W).

<sup>26</sup> [https://web.stanford.edu/dntse/Chapters PDF/Fundamentals Wireless Communication chapter2.pdf](https://web.stanford.edu/dntse/Chapters%20PDF/Fundamentals%20Wireless%20Communication%20chapter2.pdf).

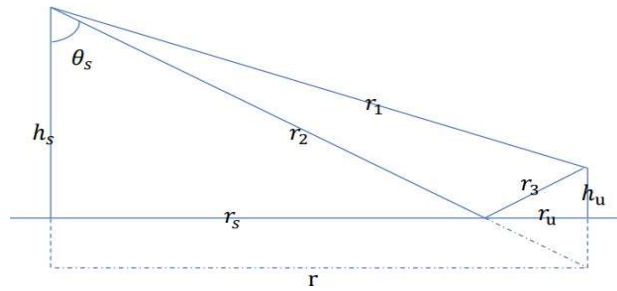


Figure 30 Reflection model of LOS by considering the heights of BS and UE

Using the reflection model, we vary the height of the receiver, and we evaluate the results of delay RMS vs a distance varying between 50 to 120 meters. Simulations results are presented in Figure 31, Figure 33 and Figure 34.

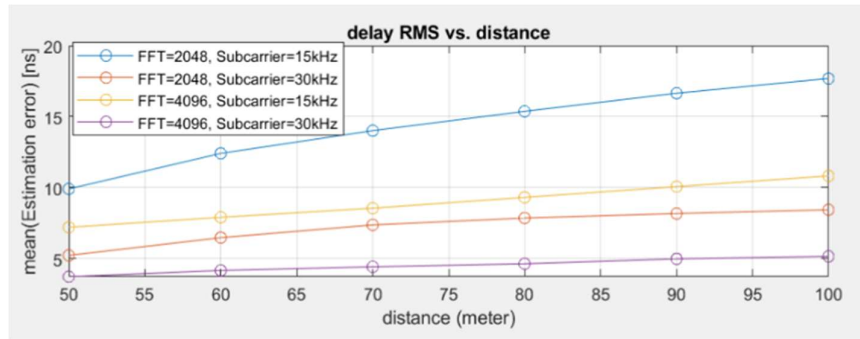


Figure 31: Delay RMS vs distance at 1.5 m UE height

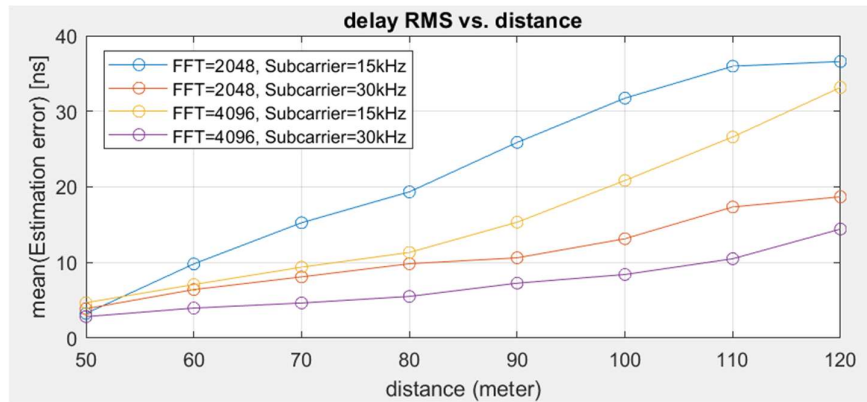


Figure 32 Delay RMS vs distance at 3 m UE height

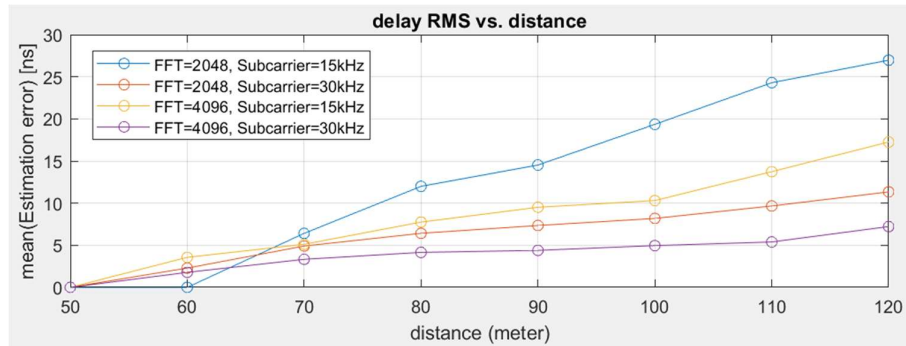


Figure 33 Delay RMS vs distance at 6 m UE height

The value of RMS error is different for each receiver height, where we can notice that for lower heights (1.5 m) the value of error is big comparing with higher heights (3 m) and (6 m). The increase of error values is due to the multiple reflected paths at lower heights. For (SCS=30 kHz, FFT=4096) the value of delay RMS is shown in Table 8.

Table 8 RMS delay w.r.t distance

Distance	RMS delay
1.5 meters	25 ns
3 meters	15 ns
6 meters	7 ns

Antenna height of the receiver has a major impact on performance in a variety of ways dependent upon the frequency in use, antenna type and size. In general, the higher the antenna the better its performance will be.

#### 4.7 Rural Macro (RMa) model in LOS and NLOS

For the presented evaluation we are assuming rural macro model deployment of 5GS. Comparing to different NPN deployment, here we assume Public Network Integrated Non-Public Network (PNI-NPN) for the smart manufacturing. In other words, macro base station is utilized to support time synchronization between UE and gNB. The pathloss models summarized in Table 7.4.1-1 in 3GPP Technical Report (TR) 38.901 [3GPP20-38901] are used in order to see the variations of error and time delay in LOS, Non line of sight (NLOS) and to investigate the variation also in a shadowing environment. Results of simulations are presented in Figure 34Figure 35Figure 36.

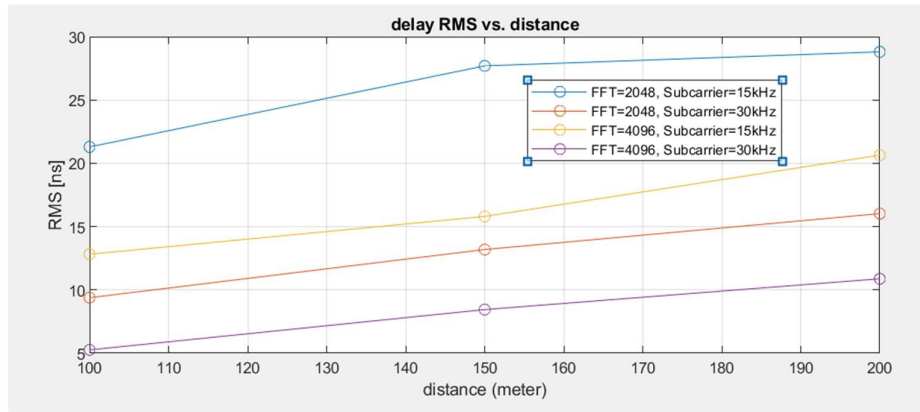


Figure 34: Variation of delay RMS in terms of distance for LOS without shadowing

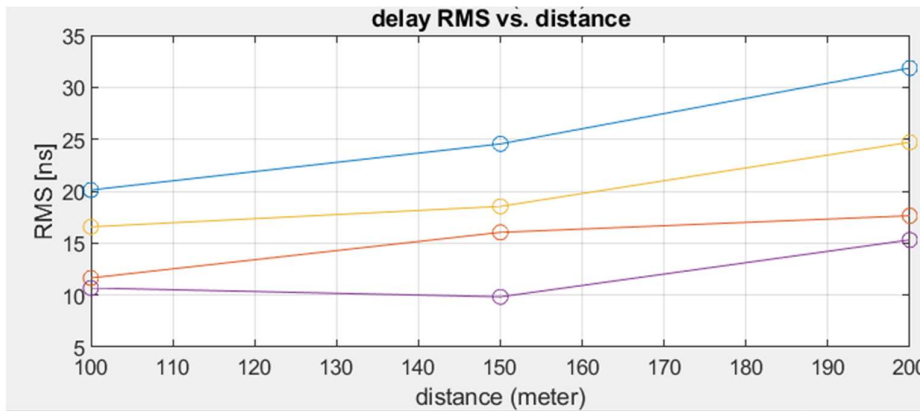


Figure 35 Variation of delay RMS in terms of distance for LOS with shadowing

The increase of delay RMS when adding shadowing are more considerable in 15 kHz SCS than the value in (30 kHz SCS). The value of the error stays stable for (FFT=4096, SCS=30 kHz) for a distance of 150 m, and then increases to a higher value for 200 m.

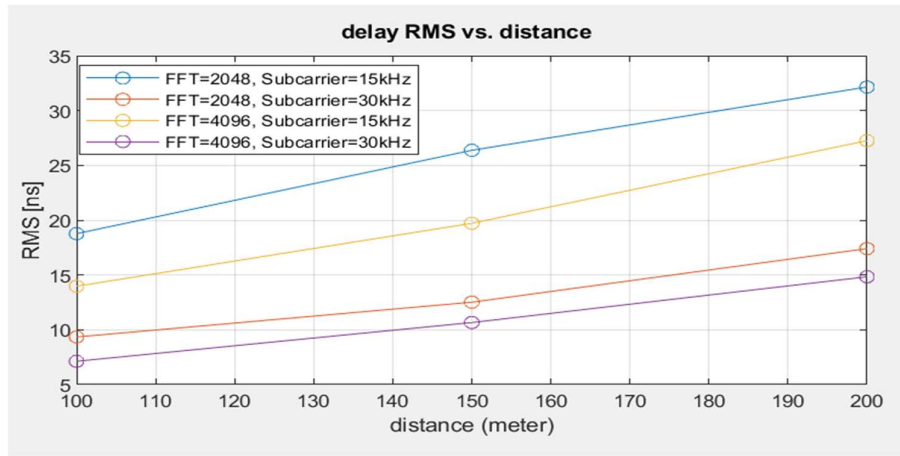


Figure 36 Variation of delay RMS in terms of distance for NLOS without shadowing

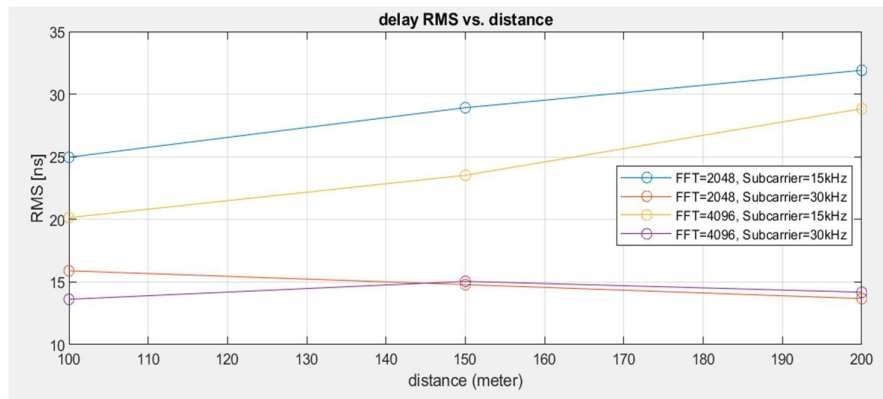


Figure 37 Variation of delay RMS in terms of distance for NLOS with shadowing

#### 4.7.1 Discussion of results

**For 15 kHz SCS:** The values of RMS error changed for higher values in line of sight when adding shadowing, where we did not notice any significant changes in NLOS.

**For 30 kHz SCS:** The values of RMS error have increased in LOS when adding shadowing but with low variations comparing with the increase in 15 kHz SCS.

In NLOS with shadowing the increase of the error is slow for a distance up to 150 m, and the error remains at the value reached at 150 m for longer distance. Higher SCS values provide lower error values for both LOS and NLOS, and it can be less affected by the environment shadowing especially in NLOS transmission.

Table 9 summarizes the above results:



Table 9 Summary of simulations results for RMS value in different scenarios

SCS (kHz)	Visibility	Shadowing effect	RMS Value (ns)
15	LOS	With	32
30	LOS	With	25
15	NLOS	Without	33
30	NLOS	Without	28

From the above simulation results, the most suitable delay RMS was at a higher value of SCS and FFT, either by varying heights toward high values or under shadowing environment in LOS or NLOS. For a network deployment at a frequency of 3.5 GHz the maximum SCS that can be used and deliver lower value of delay RMS values is 30 kHz.

#### 4.8 Conclusions and recommendations

Internal 5GS time synchronization is an essential functionality in an integrated 5G-TSN based industrial network. The 5GS can offer several internal time synchronization solutions that lead to different amounts of time error when relaying a TSN GM clock reference value between the 5GS ingress and egress. For the most demanding industrial application, a time error budget of 900 ns is assigned to the 5GS in an integrated 5G-TSN network. This report provides details on how 5GS can support such a time error budget.

A time error analysis is described for a time synchronization solution scenario typically considered in the manufacturing deployment. It is concluded that the existing solution defined by the ITU-T standards for realizing time synchronization over the transport network can be used to support some relevant industrial network scenarios (e.g., 5G-TSN based industrial network). For the analytical analysis, concerning the realization of time synchronization over the radio interface, we analysed two different techniques and we concluded that the RTT based method is the only method that is suitable for realizing the most demanding uncertainty requirements. In particular, the need for an RTT based method becomes even more important for the case where there are two radio interfaces in the 5GS ingress to egress used for relaying TSN GM clock signalling.

Furthermore, taking RTT as baseline, an extensive link level simulation analysis is performed. We have proposed an algorithm to estimate the propagation delay for RTT based estimation method. The resulting analysis shows RTT based method is the only solution that can estimate the propagation delay and maintain the requirements for time error. From the link level simulation analysis, it can be concluded that considering UE with LOS will have less time error compared to NLOS. Furthermore, the UE antenna height also has an effect on the time error (i.e., for a higher the antenna, less time error can be observed).

Also, NLOS between UE and gNB with shadowing effect will have better accuracy compared to “without shadowing” scenario. A similar effect is observed when LOS is assumed between UE and gNB. Here LOS will return more accuracy. RMS error values are lower for higher SCS for a 3.5 GHz deployment. Future link level simulation work is planned to take into consideration the below mentioned points.

- For a different frequency band other than 3.5 GHz, for example sub-1GHz and mmWave,



- For different channel models, including channel model closed to factory deployment (standalone Non-public network),
- By considering mobility of the UE.



## 5 5G positioning evaluations

Reliable positioning with high accuracy is important for navigation and tracking of devices, AGVs and persons in a large set of use cases in smart manufacturing. In this chapter we evaluate the performance of 5G radio-frequency-based positioning in a realistic industrial environment. Building upon the methods for positioning techniques as described in 5G-SMART Deliverable D5.1 [5GS20-D51], we focus on signals between 5G gNB and UE utilizing the time dimension time-of-arrival (TOA, trilateration) or time-difference-of-arrival (TDOA, multilateration). These positioning methods are both enhanced with high bandwidth as key features in 5G NR. The typical 100 MHz bandwidth has been used both for FR1 and FR2 positioning estimations. The positioning accuracy and performance have also been compared with 400 MHz BW for FR2 where more details of the multipath radio channel can be utilized. The angle of arrival (AOA) and positioning by means of triangulation could be added as a next step to further improve performance based on multi-antenna configurations as specified in the 5G radio access technology. The AOA functionality is promising as a complement to TOA and TDOA, however not evaluated in this chapter. The large interest and growing needs for enhanced positioning functionality are considered in Release 17, targeting high-precision indoor environments and industrial IoT use cases.

Similar to the industrial 5G deployment used in the 5G-SMART trial site at Fraunhofer IPT institute, one realistic environment for evaluations of positioning performance is selected. The environment is modelled both by means of the 3GPP statistical radio propagation channel and with a geometric 3D ray tracing channel where the specific objects in the trial are included. The positioning accuracy obtained from the models is related to the requirements provided, also as a comparison between the general 3GPP model and the specific geometry of the trial in the factory environment. The radio signals and, as a consequence, the positioning accuracy, are very much impacted by obstruction of objects and the multipath situation between UE and gNBs. We will thus draw conclusions on the positioning performance and on the validity of the 3GPP channel model when compared to the geometric channel model for the specific trial factory.

### 5.1 Evaluation methodology

The report considers input from one 5G-SMART trial deployment and provides details on two different evaluation methodologies. First, we have evaluated the indoor 5G-SMART trial deployment by simulations based on a geometric model (selected: 3D ray tracing model). Parallel to this, the 5G-SMART trial deployment is analyzed using a statistical 3GPP channel model. Finally, a comparison of the impact on positioning accuracy between the deterministic ray tracing model and the stochastic model is made. Figure 38 shows the evaluation methodology. The positioning performance is evaluated by considering:

- Line-of-sight probability (both models).
- Ranging performance (ray tracing model).
- Geometric effects (statistical model).
- Full positioning performance (both models).

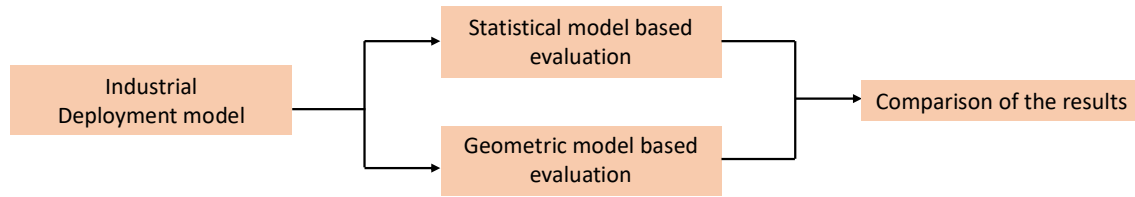


Figure 38 Evaluation methodology for positioning mechanism

The trial deployment model is utilized for the geometrical model-based evaluation and is also the baseline for the statistical model-based evaluation.

## 5.2 Geometric model-based evaluation

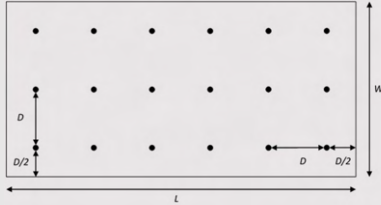
The analysis and results presented in this section are based on the use of a geometric channel model, more specifically a commercial Ray-Tracing software called Altair Winprop<sup>27</sup>. A fully deterministic approach is followed which uses a comprehensive 3D map of the environment, including a database of materials and their properties related to radio wave propagation (reflection, transmission losses, etc). This approach is complementary to the statistical model presented in the next section and together they can give valuable insights on the performance of 5G positioning systems as well as provide indications for potential areas of optimization.

### 5.2.1 Simulation setup

The simulation setup used for these investigations is based on 3GPP TR 38.901 [3GPP20-38901] and specifically on Section 5.3.4 of that document which corresponds to the indoor factory scenario. The basic parameters as adopted in this study are given in the following table Table 10.

<sup>27</sup> <https://www.altair.com/resource/altair-winprop-datasheet>.

Table 10: Simulation parameters for geometric modelling of the indoor factory scenario

Parameters	Values
Hall size	120x60 m
Room height	10 m
BS antenna configurations	1 element, Isotropic antenna gain pattern
UE antenna configurations	1 element, Isotropic antenna gain pattern
BS deployment	<p>18 BSs on a square lattice with spacing <math>D</math>, located <math>D/2</math> from the walls. (<math>L=120</math> m x <math>W=60</math> m): <math>D=20</math> m</p>  <p>BS-height = 6 m</p>
UE distribution	<p>Uniform dropping at each 2D distance of 1 m UE height = 0.5 m, 1.5 m</p>
Carrier frequency	3.5 GHz (FR1), 28 GHz (FR2)
Bandwidth	100 MHz, 400 MHz

The simulation environment was extracted from a highly detailed 3D model provided by Fraunhofer IPT which represents a realistic example of a factory shop floor. The following Figure 39Figure 40show some aspects of this 3D model.

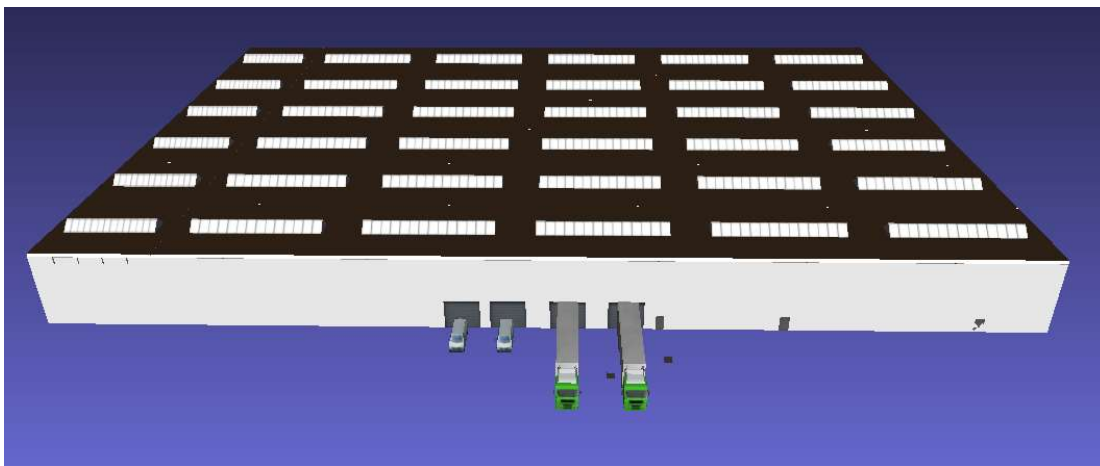


Figure 39 Outside view of 3D factory model

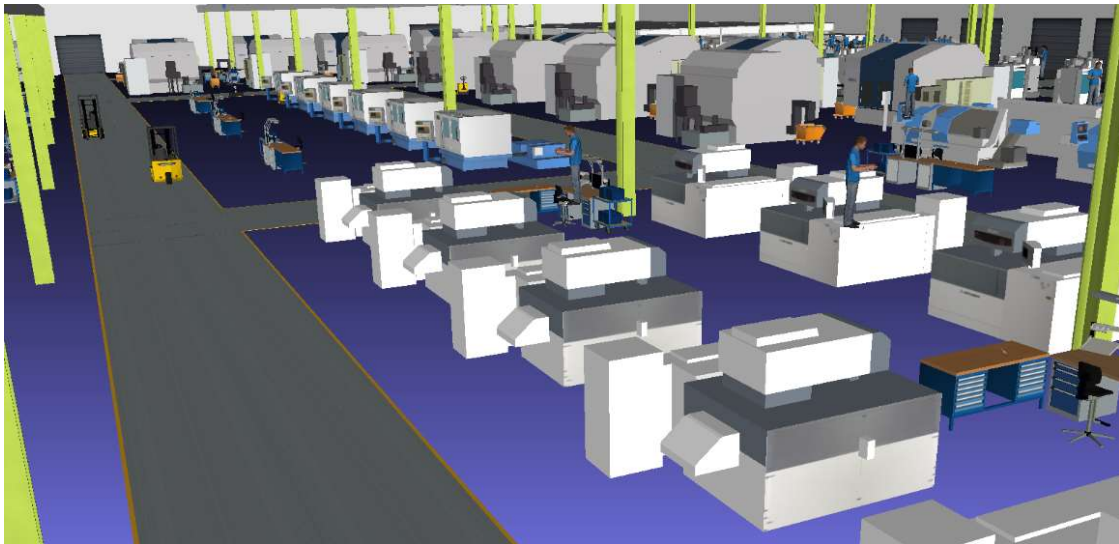


Figure 40 Inside view of 3D factory model

As seen from the pictures, the 3D model corresponds to a typical factory shop floor with multiple pieces of manufacturing equipment, areas with varying levels of clutter, some people as well as a few furniture. In addition, there are horizontal and vertical metallic beams supporting the building structure. In terms of the materials used, most of the objects in the environment are metallic, whereas the floor is made of concrete and the rooftop is made of metal and glass.

The following shows this environment as configured within the Altair WinProp simulation software. The Base station (can be considered as Radio Dot according to deployment considered for Fraunhofer IPT site) deployment topology is visible here with 18 BSs distributed every 20 m and labelled as A01, A02, etc.

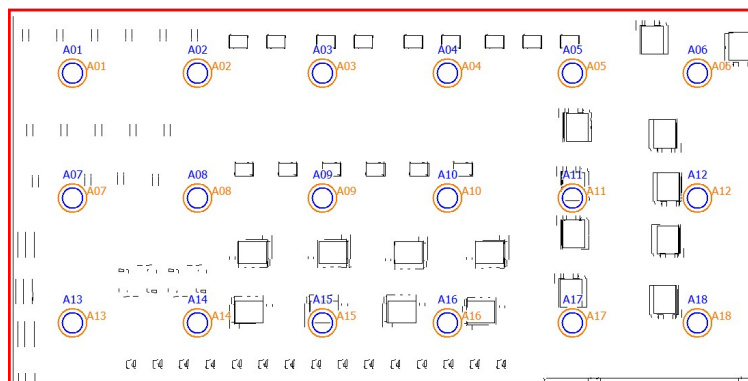


Figure 41 Deployment topology of BS in factory

### 5.2.2 LoS probability

For a time-of-flight (ToF)-based positioning technology as TOA or TDOA, distance estimation relies on the detection of the direct path between the transmitting and receiving nodes. Therefore, it is expected that the distance estimation accuracy is directly related to the existence of a line-of-sight (LoS) signal between the BS and UE. An appropriate deployment topology, such as the one described earlier, is required to maximize the availability of LoS connectivity between a UE and multiple BSs in the area of interest.

In this section, the LoS / non-LoS areas for the given scenario are estimated through a ray-tracing propagation analysis. As an example, the following figure shows the LoS visibility from the top-left BS (named A01) and all possible UE positions within the simulation area. Green areas correspond to positions with a LoS signal between the BS and UE whereas red areas correspond to positions where the received signal consists of reflected and/or diffracted rays (no direct LoS path). Finally, the blue areas correspond to positions which lay within the inside of machinery or other objects (clutter) and are therefore omitted from the following analysis.

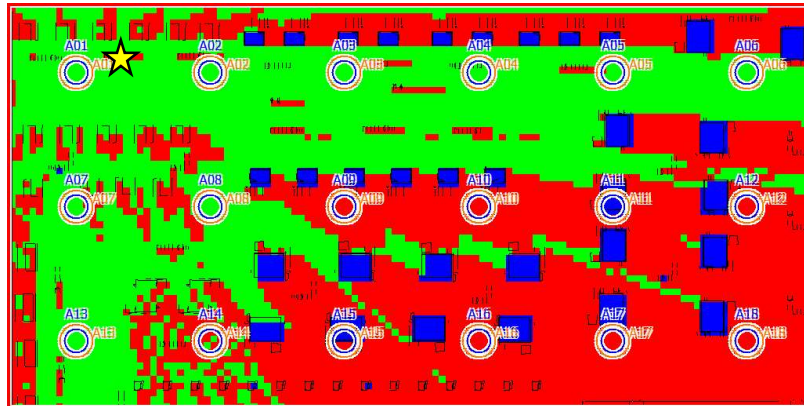


Figure 42 LoS visibility for A01 (top-left), green: LoS, red: obstructed-LoS, blue: Non-LoS. (UE height = 0.5 m)

As seen in Figure 42, a single BS can cover a large portion of the factory area when it is positioned at a high enough point (6 m in this scenario) and when the clutter is not too high (up to 3.5 m in this scenario). Another factor that influences the availability of a LoS path is the UE height. The results shown in Figure 42 consider a UE at a height of 0.5 m, when this is increased to 1.5 m there is a corresponding increase of the LoS area as shown in Figure 42.

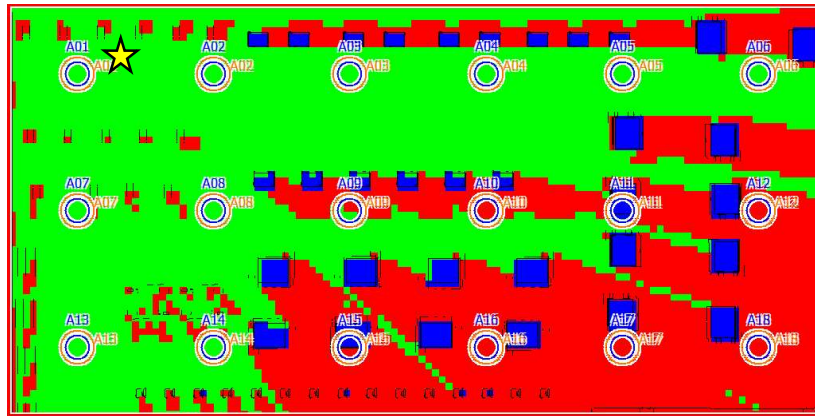


Figure 43 LoS visibility for A01 (top-left), green: LoS, red: obstructed-LoS, blue: Non-LoS. (UE height = 1.5 m)

The analysis shown in previous figures showed the LoS availability for a single BS. Using appropriate post-processing methods, the number of LoS links per UE position can be calculated as shown in Figure 44 for a UE height of 0.5 m. As shown, there is a large variance of LoS availability, with some UE positions having LoS visibility to all 18 BSs, while others have visibility to only 2-3 BSs. Such an analysis may be used to provide deployment guidelines which will optimize the deployment of BSs in a way that the variance of LoS visibility is reduced to provide a more homogeneous positioning performance.

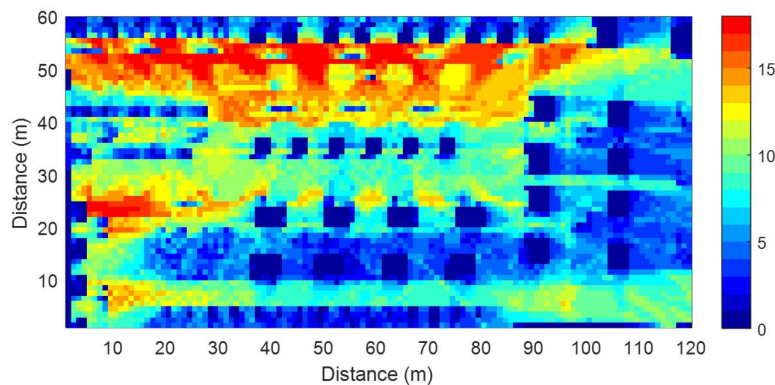


Figure 44 Number of BSs with LoS visibility for all different UE positions (UE height = 0.5 m)

Figure 45 shows the LoS visibility results for a UE height of 1.5 m. As expected, the LoS visibility is significantly improved due to reduced blockage between the UEs and BSs positions. For this scenario, an even larger area exists where there is visibility with a large number (>15) of BSs.

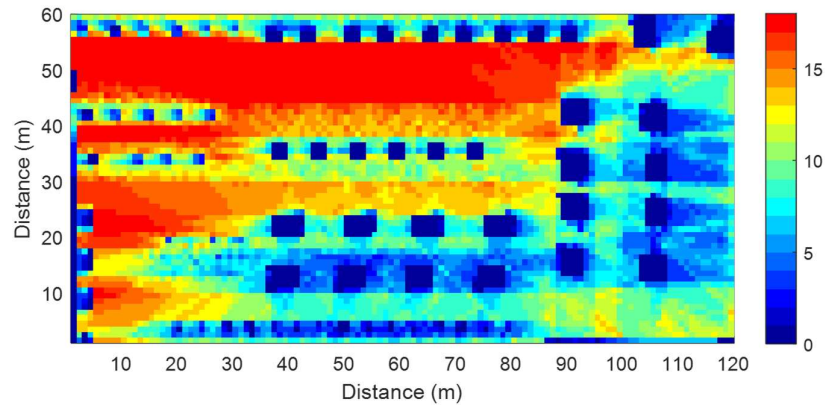


Figure 45 Number of BSs with LoS visibility for all different UE positions (UE height = 1.5 m)

Beyond the geometric visualization of the LoS visibility results it is also interesting to examine the statistics of LoS visibility in the scenario of interest. Figure 46 shows the Complementary Cumulative Distribution Function (CCDF) of the number of BSs in LoS for UE heights of 0.5 and 1.5 m. The CCDF demonstrates the probability of having LoS visibility with at least  $N$  BSs. For example, for a UE height of 0.5 m there is 52% probability of LoS visibility with at least 8 BSs, whereas, for a UE height of 1.5 m the probability rises to 66%.

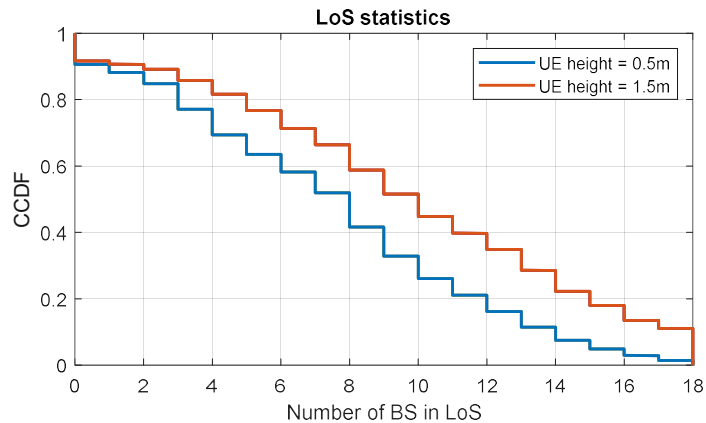


Figure 46 Statistics of BSs with LoS visibility for all different UE positions

Such statistical figures can give an indication of the expected positioning performance. For the case of multilateration i.e., the estimation of position through multiple distance measurements from known points, the minimum number of distance estimations for an unambiguous position estimation in 3D is 4. From Figure 46 the probability of LoS visibility with 4 BSs is 76% for a UE height of 0.5 m and 85% for a UE height of 1.5 m.

### 5.2.3 Ranging performance

This section outlines the findings related to the BS-UE distance measurement (referred to also as ranging) accuracy for the scenario of interest. The ranging estimation process involves the estimation of the Power Delay Profile (PDP) of the wireless channel using appropriate signal processing methods.

Once the PDP is estimated, the first ray to arrive at the receiver is considered to correspond to the LoS path and therefore its delay is converted into a distance estimate. This method has some fundamental limitations:

- The ability to resolve the delay of the first ray is directly related to the signal bandwidth
- The first signal component to arrive might not necessarily correspond to a LoS signal

Consider the example of Figure 47 where the blue lines correspond to the actual PDP, whereas the red lines correspond to the PDP perceived by the receiving device. Two main differences can be observed:

- The delay resolution of the red lines is limited and directly related to the signal sampling rate. In this example, the sampling rate is 100 MHz, therefore the delay resolution is 10 ns. Within each 10 ns interval, all PDP components appear to the receiver as a single tap.
- The delay of the first significant PDP component may have a positive or negative offset from the true delay value, depending on the synchronization between the transmitting and receiving devices.

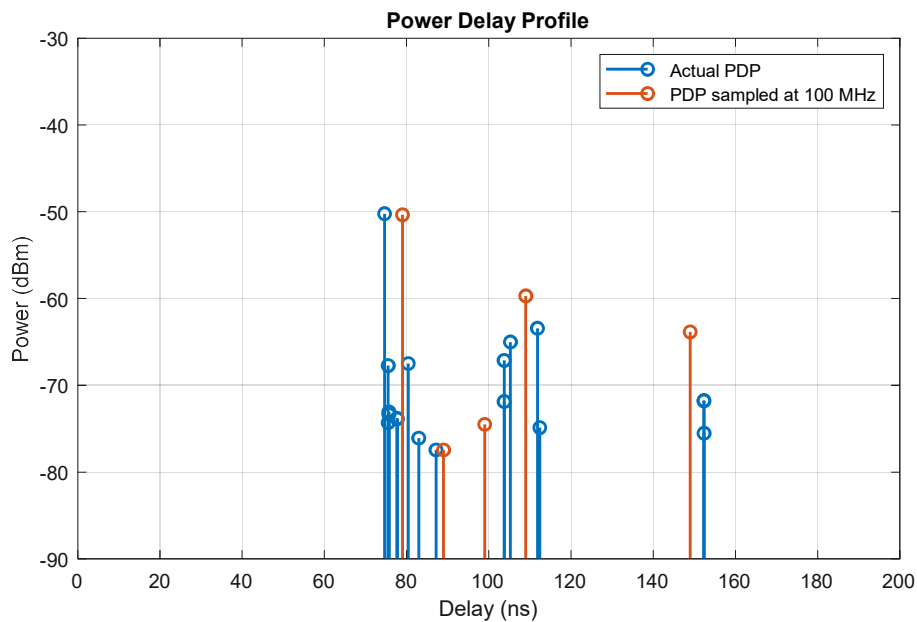


Figure 47 Power Delay Profile (actual and estimated with 100 MHz sampling rate)

Figure 48 shows another source of ranging errors, where the first PDP path is below the noise floor (-90 dBm in this example) and therefore is undetectable by the receiver. Instead, in the absence of any other filtering mechanism the receiver will perceive the second PDP tap as the first one, introducing significant error into the estimated distance.

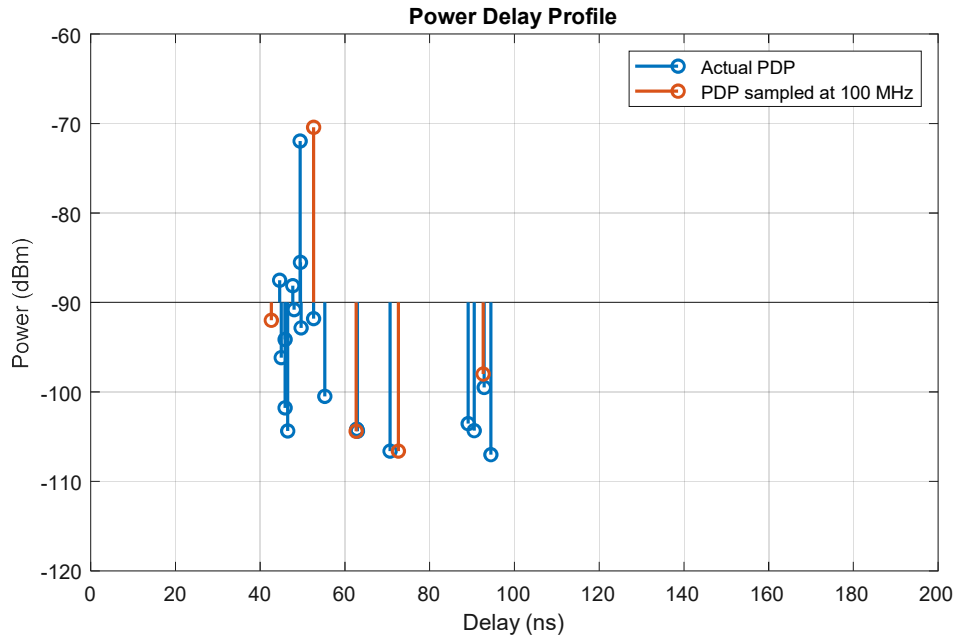


Figure 48 Power Delay Profile (actual and estimated with 100 MHz sampling rate)

In advanced (commercial) systems the bandwidth and LoS obstruction limitations may be addressed through super-resolution algorithms and LoS / non-LoS classification methods, respectively. For this project however, the baseline approach outlined above can provide adequate performance for analysing the effects of non-LoS propagation, variations in propagation between different frequency bands and the effect of available signal bandwidth. Hence any further optimization is considered outside the scope of this work.

Figure 49, shows the ranging performance for a single BS and all UE positions in the region of interest for FR1 and FR2 at two different heights. Each pixel in this figure shows the ranging error between A01 and a UE positioned at that pixel. White pixels correspond to areas where the machinery is located and therefore are omitted from this analysis. It is interesting to examine Figure 49 (a) in comparison with Figure 42, where the LoS visibility for A01 is shown.

From Figure 49 (a), it is seen that ranging errors around 1 m or less are obtained in most LoS locations, however the errors can become significantly higher, reaching 10 m or more in non-LoS areas. Similar results are obtained for other BSs, therefore these are omitted in the interest of brevity. Figure 50, shows the error statistics for all BSs in terms of the Cumulative Distribution Function (CDF) of the ranging error. The legend contains information on the CDF at 90 % Confidence Level (CL90) which is a typical metric for such applications. In this specific example, the CL90 of the error is between 1.5 m and 3.3 m, which translates to the error being 1.5 m – 3.3 m or less at 90% of the positions.

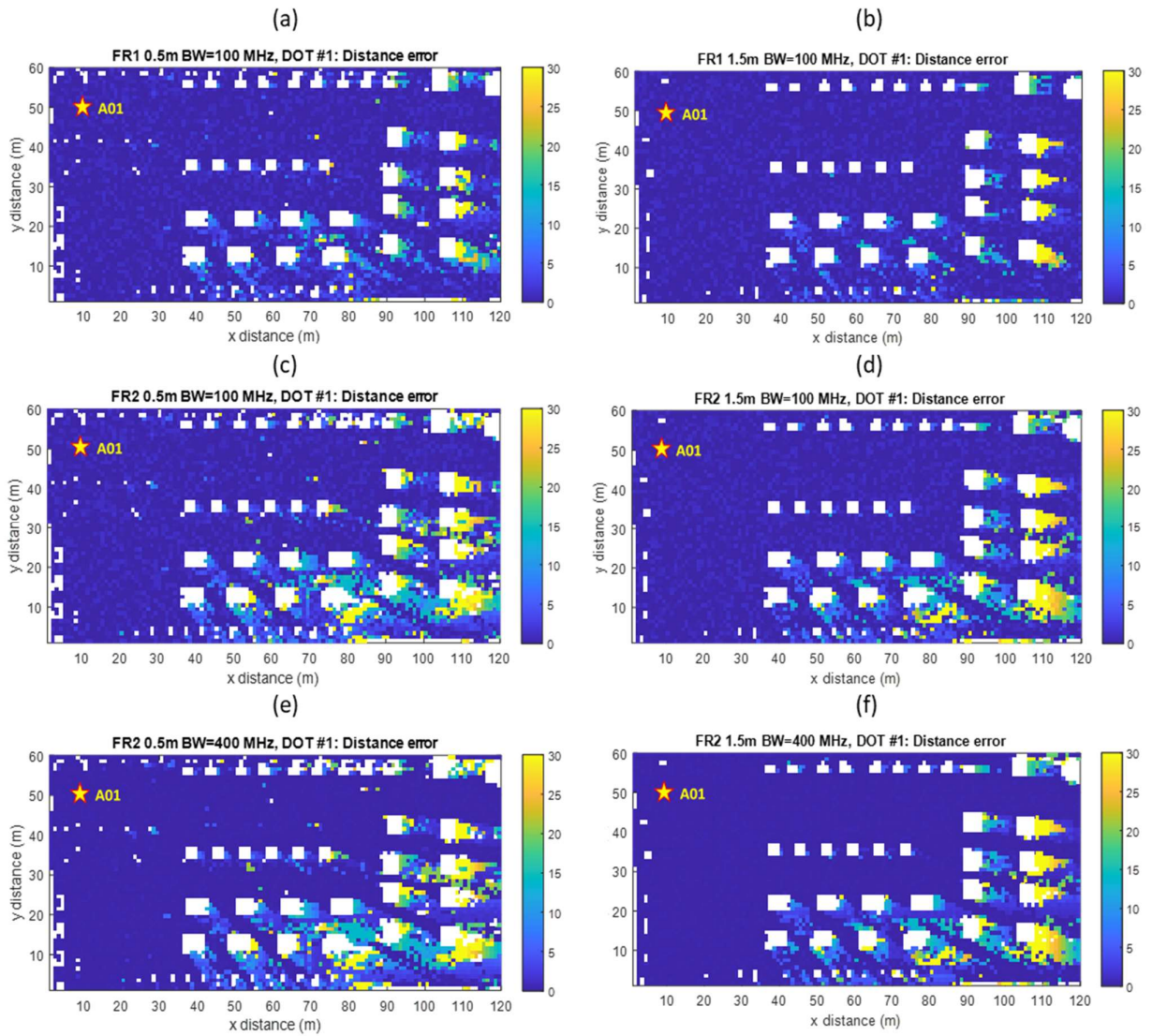


Figure 49: Distance measurements (ranging error)

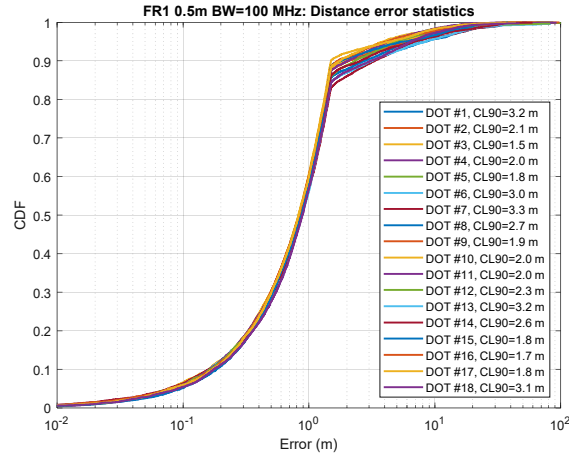


Figure 50 Ranging error statistics for all BSs (FR1, 100 MHz, UE height = 0.5 m)

Several observations can be drawn from Figure 50. Firstly, there are two distinct regions (below and above 1.5 m error) with a different slope. These regions are related to the two main limitations of the ranging algorithm mentioned previously, more specifically, the finite signal bandwidth and the non-availability of a LoS path. In detail, the first region (up to 1.5 m error) corresponds to the finite resolution offered by the 100 MHz bandwidth which corresponds to a sampling time of 10 ns. Assuming a uniformly distributed synchronization, the potential error becomes  $(10 \times 10^{-9}) \times (3 \times 10^8) = 3 \text{ m}$  or  $\pm 1.5 \text{ m}$  when synchronization occurs around the nominal time. The second region corresponds to errors coming from the non-LoS regions. In these regions the error is significantly higher than the synchronization error, hence a logarithmic x-axis is used to capture the whole range of errors.

In Figure 49 (b) UE height of 1.5 m has been used. When compared with Figure 49 (a) we see a similar error performance, however, the errors are more localized due to the larger LoS areas compared to those for the case of a lower UE height of 0.5 m. The error statistics in Figure 51 also show a similar trend; therefore, the first segment of the error CDF ( $< 1.5 \text{ m}$ ) remains unaffected, however in this scenario the amount of non-LoS locations is smaller and can be estimated to be 5-10% depending on the BS of interest. In Figure 49(c) the results for FR2, i.e. for a system with a mm-wave carrier frequency at 28 GHz. Comparing these results with Figure 49 (a) for FR1 (3.5 GHz) there are higher errors in non-LoS regions. This can be attributed to the higher attenuation at this frequency which limits the amount of multipath. Hence, in non-LoS regions there are fewer paths and therefore the probability of choosing a path which is further away from the true distance (and thus making a larger error) is higher. The error mechanism outlined above is also visible at the statistics plot Figure 52, where a 15-25% of positions in non-LoS can be estimated from the breakpoint location at the 1.5 m error. This is an important finding, as it is showing that a move of 5G to the highest frequencies does not come without limitations, especially for the case of using the same bandwidth configuration of 100 MHz as in FR1.

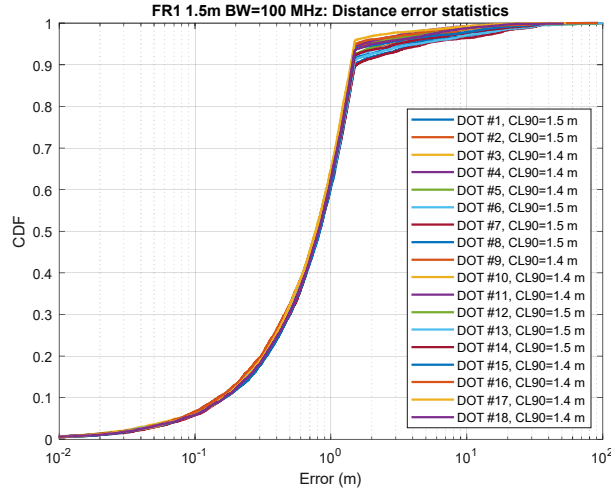


Figure 51 Ranging error statistics for all BSs (FR1, 100 MHz, UE height = 1.5 m)

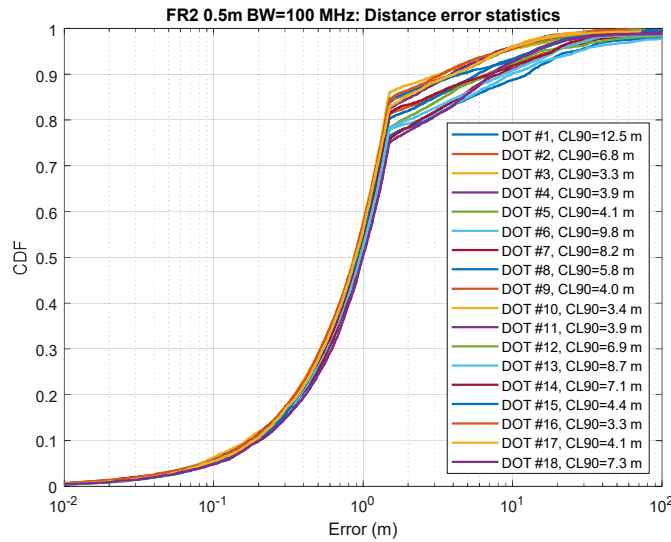


Figure 52 Ranging error statistics for all BS (FR2, 100 MHz, UE height = 0.5 m)

Figure 49 (d) shows results for FR2 and a UE height of 1.5 m. The results in comparison to Figure 49 (c) are clearly improved, however, the errors are still higher than the corresponding case of FR1. The above observations are also confirmed from the plot in Figure 53, where the distance error statistics are worse than the corresponding FR1 results of Figure 51.

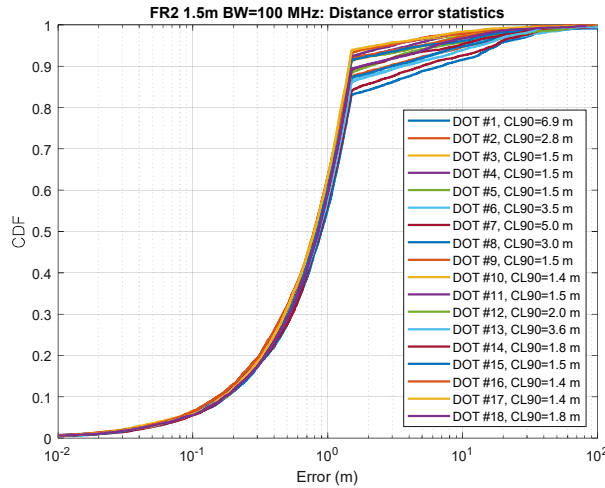


Figure 53 Ranging error statistics for all BSs (FR2, 100 MHz, UE height = 1.5 m)

The results in Figure 49 (e) correspond again to the FR2 (mm-wave) scenario, however, for the larger bandwidth that is available at that band which is 400 MHz. A comparison of this figure with Figure 49 (c) shows that even though there is no visible improvement in the non-LoS performance, there is a significant improvement in the LoS regions. The improvement in LoS performance for the case of 400 MHz of bandwidth is more clearly observed in the statistics plots in Figure 54. Here, as expected, the first segment of the distance error CDF is now moved from the 1.5 m to 37.5 cm (a factor of 4) due to the 4-times improvement in signal bandwidth and corresponding increase of sampling rate. In contrast to this result, the second CDF segment which relates to errors due to non-LoS propagation remains unaffected from the bandwidth improvement.

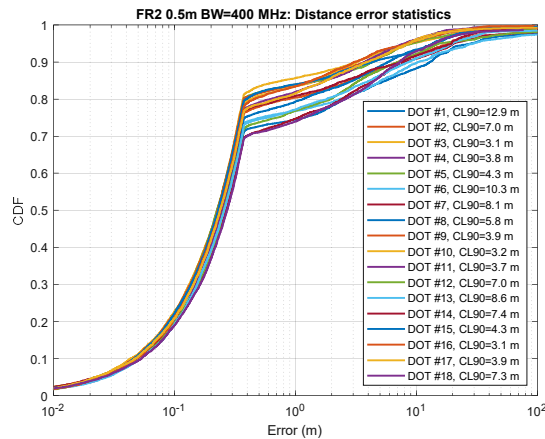


Figure 54 Ranging error statistics for all BS (FR2, 400 MHz, UE height = 0.5 m)

In Figure 49 (f) the results for FR2, 400 MHz and a UE height of 1.5 are shown. Here again, there is a clearly observable improvement in the LoS areas, whereas the non-LoS areas show significant errors.

The error statistic plots in Figure 55 confirm the improvement of LoS performance as well as the lower errors due to non-LoS propagation for this higher UE height. It is interesting to note that for this scenario there are several BSs (Radio Dots) with ranging errors below 1 m at confidence level of 90 %.

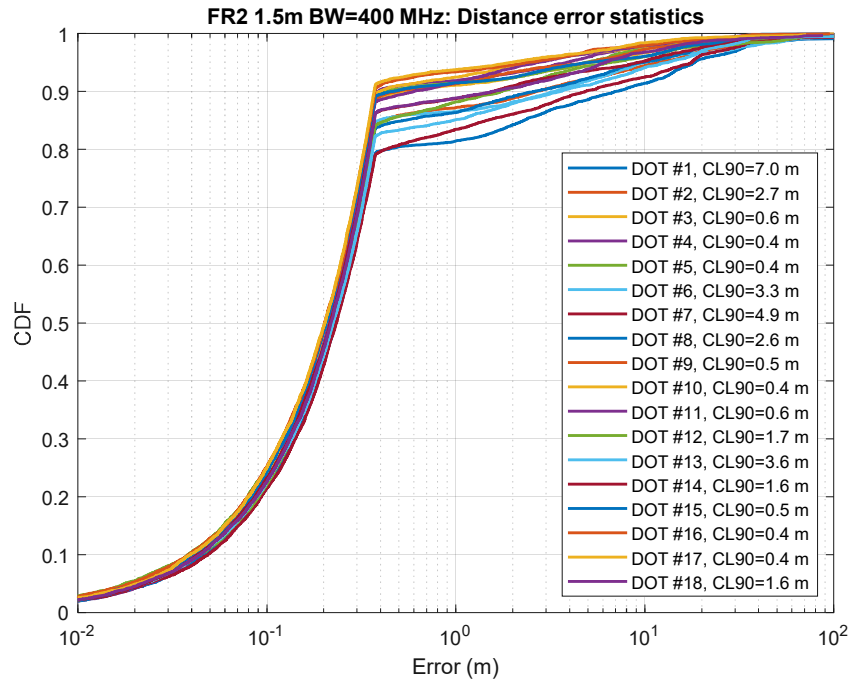


Figure 55 Ranging error statistics for all BSs (FR2, 400 MHz, UE height = 1.5 m)

#### 5.2.4 Positioning performance

So far, the performance of distance estimation was evaluated, however, the goal is to estimate the position of a UE within the area of interest. As mentioned before, a common position estimation method uses the estimated distances from multiple BSs through a process known as trilateration (for 3 known points) or multilateration (for N known points) as shown in Figure 56.

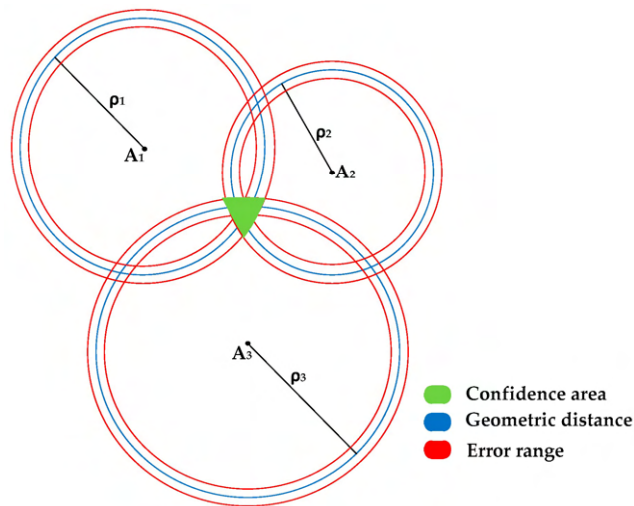


Figure 56 Trilateration (taken from [KR+16])

Clearly, the number of distance measurements to be used by the multilateration algorithm can influence the positioning performance. Therefore, a trade-off needs to be made between exploiting the information from reliable distance measurements (e.g. when BS is in LoS) and avoiding potential errors introduced from unreliable measurements (e.g. when BS is in non-LoS). Advanced methods exist to determine and weigh accordingly between sources of measurements with varying levels of reliability; however, these are considered beyond the scope of this work. For this analysis, the assumption taken was to assume that the 6 measured distances with the lower values are considered during multilateration. It is expected, that in most cases this straight-forward assumption will lead to a selection of the 6 nearest BSs, which are the ones where LoS is most likely.

Using the estimated distances from multiple BSs it is possible to estimate the position of the UE. For this analysis it was assumed that from all measured distances the 6 lower values would be used. Also, it is assumed that the BS positions are known in advance from the positioning engine.

The plots in Figure 57 shows the positioning error throughout the area of interest for different UE heights. Please note that contrary to previous plots the results shown here correspond to the positioning estimate when combining information from multiple BSs (6 as mentioned above) and not just for BS A01. Moreover, the positioning errors are expressed as two components corresponding to the azimuth plane error (x and y axes) and elevation / height plane error (z axis).

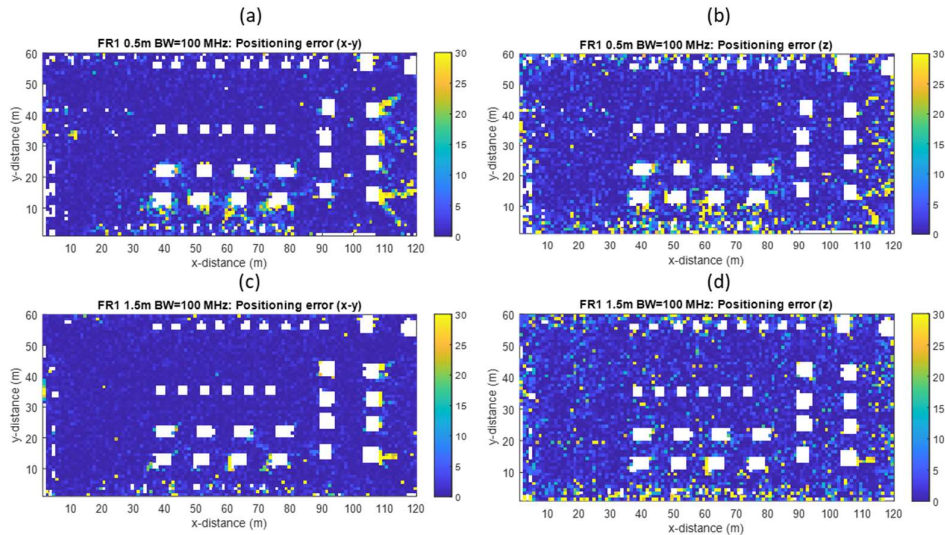


Figure 57 Positioning error in azimuth plane (X,Y) and elevation plane (Z) (FR1, 100 MHz, MS height = 0.5 and 1.5 m)

Figure 57 (a) and (b) above show results which are expected from previous analysis, that is, a low error in areas with LoS visibility to many BSs and higher error in areas with limited LoS visibility. It is also interesting to note the correlation between the positioning error performance and the LoS visibility shown in Figure 44.

Regarding the error levels in the x-y and z axes, it is clear that the latter show a higher error than the former. Such behaviour could be attributed to using the same height for all BSs, which in turn can lead to a reduced diversity between different height measurements. Figure 57 (c) and (d) show the errors for FR1 and a UE height of 1.5 m. As expected, the positioning error is reduced compared to the case of a UE height of 0.5 m.

Figure 58 show the errors for FR2 and a UE height of 0.5 and 1.5m, respectively. As in the case of ranging errors, the increased propagation losses at the mm-wave frequencies are resulting in higher errors than the corresponding case of FR1. The positioning error for 1.5m is significantly reduced compared to the case of a UE height of 0.5 m.

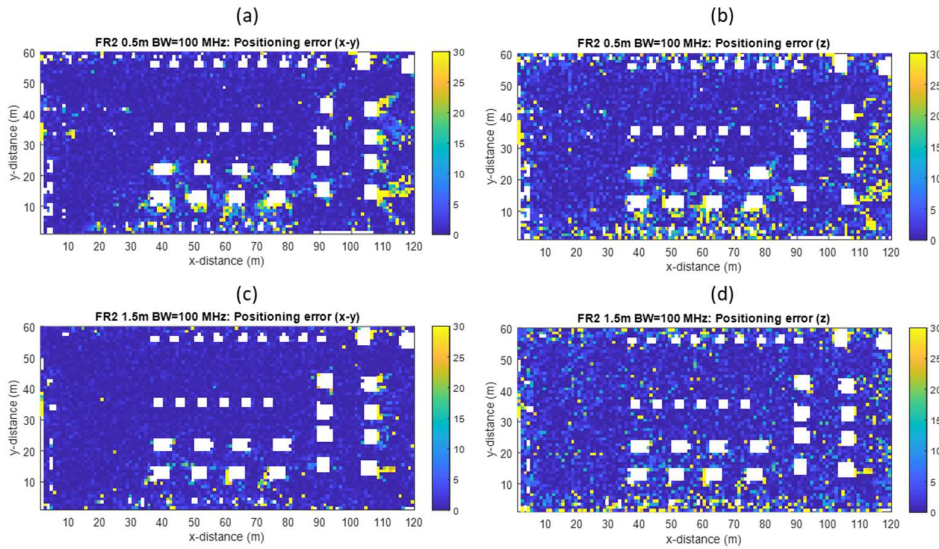


Figure 58 Positioning error in azimuth plane (X,Y) and elevation plane (Z) (FR2, 100 MHz, MS height = 0.5 and 1.5 m)

Figure 59 (a) and (b) show the errors for FR2, MS height of 0.5 m with a bandwidth of 400 MHz. As in the case of ranging errors, the positioning error is significantly reduced in LoS areas, however the errors remain at relatively high levels in non-LoS. The final set of positioning error figures (Figure 59 (c) and (d)) correspond to the case of FR2, UE height of 1.5 m and bandwidth of 400 MHz. This is the best case scenario where a wide range of positions show errors at 1 m or below.

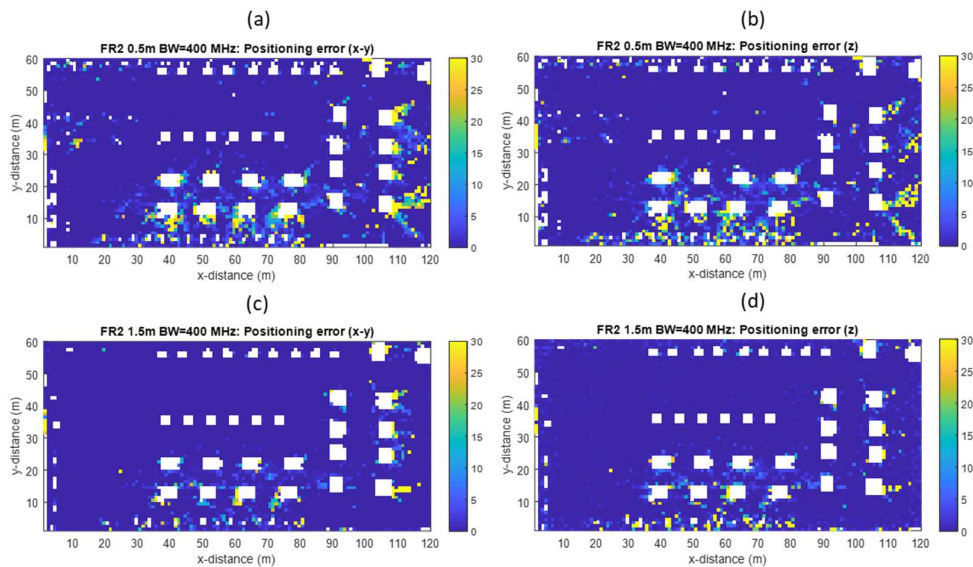


Figure 59 Positioning error in azimuth plane (X,Y) and elevation plane (Z) (FR2, 400 MHz, MS height = 0.5 and 1.5 m)

In addition to the geometric interpretation of results it is also important to investigate the statistical behaviour of the positioning errors in the above scenarios. Figure 60 shows the CDF of positioning errors in the 6 scenarios corresponding to the different carrier frequencies (FR1, FR2), UE height levels (0.5 m and 1.5 m) as well as the bandwidth (100 MHz and 400 MHz). From these curves, the increase in bandwidth shows a pronounced improvement in positioning performance from m-level to dm-level. However, this improvement corresponds to the LoS positions, whereas the positioning error on the non-LoS areas is not improved by the increased bandwidth. According to this figure, in those areas the positioning error can be improved by a higher level of the UE position.

Considering the 90% confidence level as a reference point, it is interesting to see that the FR2 scenario with 400 MHz bandwidth and a UE height of 1.5 m has demonstrated positioning errors below 30 cm, which is a promising result for use cases with enhanced positioning error requirements.

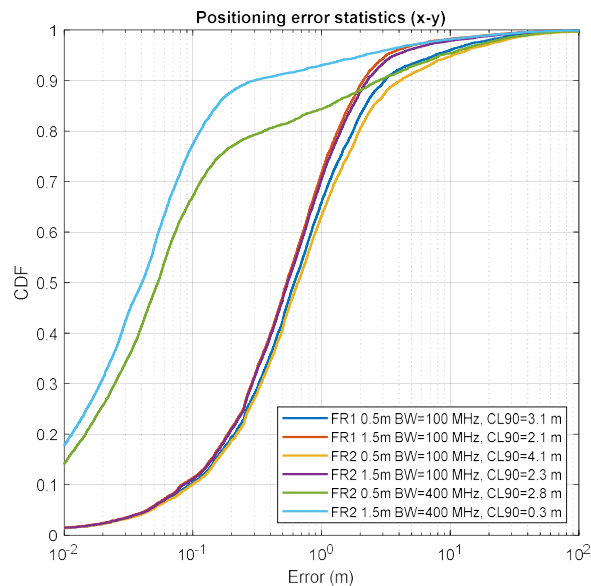


Figure 60 Positioning error statistics in azimuth plane for all configurations

An investigation of errors in the elevation plane shows a similar behaviour with the azimuth plane (Figure 61). However, the error values are higher than in the former in all cases. Considering the dimensions of this scenario (roof height of 10 m) the observed levels of positioning error reduce even further the usability of these positioning estimates. As a solution, the authors would recommend a different deployment methodology, possibly with BSs at different heights and/or positioned in the side walls of the building.

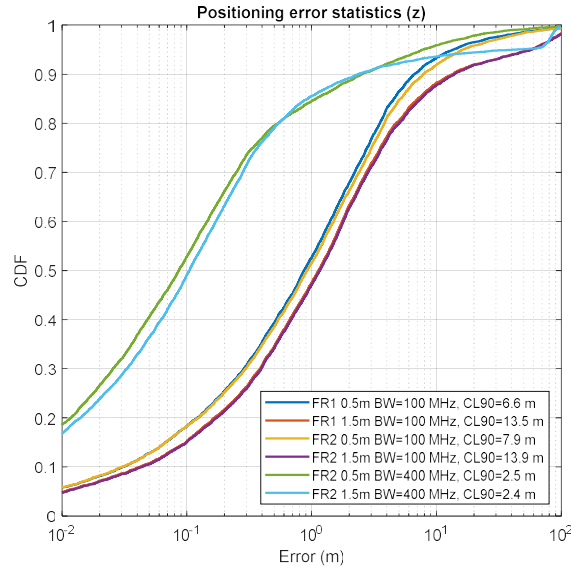


Figure 61 Positioning error statistics in elevation plane for all configurations

### 5.3 Statistical model-based evaluation

In this section, results from statistical simulations using the 3GPP Indoor Factory (InF) model are presented. The model is used to analyse the LoS visibility and the effect of the deployment geometry on the error in the position estimate (dilution of precision) for different factory setups. Also, the positioning accuracy using realistic signal conditions is analysed using the same model.

A detailed specification of the InF model can be found in 3GPP TR 38.901. The model builds on many measurements and ray-tracing experiments. It follows a traditional stochastic modelling approach where the various objects that are present in a factory hall are implicitly considered through their effect on the path loss and multipath parameters.

The model contains parameters describing the clutter size, clutter density and clutter height in the factory hall. The term “clutter” is taken to represent all small and large objects (e.g., conveyor belts, machinery, storage shelves, vehicles) that obstruct the radio waves propagation. All clutter is assumed to be metallic and thus highly reflective. The clutter parameters can be varied, within certain limits, and has impact on the path loss model and the LoS probability. Generally, the path loss is low in the InF scenarios, due to plentiful reflections from walls, ceiling, and metallic objects even in nLoS conditions.

How to select clutter height, clutter size and clutter density depends on the type of factory hall that should be modelled. The *clutter height* used in the model represents the fixed height for all clutter. Above this, it is assumed to be free space. The *clutter density* describes the density of clutter in terms of percentage of the surface area that is covered. The *clutter size* is the average size of the objects in the hall, when observed in different directions. To what extent clutter causes nLoS propagation depends also on the UE height.



### 5.3.1 Simulation setup

Two simulations were performed using the same factory layout and BS deployment as in the previous section. In the first simulation the parameters were chosen to resemble the environment considered in Section 5.2. The parameters used in the second simulation are identical to those used for evaluation of position calculations were the same model was used. The parameters are summarized in Table 11.

Table 11: Simulation parameters for statistical modelling of the indoor factory scenario.

Parameters	Simulation 1	Simulation 2
BS height	6 m	8 m
Clutter height	3 m	4 m
Clutter density	30 %	40 %
Clutter size	6 m	6 m
UE height	0.5 m and 1.5 m	0.5 m and 1.5 m

### 5.3.2 Evaluation of LoS probability

In Figure 62 the probability of having a LoS link to the BS in the top left corner is shown for Simulation 1 assuming a UE height of 0.5 m and 1.5 m. The LoS probability in the InF model depends on the horizontal distance between the BS and the UE as can be seen in the lowest plot. One BS can cover a significant part of the factory in this case, in particular when the UE is placed at a height of 1.5 m. This can be compared with the results shown in Figure 63 for Simulation 2. In this case the BS covers a smaller part of the factory. Due to the height of the clutter and the BS's the difference between placing the UE at 0.5 m and 1.5 m is also smaller.

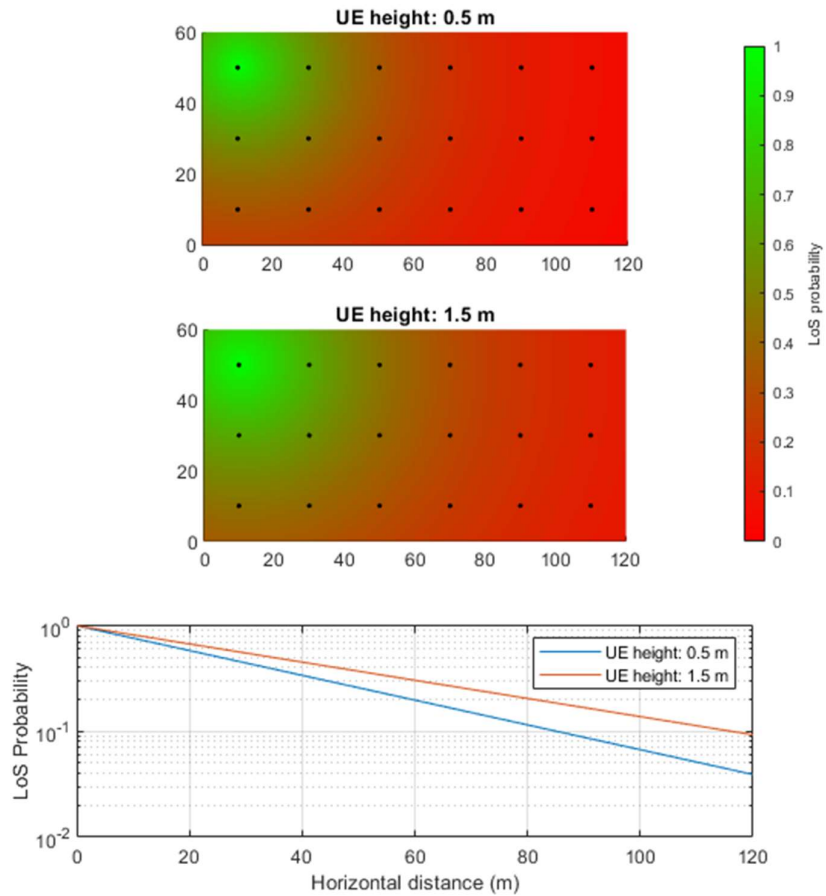


Figure 62: LoS probability for the BS in the top left corner using the assumptions for Simulation 1

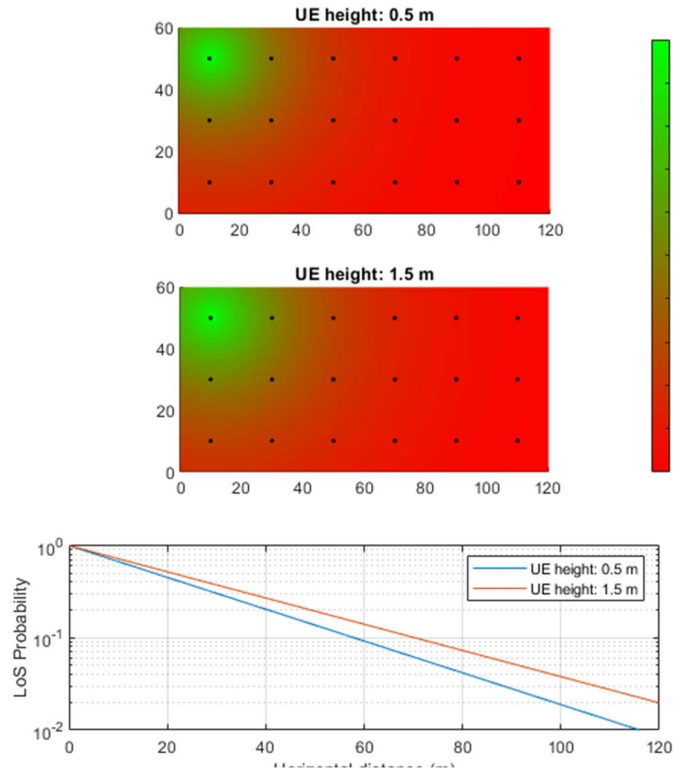


Figure 63: LoS probability for the BS in the top left corner using the assumptions for Simulation 2

The number of LoS links from a UE in a specific location to any BS, also connected to the possibility of using different radio-based techniques for positioning at this location, is shown in Figure 64 for Simulation 1 and Figure 65 and Figure 66 for Simulation 2. To be able to use time-of-arrival to calculate the 3D position of the UE at least 4 LoS links will be necessary. Using the same techniques to calculate a 2D position requires at least 3 LoS links. If angle-of-arrival is used instead, it is sufficient with 2 LoS links. If only 1 LoS link is available, the position can still be calculated using ranging in combination with angle-of-arrival.

In Figure 64 it can be seen that there are enough LoS links to be able to use any of the algorithms mentioned above, with only slightly reduced probability of having at least 4 LoS links in the corners if the UE is placed 0.5 m above the floor. This is in contrast to the results in Figure 65 which indicates that only 2 LoS links can be expected with a reasonable reliability in the whole factory while 3 or 4 LoS links, which is needed for ToA based positioning in 2D or 3D, only can be obtained in a limited area in the center part of the factory hall. In Figure 66 the probability of obtaining at least three LoS links is shown for a few different deployments, which are further discussed in Section 5.3.4. As expected, reducing the ISD (and thereby increasing the number of BSs) or reducing the clutter density increases the probability of obtaining enough LoS links significantly whereas an increase of the ISD (resulting in fewer BSs) reduces the chances of obtaining enough LoS links.

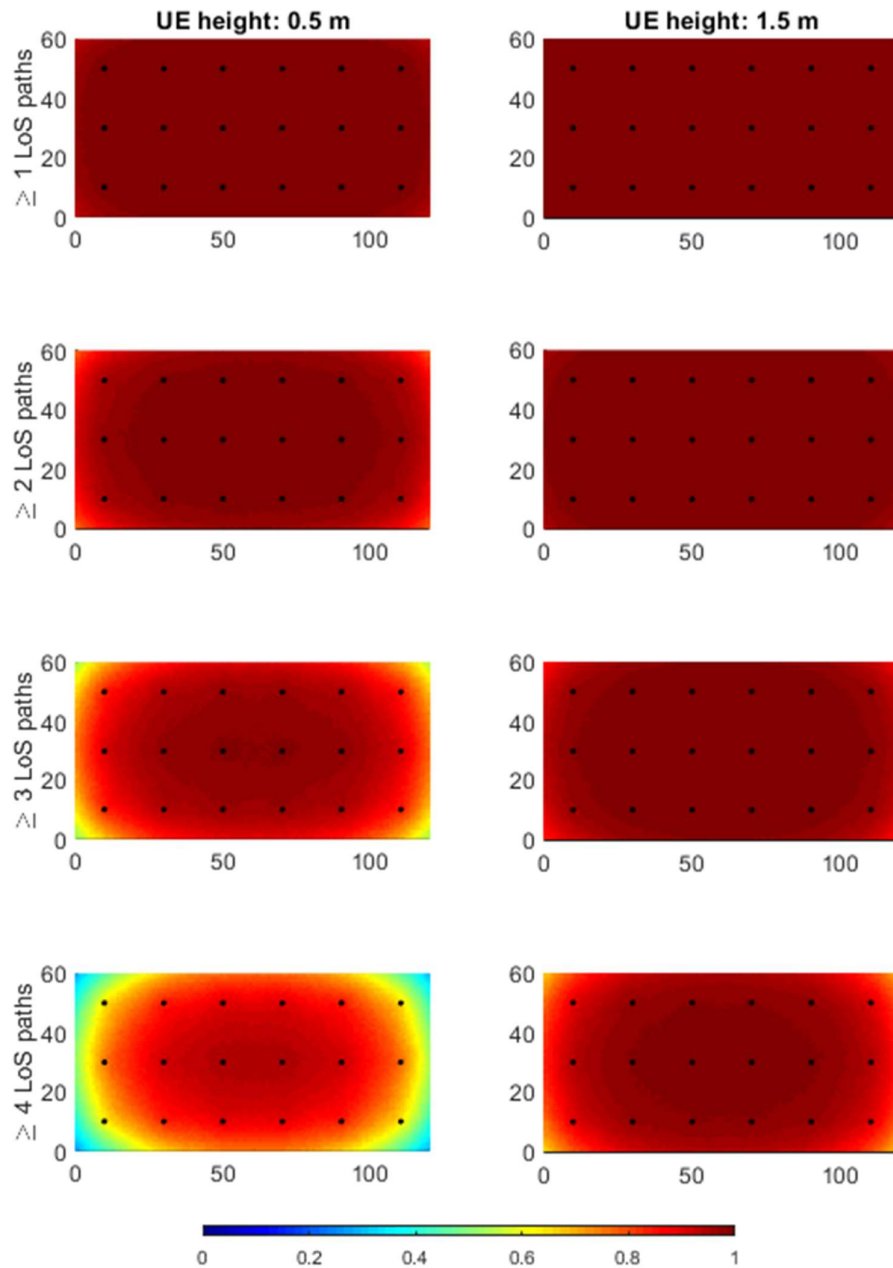


Figure 64: The probability of having at least a given number of LoS links using the assumptions for Simulation 1

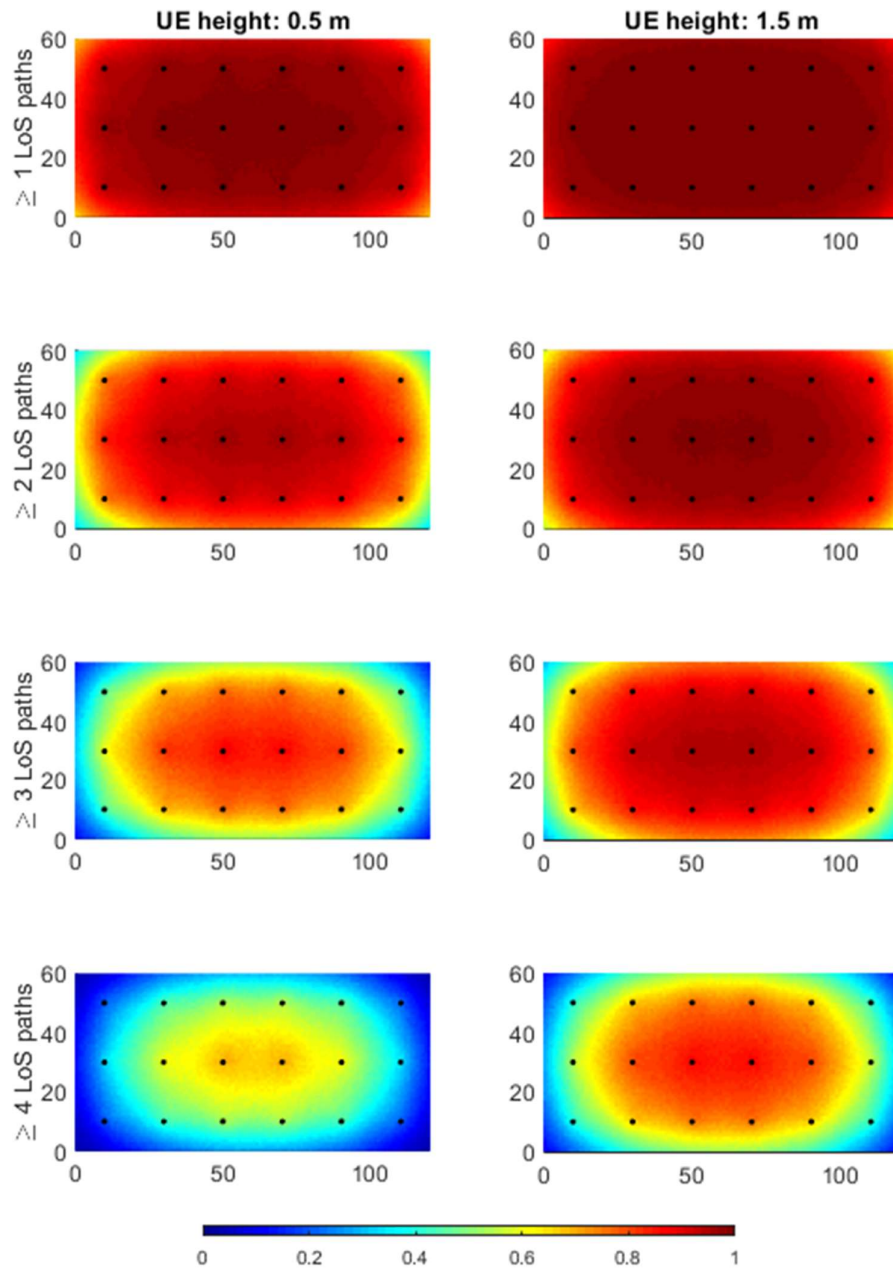


Figure 65: The probability of having at least a given number of LoS links using the assumptions for Simulation 2

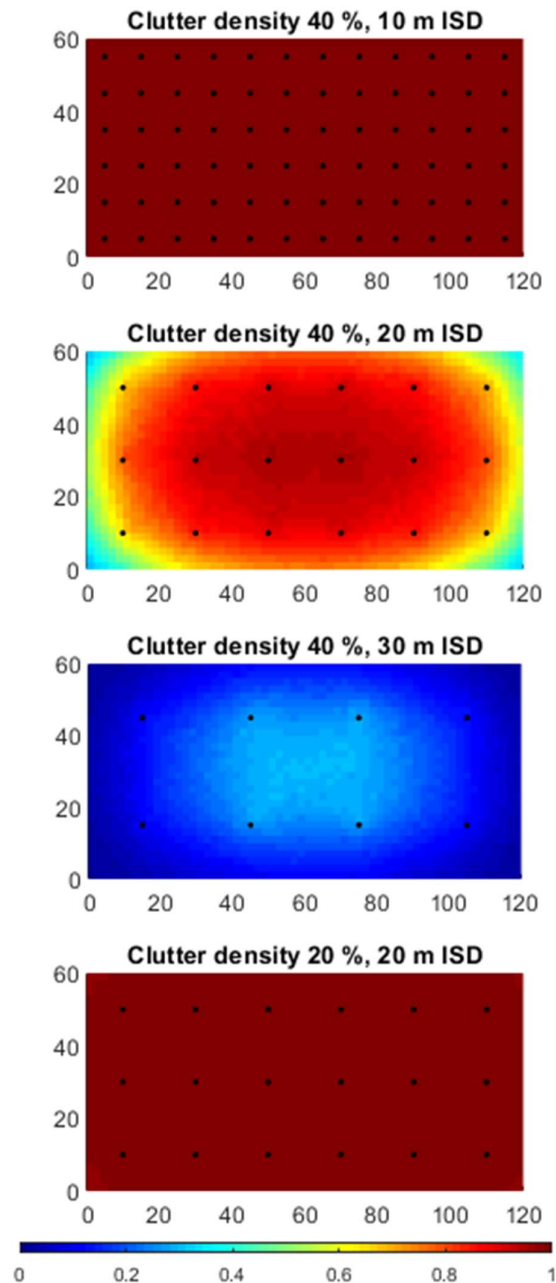


Figure 66: The probability of having at least three LoS links using the assumptions for Simulation 2. The results are here shown for different ISDs and clutter densities.

The probability of obtaining at least four LoS links for all positions in the factory is shown in Figure 67 for Simulation 1. It can be seen that the probability of obtaining 4 LoS links is approximately 78 % for a UE at a height of 0.5 m and 95 % for a UE at a height of 1.5 m. The probability of obtaining a larger number of LoS links is somewhat lower than what is seen in Figure 46 for the geometrical model.

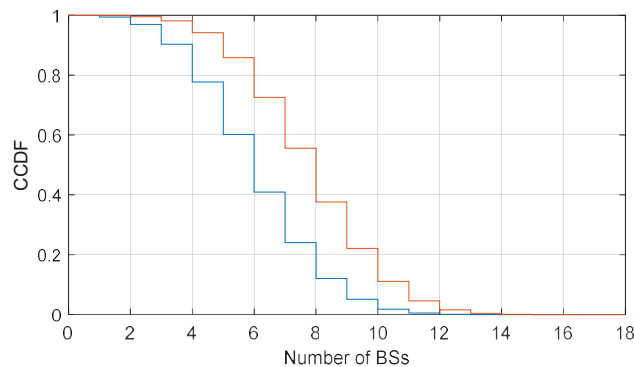


Figure 67: The probability of having at least four LoS links using the assumptions for Simulation 1

### 5.3.3 Evaluation of geometric effects on the positioning performance

The position accuracy might be significantly degraded by the geometry of the deployed BSs. This effect is called dilution of precision (DOP) and is explained in detail in [KR+16]. It is defined as the ratio of the variance of the position estimate to the variance of the ranging measurement. It is thus desired to have as low DOP value as possible, ideally less than 1 also shown in the report<sup>28</sup>. In Figure 68 the maximum horizontal DOP (how the geometry affects the horizontal positioning error), denoted HDOP in the figure that is achieved with 90 % probability is shown for Simulation 1. As can be seen the DOP is low over most of the factory floor but significantly increased in the corners, especially for the case with the UE at 0.5 m height. This means that even if there are enough LoS links available it will likely not be possible to obtain a reasonably accurate position estimate in the corners. This can to a certain extent be mitigated by placing BSs on the wall and in the corners, but this will not be optimal from a communication point of view and might thus require more BSs to be deployed.

<sup>28</sup> A DOP of less than 1 is possible if the number of measurements is larger than the number of unknowns, i.e. more than four measurements if a 3D position (and clock offset) is to be estimated.

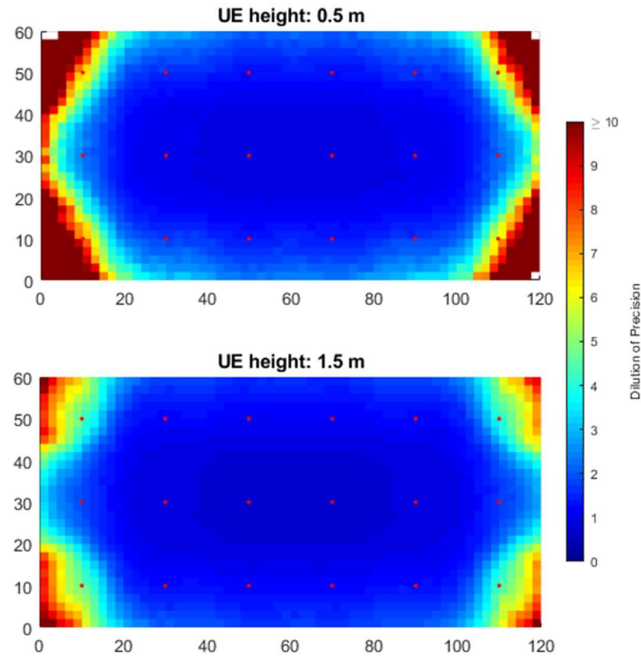


Figure 68: The 90<sup>th</sup> percentile of the HDOP using the assumptions for Simulation 1.

#### 5.3.4 Positioning simulation results

The NR positioning performance for DL-TDOA has been simulated. In the simulations, perfect synchronization between the different BSs is assumed. Only 2D positioning in the horizontal plane is considered here and the vertical position is the known UE height. This reduces the number of unknowns when estimating the position and slightly better results can be achieved compared to if 3D positioning is required. In the simulations the positioning is assumed to be performed in downlink although due to the assumptions made, for example on the orthogonality of the reference signals, the results would be very similar in uplink. No averaging is used in these results which means that some improvement in the accuracy could be gained, especially in stationary use cases.

As previously, the results are shown for a 120-by-60 m hall with an ISD of 10, 20 and 30 m with a BS layout as shown in Figure 69. The height of the BSs is however 8 m instead of 6 m which was used previously. Other simulation parameters are summarized in Table 12.

Table 12: Simulation parameters used for simulation of positioning performance using the InF model.

Parameter	Value
Carrier frequency	3.5 GHz
Sub-carrier spacing	30 kHz
Bandwidth	100 MHz = 272 PRBs
Antennas	Omni-directional X-polarized antennas at both UEs and base stations
Base station height	8m
UE height	1.5m
Reference signals used for positioning	Orthogonal positioning reference signals (PRS) defined in Rel-16
Averaging	No positioning averaging, one single positioning occasion
Base station TX power	23 dBm
Number of base stations	72 for 10m ISD, 18 for 20m ISD and 8 for 30m ISD

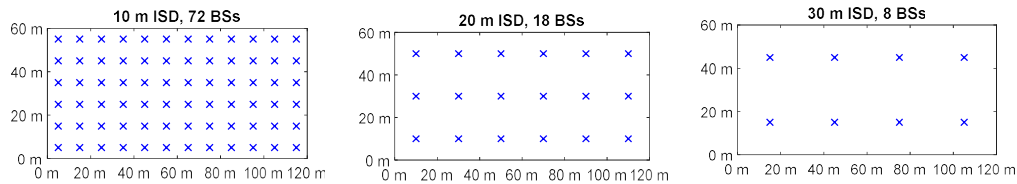


Figure 69: Location of the BSs in a 120-by-60 m hall for 10, 20 and 30 m ISD

In Figure 70, the probability of having a certain number of line-of-sight (LoS) links is shown for different inter-site distances (ISDs). For each simulation, the probability distribution and the complementary cumulative distribution function (CCDF) of the number of LoS links is shown. The CCDF can be interpreted as the probability that the number of LoS links is at least a certain number.

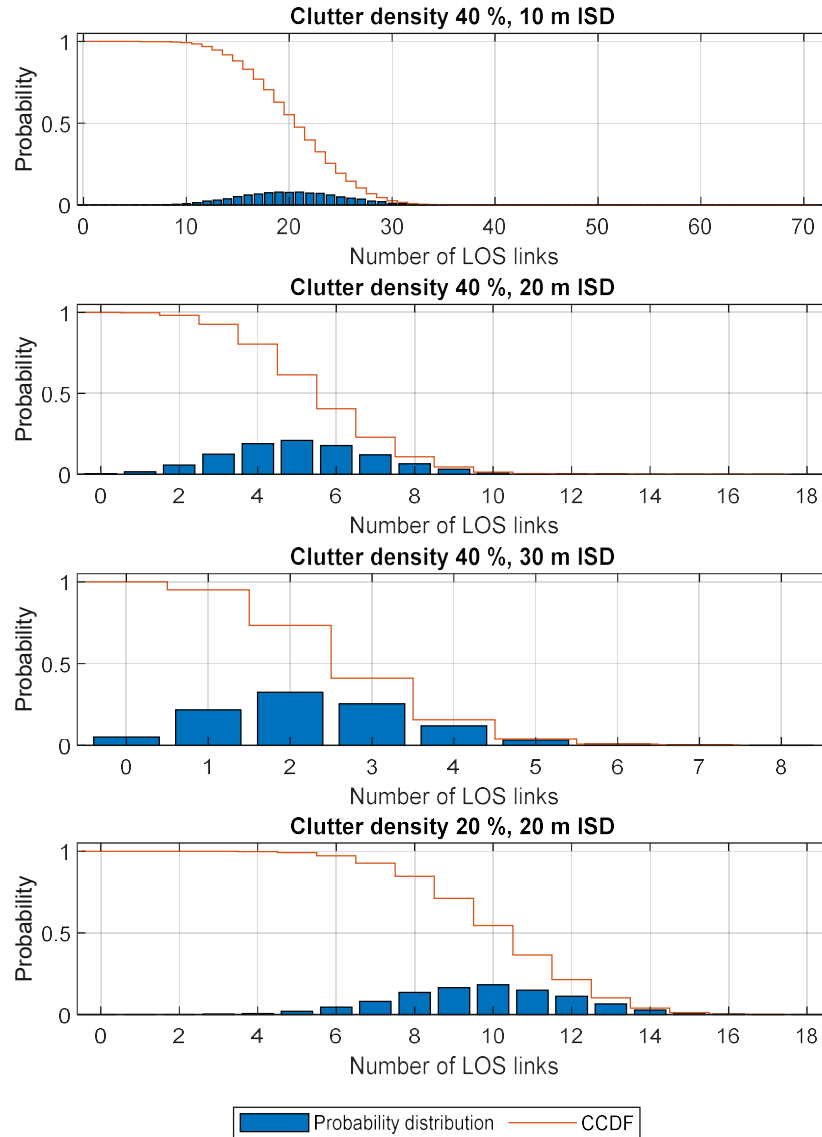


Figure 70: Number of LoS links assuming a clutter size of 6 m and a clutter height of 4 m. The BS height is in this case 8 m

The cumulative probability of the horizontal position errors is shown in Figure 71 for the case when the clutter size is 6 m and the clutter height is 4 m. In the “No LoS detection” case there is no attempt to distinguish between LoS and nLoS signals and the latter signals are therefore included in the position solution. The “LoS oracle” always makes a correct LoS/nLoS classification. The performance for this case can be seen as a lower bound on the achievable performance if perfect algorithms for LoS detection are implemented. It is obvious in Figure 71 that a LoS detector has a significant impact

on the position accuracy. An exception is when the ISD is large, and hence the number of BSs low, where the position accuracy seen for the case without any LoS detection at the higher percentiles (around the 90<sup>th</sup> percentile) is slightly better than the LoS oracle cases. In this case the position accuracy in the latter cases is slightly reduced due to too few LoS links resulting in higher DOP values. It should be noted that other errors, e.g. synchronization errors between the BSs, will exist in a real deployment and these results are therefore optimistic. These results indicate that it will be challenging to obtain an accurate position in 99% of the cases and that both a short ISD and LoS detection will be necessary to obtain an accurate position in 90% of the cases. The sparser scenario with 20% clutter density results in a smaller position error. The difference is particularly large when using LoS detection or a LoS oracle. It should be noted that these are the statistics for the whole factory and that knowledge about the LoS probability and the multipath environment in different parts of the factory can increase the reliability and integrity<sup>29</sup> of the position estimates significantly.

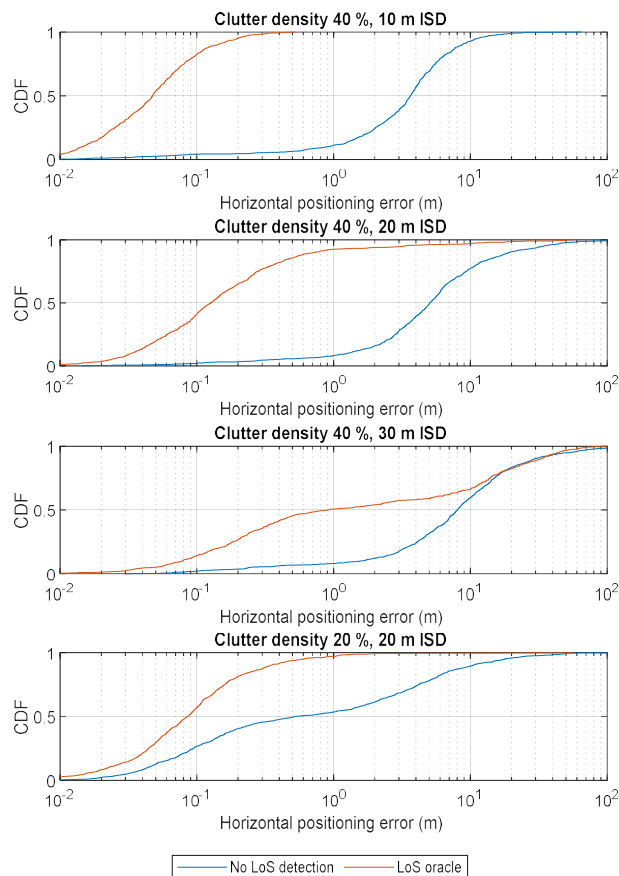


Figure 71: Simulated horizontal position accuracy. The clutter size is 6 m and the clutter height is 4 m. The height of the BSs is in this case 8 m.

<sup>29</sup> The ability to detect when the positioning requirements cannot be met.

#### 5.4 Comparison between Geometric based model and 3GPP based statistical model

In this section the performance of the statistical InF model used in Section 5.3 is compared to the geometric model used in Section 5.2. The results presented in Figure 46 and Figure 67 are combined in Figure 72. It can be seen that using the InF model the probability of having at least one LoS link anywhere in the factory is found to be very high (above 99 %), whereas the corresponding probability when using the geometric model is lower (90 % for the UE at 1.5 m height and 88 % for the UE at 0.5 m height). The InF model thus overestimates the LoS visibility of the areas in the factory with the poorest LoS coverage when compared to the geometric model. Also, it can be seen that the InF model underestimates the LoS visibility of the areas in the factory with the best LoS coverage.

The reason for this discrepancy can be seen by studying Figure 73 which shows the LoS visibility for different parts of the factory (the median value is shown for the InF model). Since the InF model assumes a homogeneous distribution of the clutter in the factory, the result is less variation in the LoS probabilities for different parts of the factory. Conversely the geometric model describes a particular factory which often have a larger variation in the distribution of the clutter. Parts of the factory consist of open areas with almost no clutter where the number of available LoS links is very high, see upper left part in the right column in Figure 73, and other parts have significant clutter resulting in nearly no LoS visibility, see lower right part in the right column in Figure 73. Thus, the positioning accuracy obtained in a real deployment can be expected to be significantly better than the results obtained using the InF model (see Section 5.3.4) in areas with high LoS visibility whereas it will likely be worse in areas with low LoS visibility.

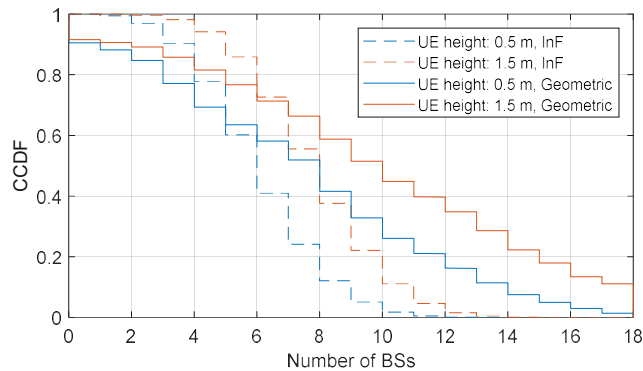


Figure 72: Comparison of the estimated number of LoS links for the InF model and the geometric model.

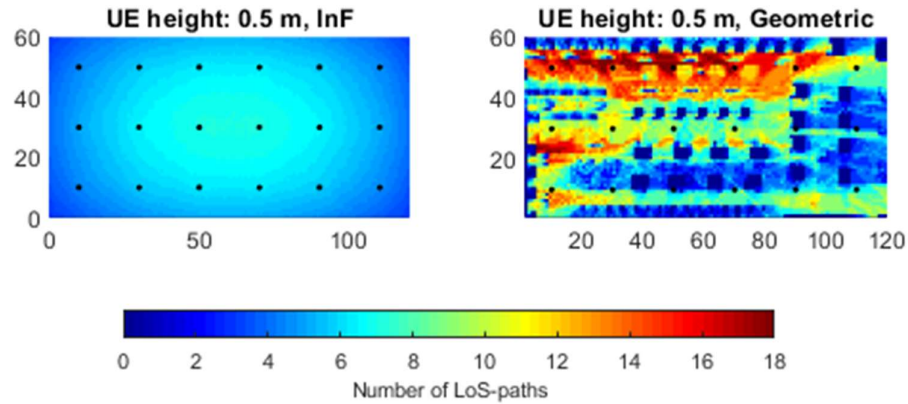


Figure 73: Comparison of the LoS visibility for different positions in the factory. For the InF model the median value is shown.

## 5.5 Conclusions and recommendations

In this chapter the performance of 5G positioning in a factory was evaluated using both a ray tracing model and a statistical model. The positioning performance in this type of environment will be limited mainly by multipath propagation and the lack of line-of-sight paths. Any error in the ranging estimates might also be amplified by geometric effects (DOP) in situations with poor geometric spread of the signals. These error sources depend significantly on the LoS probability in different parts of the factory. To improve the positioning performance, it is important both to have enough LoS signals and to know whether a particular signal is LoS or non-LoS.

The comparison between the ray tracing model and the 3GPP InF model in terms of LoS probability shows that, in this particular case, there is a difference in the determined LoS probability, which in turn corresponds to a difference in achievable positioning accuracy. This is to be expected, since the ray tracing model describes one particular factory whereas the 3GPP InF model describes a generic factory in statistical terms. The general conclusions from using both the models are however very similar.

To improve the positioning performance, it is recommended that:

- The indoor infrastructure deployment is carefully planned



- Line-of-sight (LoS) signal is essential for all radio-based positioning solutions, including 5G-based positioning. The number of base stations (or transmit and reception points) must therefore be large enough to provide LoS between UEs and the BSs. Wireless communication works well in multipath environments where nLoS components are dominating, however, positioning may require a denser deployment than wireless communication given the above observations, especially in an industrial environment with lots of clutter.
- The above observation also leads to lower positioning accuracy in areas with few surrounding BSs, like in corners and close to the walls, due to high dilution of precision. To achieve better positioning accuracy in these areas, it is recommended to deploy additional BSs along the walls and in the corners of the factory.
- Algorithms for detection of LoS paths are considered
  - As non-LoS path takes longer to travel than the LoS path between a UE and a BS. If a non-LoS path is used for TDOA-based positioning, it may lead to an additional timing error. By considering algorithms for detection of LoS/non-LoS paths and hence to distinguish between the two, the positioning accuracy can be greatly improved.

The standardization direction and performance targets for Industrial IoT positioning in 3GPP Release 17 look promising, as it provides additional support for industrial IoT use cases which demand high accuracy positioning. However, similar to legacy positioning solutions, given the diverse factory settings and various signal propagation conditions, there is no one-size-fits-all solution. Hence to commercially deploy those solutions, tight eco-system collaboration is essential to ensure practical deployment success but also commercial viability. Standardization is an enabler, but commercialization of such feature requires efforts of the industry through engagement in, for example, 5G-ACIA to foster adoption and ultimately help scale the solution.

Other further enhancements consideration, from product improvements perspective as an example, would be to provide accurate measurements of network synchronization uncertainties. Further deployment consideration is a dense indoor nodes deployment to provide richer LoS paths for the TDoA positioning approach. As the positioning error is highly dependent on the number of base stations which have a line-of-sight (LoS) path to the UE a dense deployment is hence beneficial. For indoor use cases, there is therefore typically a main advantage with indoor systems utilizing densely deployed nodes.

As mentioned, 3GPP Release 17 studied NR positioning for industrial IoT use cases, evaluated the achievable positioning accuracy and latency with the Release 16 positioning solutions in (industrial) IoT scenarios, and it is now specifying solutions to enable RAT dependent and RAT independent NR positioning enhancements for improving positioning accuracy, latency, network and/or device efficiency.

5G-SMART will closely monitor the development in 3GPP especially with respect to the above-mentioned gaps and point out any missing aspects that have not been addressed in future releases.

- Future work for positioning



- Solutions based on angle-of-arrival (AoA) measurements can provide localisation of a UE even with fewer BSs within LoS settings. The combination of TDOA and AoA has not been addressed in this report, however it would be an interesting approach to reduce the need for very dense deployments in cluttered industrial environments.
- The current evaluation assumes no sync error between the BSs. Understanding the various sync errors between BSs for specific deployment and technologies can be further investigated.
- Algorithms for non-LoS detection are important as almost all radio-based positioning solutions require LoS.
- System integrity information for ensuring reliable operation, particularly for safety-critical applications such as autonomous navigation inside the factory (e.g. drones, AGVs).
- Future work on the reliable estimation of positioning techniques (e.g. detection of outlier).



## 6 Summary and Future work

Moving forward from Release 15 based 5G technology, new 5G technical features introduced in Release 16 such as 5G-TSN integration, time synchronization and cellular-based positioning are key enablers for new smart manufacturing use cases. For adoption of such features in a 5GS deployment, there is need for the feature investigation and evaluation when these need to be realized for a specific use case.

This report provides an in-depth evaluation of these features along with results and implications of those 5G novel capabilities. It also goes beyond in the technical features aspect by introducing DetNet as a potential technology for future smart manufacturing applications. Furthermore, a 5G-DetNet architecture is proposed which is tailored for the smart manufacturing deployment. Concerning 5G-TSN integration, a new scheduling mechanism is proposed and evaluated for an integrated 5G-TSN network, by utilizing system-level simulation methodology. The use case considered for evaluation relates to a trialled 5G-SMART use case. A time error analysis is presented for typical smart manufacturing deployment. An E2E chain, including all the components within 5GS contributing to overall time error budget, is identified. Within 5GS, the radio link between base station and user equipment is seen as a major factor contributing to overall 5GS time error budget. Uncertainty introduced from estimation of the downlink propagation delay is the major factor. An evaluation of 5G-based positioning in a realistic environment adopted from a 5G-SMART trial site is presented. Key learnings for all the features are summarized in the table below. It is observed from the positioning evaluations that the performance of the positioning does not only depend upon the positioning mechanism utilized but also on the 5GS deployment and configuration.

Technical features	Key learnings and insights
5G-TSN integration	<p>New scheduling optimization is proposed for an integrated 5G-TSN network, where it shown that a CNC can design more efficient TSN schedule based on additional information from 5GS bridge capabilities, such as channel conditions and variability of the radio link.</p> <p>The downside of using these additional values to be considered in TSN scheduling generation, however, increases complexity, as the simple black-box integration of the logical 5GS bridge does not apply anymore. There is a clear trade-off between complexity and efficiency that can be achieved with the integrated TSN and 5G network concept.</p>
Time synchronization	<p>Time error analysis investigation indicates that a 5GS is able to support stringent time error budget of 900 ns. From the transport network, an existing solution defined by ITU-T standard can support some relevant 5G-TSN based industrial network synchronization requirements. From the radio network perspective, accurate propagation delay estimation method is very crucial to achieve minimal time error between UE and base station. Two propagation estimation delay methods are investigated, namely RTT and Timing Advance. The result indicates that the RTT can achieve lower time error compared to the Timing Advance.</p> <p>Furthermore, an extensive link level simulation is performed by considering the RTT method. To evaluate a certain radio deployment scenario, new algorithm is proposed to estimate downlink propagation</p>



	delay based on the detection of primary synchronization signal (PSS). The results from the simulation provide guidelines on the suitable radio configurations (e.g., subcarrier spacing and UE antenna height) required to achieve target time synchronization performance.
Positioning	The industrial 5G deployment of a 5G-SMART trial (from the site in Aachen) is selected as a realistic environment for the positioning evaluation. 5G radio frequency-based positioning is evaluated with ray tracing model (also known as geometric model) and statistical model. The results show that the positioning performance will be limited due to multipath propagation and lack of line of sights. Furthermore, it is concluded that, in order to improve positioning performance, more accurate estimation of both enough LOS signals and estimation of whether a signal is LoS or non-LoS is important. Finally, a set of recommendations is provided to improve positioning performance.



## References

- [5GS20-D51] 5G-SMART Deliverable D5.1, "First report on new technological features to be supported by 5G standardization and their implementation impact", November 2020. <https://5gsmart.eu/deliverables/>
- [5GS20-D11] 5G-SMART Deliverable D1.1, "Forward looking smart manufacturing use cases, requirements and KPIs", June 2020. <https://5gsmart.eu/deliverables/>
- [5GS20-D52] 5G-SMART Deliverable D5.2, "First report on 5G network architecture options and assessments", November 2020.
- [IEEE18-8021QCC] IEEE, "P802.1Qcc Draft Standard for Local and metropolitan area network - Bridges and Bridged Networks - Amendment:Stream Reservation Protocol (SRP) Enhancements and Performance Improvements," IEEE, 2018.
- [IEEE18-8021Q] IEEE, "IEEE standard for Local and Metropolitan Area Networks - Bridges and Bridged Networks IEEE Std 802.1Q-2018," IEEE, 2018.
- [MS+21] M. S. D. C. J. F. J. P.-R. Maik G. Seewald, "Configuration Enhancements for Wireless TSN," 17 08 2021. [Online]. Available: <https://www.ieee802.org/1/files/public/docs2021/dj-seewald-wireless-tsn-0721-v01.pdf>.
- [RG+21] R. G. M. S. H. D. S. David Ginthoer, "Robust End-to-End Schedules for Wireless Time-Sensitive Networks under Correlated Large-scale Fading," in *2021 17th IEEE International Conference on Factory Communication Systems (WFCS)*, 2021
- [3GPP20-22104] 3GPP technical specification TS 22.104, "Service requirements for cyber-physical control applications in vertical domains", October, 2020
- [IG+20] I. Godor *et al.*, "A Look Inside 5G Standards to Support Time Synchronization for Smart Manufacturing," in *IEEE Communications Standards Magazine*, vol. 4, no. 3, pp. 14-21, September 2020, doi: 10.1109/MCOMSTD.001.2000010.
- [3GPP20-22261] 3GPP technical specification TS 22.261, "Service requirements for the 5G system", March 2020
- [3GPP20-23700] 3GPP technical report TR 23.700-20, "Study on enhanced support for industrial Internet of things in the 5G system (5GS)", November, 2020
- [3GPP20-23434] 3GPP technical specification TS 23.434, "Service Enabler Architecture Layer for Verticals (SEAL); Functional architecture and information flows" Service Enabler Architecture Layer for Verticals (SEAL), September, 2020
- [3GPP20-TS23501] 3GPP technical specification TS 23.501, "System architecture for the 5G System (5GS)", Release 16, August, 2020
- [5GS20-CT] 5G-SMART report, "5G common terminology report", 2020 <https://5gsmart.eu/deliverables/>
- [SR+21] Stefano Ruffini, Mikael Johansson, Björn Pohlman, Magnus Sandgren, "5G synchronization requirements and solutions" Ericsson Technology Review, January 2021.
- [ITU20-G82752] ITU-T G.8275.2, "ITU-T G.8275.2, "ITU-T PTP Profile for Phase and Time Distribution with Frequency Support", March, 2020.



[ITU20-G82751]	ITU-T G.8275.1 : Precision time protocol telecom profile for phase/time synchronization with full timing support from the network,2020
[3GPP21-2010837]	R2-2010837, 3GPP TSG RAN WG2 Meeting #112, Reply to LS on propagation delay compensation enhancements.
[ITU20-G8721]	ITU-T G.8721.1 Network limits for time synchronization in packet networks with full timing support from the network, February 2020.
[3GPP21-38133]	3GPP TS 38.133, "NR; Requirements for support of radio resource management," v. 16.7.0, January, 2021
[3GPP21-38331]	3GPP TS 38.331, "NR; Radio Resource Control (RRC); protocol specification" v. 16.6.1, January, 2021
[3GPP21-38211]	3GPP TS 38.211, "NR; Physical channels and modulation" v. 16.6.1, January, 2021
[3GPP21-38213]	3GPP TS 38.213, "NR; Physical layer procedures for control" v. 16.4.0, January, 2021
[3GPP20-38901]	3GPP TR 38.901, "Study on channel model for frequencies from 0.5 to 100 GHz", November, 2020
[KR+16]	K. R. e. al, "A Novel 3D Multilateration Sensor Using Distributed Ultrasonic Beacons for Indoor Navigation," <i>Sensors</i> , 2016.
[5GS20-D14]	5G-SMART Deliverable D1.4, "Radio network deployment options for smart manufacturing", December 2020. <a href="https://5gsmart.eu/deliverables/">https://5gsmart.eu/deliverables/</a>
[5GS20-D21]	5G-SMART Deliverable D2.1, "Design of 5G-based testbed for industrial robotics", May 2020. <a href="https://5gsmart.eu/deliverables/">https://5gsmart.eu/deliverables/</a>
[5GS20-D32]	5G-SMART Deliverable D3.2, "Report of system design options for monitoring of workpiece and machine", May 2020. <a href="https://5gsmart.eu/deliverables/">https://5gsmart.eu/deliverables/</a>



## List of abbreviations

3GPP	3 <sup>rd</sup> Generation Partnership Project
5GS	5G system
A-GPS	Assisted-GPS
AF	Application Function
AGV	Automated Guided Vehicle
AoA	Angle of Arrival
AR	Augmented Reality
ARP	Antenna Reference Point
AMC	Advance Modulation Coding
DRB	Data Radio Bearer
BMCA	Best Master Clock Algorithm
CCDF	Complementary Cumulative Distribution Function
CPF	Control Plane Function
CLP	Centralized or Distributed Localization Protocols
CM	Clock Master
CNC	Centralised Network Configuration
CP	Constraint programming
CQI	Channel Quality Indicator
CS	Clock Slave
CSI	Channel State Information
CUC	Centralised User Configuration
DetNet	Deterministic Networking
DOP	Dilution of precision
DS-TT	Device Side TSN Translators
DSCP	DiffServ Code Point
eNB	Enhanced NodeB
ePRC	Enhanced Primary Reference Clock
ePRTC	Enhanced Primary Reference Time Clock
FME	Flow Management Entity
GM	Grand Master
gNB	Next generation NodeB
GNSS	Global Navigation Satellite System
GPS	Global Position System
gPTP	generalized Precision Time Protocol
IETF	Internet Engineering Task Force
InF	Indoor Factory
ISD	Inter-site distance
ITU-T	International Telecommunication Union
LO	Local Oscillator



LoS	Line of Sight
LPP	Location and Positioning Protocol
LRP	Link Local Registration Protocol
LTE	Long Term Evolution
M2M	Machine to Machine
MES	Manufacturing Execution System
MILP	Mixed Integer Linear Programming
MME	Mobility Management Entity
MMRP	Multiple MAC Registration Protocol
MPLS	Multiprotocol Label Switching
MSRP	Multiple Stream Registration Protocol
MCS	Modulation Coding Scheme
MVRP	Multiple VLAN Registration Protocol
NIC	Network Interface Card
NME	Network Management Entity
NPN	Non-Public Network
NRTK	Network Real-time kinematic
NTP	Network Time Protocol
NW-TT	Network Side TSN Translator
OTDOA	Observed time of arrival
PAR	Project Authorization Request (RAP)
PCE	Path Computational Element
PCE	Path Computation Engine
PCF	Policy Coordination Function
PCI	Physical Cell Identifier
PDU	Packet Data Unit
PEF	Packet Elimination Function
POF	Packet Ordering Function
PPP	Precision Point Positioning
PREOF	Packet Replication Elimination and Ordering Functions
PRF	Packet Replication Function
PRTC	Primary Reference Time Clock
PSN	Packet Switched Network
QoS	Quality of Service
RAN	Radio Access Network
RAP	Resource Allocation Protocol
RIBM	Radio-Interface Based Monitoring
RRC	Radio Resource Control
RSRP	Reference Received Signal Power
RSSI	Received Signal Strength



RTT	Round Trip Time
SDO	Standard Development Organization
SFN	System Frame Number
SIB	System Information Block
SMT	Satisfiability Modulo Theories
SRP	Stream Reservation Protocol
SSR	State Space Representation
SyncE	Synchronous Ethernet
T-BC	Telecom Boundary Clock
TBS	Terrestrial Beacon System
TDofA	Time Difference of Arrival
TG	Task Group
ToA	Time of Arrival
TSC	Time Sensitive Communications
TSN	Time Sensitive Networking
TT	TSN Translators
U-OTDA	Uplink time-difference-of-arrival
UAV	Unmanned Aerial Vehicle
UCI	Uplink Control Information
UE	User Equipment
UNI	User /Network Interface
UPF	User Plane Function

Table 13: List of abbreviations